CHARACTERIZATION OF THE AUTONOMIC NERVOUS SYSTEM RESPONSE UNDER EMOTIONAL STIMULI THROUGH LINEAR AND NON-LINEAR ANALYSIS OF PHYSIOLOGICAL SIGNALS

A thesis presented for the degree of Doctor of Biomedical Engineering

Author: María Teresa Valderas Yamuza

Directors:

Dr. Raquel Bailón Luesma[1]

Dr. Montserrat Vallverdú Ferrer[2]

[1]Biomedical Signal Interpretation and Computational Simulation (BSICoS), Aragón Institute for Engineering Research (I3A), IIS Aragón, University of Zaragoza, Spain.

[2]Department ESAII, Centre for Biomedical Engineering Research, Universitat Politècnica de Catalunya, Barcelona, Spain.

Zaragoza 2019

Remain steadfast on the path with a pristine heart, unmoveable faith and a desperate thirst. You shall assuredly discover your own self.

Sri Ma Anandamayí

To Gerard, Zipi and Zape.

Acknowledgments

The research developed within this PhD thesis, entitled "Characterization of the autonomic nervous system response under emotional stimuli through linear and non-linear analysis of physiological signals", was supported by Agencia Estatal de Investigación (AEI) and Fondo Europeo de Desarrollo Regional (FEDER) under the projects RTI2018-097723-B-I00, DPI2016-75458-R and DPI2017-89827-R, by Centro de Investigación Biomédica en Red (CIBER) de Bioingeniería, Biomateriales y Nanomedicina through Instituto de Salud Carlos III, and by Gobierno de Aragón and FEDER under project LMP44-18 and BSICoS group (T39-17R).

The computation was performed using the ICTS "NANBIOSIS", more specifically by the High Performance Computing Unit of the CIBER in Bioengineering, Biomaterials & Nanomedicine (CIBERBBN). This work has been developed within a joint PhD program in biomedical engineering at both the University of Zaragoza and the Universitat Politècnica de Catalunya. The collaboration between both universities has been fundamental for the performance of this thesis.

I would like to express my sincere gratitude to all the people who have been part of this thesis and who have contributed to its development.

Firstly, I feel immensely grateful to my two thesis directors Dr. Raquel Bailón and Dr. Montserrat Vallverdú for encouraging my research, for their continuous support, for their patience, motivation, and immense knowledge. Their guidance helped me in all the time of research and writing of this thesis. I could not have imagined having better advisors and mentors for my PhD study. Your advice on my research has been priceless.

Besides my two thesis directors, I would like to thank Dr. Pablo Laguna, and Dr. Pere Caminal, who provided me an opportunity to join their teams in my special situation of doing the research from home and part-time. Without they precious support it would not be possible to conduct this research. Especially, I would like to thank Dr. Pablo Laguna for his meticulous involvement in the corrections of the papers.

My sincere thanks also goes to Dr. Juan Bolea for enlightening me the first glance of research, for the stimulating discussions, and all his help that he provided me to improve my thesis in the last five years.

I would also like to thank to Dr. Michele Orini for his support in adapting his ARMA model algorithm to generate simulated signals, and to Dr. Carlos Orrite for provide me the emotion database.

Also I thank my friends in the following institutions: Biomedical Signal Interpretation and Computational Simulation at the University of Zaragoza and Centre for Biomedical Engineering Research at the Universitat Politècnica de Catalunya.

Last but not the least, I would like to thank my husband Gerard García Porlan for supporting me spiritually throughout writing this thesis and in my life in general.

Abstract

In this dissertation, linear and non-linear methodologies applied to physiological signals are presented, with the purpose of characterizing the autonomic nervous system response under emotional stimuli. This study is motivated by the necessity of developing a tool which identifies emotions based on their effect on cardiac activity, since it may have a potential impact on clinical practice for diagnosing psycho-neural illnesses.

The hypotheses of this PhD thesis are that emotions induce noticeable changes in autonomic nervous system and that these changes can be capture from the analysis of physiological signals, in particular, from the joint analysis of heart rate variability (HRV) and respiration.

The analyzed database contains the simultaneous recording of electrocardiogram and respiration of 25 subjects during video-induced emotion elicitation, including the following emotions: joy, fear, sadness and anger.

In this dissertation, two methodological studies are described.

A method based on the linear analysis of HRV guided by respiration is proposed. The method was based on redefining the high frequency (HF) band, not only to be centered at the respiratory frequency, but also to have a bandwidth dependent on the respiratory spectrum. Firstly, the method was tested using simulated HRV signals, yielding the minimum estimation errors as compared to classic HF band and even the HF band centered at respiratory frequency but with constant bandwidth, independently of the values of the sympathovagal ratio. Then, the proposed method was applied to discriminate emotions in a database of video-induced elicitation. Not

only the proposed redefined HF band outperformed the other HF band definitions in emotion discrimination but also the maximum correlation between HRV and respiration spectra discriminated joy vs. relax, joy vs. each negative valence emotion, and fear vs. sadness with p-value ≤ 0.05 and AUC ≥ 0.70.

Non-linear techniques as the Auto-Mutual and the Cross-Mutual Information Function, the AMIF and the CMIF respectively, are also used in this PhD thesis for human emotion recognition. The AMIF technique was applied to HRV signals to study complex interdependencies, and the CMIF technique was considered to quantify the complex coupling between HRV and respiratory signals. Both algorithms were adapted to short-term RR time series. Traditional band pass filtering was applied to the RR series at low frequency and high frequency bands, and a respiration-based filter bandwidth was also investigated.

The results revealed that the AMIF applied to the RR time series filtered in the redefined HF band was able to discriminate between: relax and joy and fear, joy and each negative valence conditions and finally fear and sadness and anger, all with a statistical significance level (p-value ≤ 0.05, AUC ≥ 0.70). Furthermore, the parameters derived from the AMIF and the CMIF allowed the low signal complexity presented during fear to be characterized in front of any of the studied elicited states.

Finally, the ability of a combination of linear and non-linear characteristics to discriminate between pairs of emotions and between emotional valences is investigated. The results extracted from this chapter suggested that relax vs. joy, positive vs. all negative valences, joy vs. fear, joy vs. sadness, joy vs. anger and fear vs. sadness can be discriminated by means of HRV analysis.

The joint analysis of HRV and respiration increases the discriminatory capacity of HRV, being the maximum correlation between HRV and respiration spectra one of the best indices for the discrimination of emotions. The analysis of mutual information, even in short-term signals, adds relevant information to the linear indices for the discrimination of emotions.

Resumen

En esta disertación se presentan metodologías lineales y no lineales aplicadas a señales fisiológicas, con el propósito de caracterizar la respuesta del sistema nervioso autónomo bajo estímulos emocionales. Este estudio está motivado por la necesidad de desarrollar una herramienta que identifique emociones en función de su efecto sobre la actividad cardíaca, ya que puede tener un impacto potencial en la práctica clínica para diagnosticar enfermedades psico-neuronales.

Las hipótesis de esta tesis doctoral son que las emociones inducen cambios notables en el sistema nervioso autónomo y que estos cambios pueden capturarse a partir del análisis de señales fisiológicas, en particular, del análisis conjunto de la variabilidad del ritmo cardíaco (HRV) y la respiración.

La base de datos analizada contiene el registro simultáneo del electrocardiograma y la respiración de 25 sujetos elicitados con emociones inducidas por vídeos, incluyendo las siguientes emociones: alegría, miedo, tristeza e ira.

En esta disertación se describen dos estudios metodológicos.

En el primer estudio se propone un método basado en el análisis lineal de la HRV guiado por la respiración. El método se basó en la redefinición de la banda de alta frecuencia (HF), no solo centrándose en la frecuencia respiratoria, sino también considerando un ancho de banda que dependiera del espectro respiratorio. Primero, el método se validó con señales de HRV simuladas, obteniéndose errores mínimos de estimación en comparación con la definición de la banda de HF clásica e incluso con la banda de HF centrada en la frecuencia respiratoria pero con un ancho de banda constante, independientemente de los valores del ratio simpático-vagal.

Después, el método propuesto se aplicó en una base de datos de elicitación emocional inducida mediante vídeos para discriminar entre emociones. No solo la banda de HF redefinida propuesta superó a las otras definiciones de banda de HF en discriminación emocional, sino también la correlación máxima entre los espectros de la HRV y de la respiración discriminó alegría y relajación, alegría y cada emoción de valencia negativa y entre miedo y tristeza con un p-valor ≤ 0.05 y AUC ≥ 0.70.

En el segundo estudio, técnicas no lineales como la Función de Auto Información Mutua y la Función de Información Mutua Cruzada, AMIF y CMIF respectivamente, son también propuestas en esta tesis doctoral para el reconocimiento de emociones humanas. La técnica AMIF se aplicó a las señales de HRV para estudiar interdependencias complejas, y se consideró la técnica CMIF para cuantificar el acoplamiento complejo entre las señales de HRV y de respiración. Ambos algoritmos se adaptaron a las series temporales RR de corta duración. Las series RR fueron filtradas en las bandas de baja y alta frecuencia, y también se investigaron las series RR filtradas en un ancho de banda basado en la respiración.

Los resultados revelaron que la técnica AMIF aplicada a la serie temporal RR filtrada en la banda de HF redefinida fue capaz de discriminar entre: relajación y alegría y miedo, alegría y cada valencia negativa y finalmente miedo y tristeza e ira, todos con un nivel de significación estadística (p-value ≤ 0.05, AUC ≥ 0.70). Además, los parámetros derivados de AMIF y CMIF permitieron caracterizar la baja complejidad que la señal presentaba durante el miedo frente a cualquier otro estado emocional estudiado.

Finalmente se investiga, mediante un clasificador lineal, las características lineales y no lineales que discriminan entre pares de emociones y entre valencias emocionales para determinar qué parámetros permiten diferenciar los grupos y cuántos de éstos son necesarios para lograr la mejor clasificación posible. Los resultados extraídos de este capítulo sugieren que pueden ser clasificadas mediante el análisis de la HRV: relajación y alegría, la valencia positiva frente a todas las negativas, alegría y miedo, alegría y tristeza, alegría e ira, y miedo y tristeza.

El análisis conjunto de la HRV y la respiración aumenta la capacidad discriminatoria de la HRV, siendo la máxima correlación entre los espectros de la HRV y la respiración uno de los mejores índices para la discriminación de emociones. El análisis de la información mutua, aun en señales de corta duración, añade información relevante a los índices lineales para la discriminación de emociones.

Resum

En aquesta dissertació es presenten metodologies lineals i no lineals aplicades a senyals fisiològics, amb el propòsit de caracteritzar la resposta del sistema nerviós autònom sota estímuls emocionals. Aquest estudi està motivat per la necessitat de desenvolupar una eina que identifiqui emocions en funció del seu efecte sobre l'activitat cardíaca, ja que pot tenir un impacte potencial en la pràctica clínica per diagnosticar malalties psico-neuronals.

Les hipòtesis d'aquesta tesi doctoral són que les emocions indueixen canvis notables en el sistema nerviós autònom i que aquests canvis es poden capturar a partir de l'anàlisi de senyals fisiològics, en particular, de l'anàlisi conjunta de la variabilitat del ritme cardíac (HRV) i la respiració.

La base de dades analitzada conté l'enregistrament simultani de l'electrocardiograma i la respiració de 25 subjectes durant l'elicitació d'emocions induïda per vídeo, incloent les emocions següents: alegria, por, tristesa i ira.

En aquesta dissertació es descriuen dos estudis metodològics.

En el primer estudi es proposa un mètode basat en l'anàlisi lineal de la HRV guiat per la respiració. El mètode es va basar en la redefinició de la banda d'alta freqüència (HF), no només per centrar-se en la freqüència respiratòria, sinó també per tenir un ample de banda que depengués de l'espectre respiratori. Primer, el mètode es va validar amb senyals de HRV simulades, obtenint errors mínims d'estimació en comparació amb la definició de la banda HF clàssica i fins i tot amb la banda HF centrada en la freqüència respiratòria però amb un ample de banda constant, independentment dels valors de la ràtio simpàtico-vagal. Després, el mètode proposat

es va aplicar en una base de dades d'elicitació emocional induïda mitjançant vídeos per discriminar entre emocions. No només la banda HF redefinida proposta va superar les altres definicions de banda HF en discriminació emocional, sinó també la correlació màxima entre els espectres de la HRV i de la respiració va discriminar entre l'alegria i la relaxació, entre l'alegria i cada emoció de valència negativa i entre la por i la tristesa amb un p-valor ≤ 0.05 i AUC ≥ 0.70.

En el segon estudi, tècniques no lineals com la Funció d'Auto Informació Mútua i la Funció d'Informació Mútua Creuada, AMIF i CMIF respectivament, també es proposen en aquesta tesis doctoral per al reconeixement d'emocions humanes. La tècnica AMIF es va aplicar als senyals de HRV per estudiar interdependències complexes, i es va considerar la tècnica CMIF per quantificar l'acoblament complex entre els senyals de HRV i de respiració. Tots dos algoritmes es van adaptar a les sèries temporals RR de curta durada. Les sèries RR van ser filtrades a les bandes de baixa i d'alta freqüència, i també es van investigar les sèries RR filtrades en un ample de banda basat en la respiració.

Els resultats van revelar que l'AMIF aplicada a la sèrie de temps RR filtrada a la banda HF redefinida va ser capaç de discriminar entre: la relaxació i l'alegria i la por, l'alegria i cada emoció de valència negativa i finalment entre la por i la tristesa i la ira, tots amb un nivell de significació estadística (p-value ≤ 0.05, AUC ≥ 0.70). A més, els paràmetres derivats de l'AMIF i la CMIF van permetre caracteritzar la baixa complexitat del senyal presentada durant la por davant de qualsevol dels estats emocionals estudiats.

Finalment s'investiga, mitjançant un classificador lineal, les característiques lineals i no lineals que discriminen entre parells d'emocions i entre valències emocionals per determinar quins paràmetres permeten diferenciar els grups i quants d'aquests són necessaris per aconseguir la millor classificació possible. Els resultats extrets d'aquest capítol suggereixen que es poden classificar mitjançant l'anàlisi de la HRV: la relaxació i l'alegria, la valència positiva i totes les valències negatives, l'alegria i la por, l'alegria i la tristesa, l'alegria i la ira, i la por i la tristesa.

L'anàlisi conjunta de la HRV i la respiració augmenta la capacitat discriminatòria de la HRV, sent la màxima correlació entre els espectres de la HRV i la respiració un dels millors índexs per a la discriminació d'emocions. L'anàlisi de la informació mútua, fins i tot en senyals de curta durada, afegeix informació rellevant als índexs lineals per a la discriminació d'emocions.

Contents

List of Figures

List of Tables

Chapter 1

Introduction

Contents

1.1 Motivation

Emotions are an essential part of human existence because they determine the quality of our lives. These represent the evaluation of what happens in our life, but in some people, the affections are disconnected from reality. They have feelings of extreme euphoria (mania) or of desperation (depression) [19, 34]. Depression, according to the World Health Organization[1], is the world's leading cause of disability and contributes very significantly to the global burden of disease affecting 350 million people worldwide.

The emotional responses are formed by behaviors to face specific situations and by physiological responses, both neurovegetative and hormonal, that support these behaviors. The emotional reactions of people to aversive stimuli can harm their health. For example, the stress response, which Cannon called a fight or flight response [18], is useful as a short-term reaction to threatening stimuli, but in the long terms it is detrimental. The autonomic nervous system (ANS) exerts an antagonistic regulation in the organs and target tissues, thanks to the action of its two branches, one sympathetic and the other parasympathetic. Therefore, the stress response includes an increase in the activity of the sympathetic branch of the neurovegetative system and an increase in the secretion of hormones from the adrenal gland: adrenaline, noradrenaline and glucocorticoids. Prolonged exposure to high levels of these hormones can raise blood pressure (BP), damage muscle tissue, lead to infertility, slow growth, inhibit the inflammatory response and depress the activity of the immune system [19, 29].

The organs of the immune system are also terminal organs of direct autonomic innervation [36, 90], especially of the sympathetic nervous system [35]. The sympathetic denervation of the immune organs results in an increase in susceptibility to infectious and inflammatory diseases [90]. And on the other hand, there is a circuit of the nervous system composed of the limbic cortex, the limbic regions of the forebrain, the hypothalamus and the autonomous nuclei of the brainstem, which

[1] http://www.who.int/

regulates autonomic and neuroendocrine flow and, thereby, contributes to modulate the immune system [36]. In addition, specifically the cortical areas and the limbic system of the forebrain mediate the affective and cognitive processes and, consequently, may be involved in the response to stressors, in states and affective disorders [51], and in aversive conditioning [36].

In addition, both the sympathetic and parasympathetic branches innervate the heart, specifically in the sinoatrial node (SA node), which allows the corresponding neurotransmitters to modulate their activity. The different emotional states cause a reaction in the ANS, which is reflected in the heart rhythm, due to this neuromodulation. Sympathetic hyperactivity, observed in response to sexual or combative nature can cause extra systole or tachycardia. Parasympathetic hyperactivity, observed in responses to aversive emotions, usually olfactory or visual origin, can cause bradycardia or cardiac arrest [29, 95].

Therefore, emotional disorders are the result of the interaction between multiple factors, which depend both on the individual′s environment and the individual′s characteristics such as genetic, endocrine, nervous, immunological, emotional, cognitive and behavioral characteristics, gender, life experiences and psychosocial factors such as personal support and the perception of control. In addition, stressful situations processed by the interpretative belief system, typical of each individual, can generate negative feelings of fear, anger, depression, helplessness and hopelessness. These attitudes and emotions activate biochemical mechanisms, at the level of the hypothalamus, pituitary gland and adrenal glands, which tend to depress and/or suppress the immune response, which makes possible the development of diverse pathological processes [35, 51, 95].

Developing a tool which identifies human emotions may have a potential value in several fields. First, in the clinical practice, it may have value to reduce the diagnostic time of a psycho-neural illness, and, subsequently, it could directly represent a beneficial economic impact for the health system. Secondly, it can improve on the human-machine interaction since it could provide knowledge regarding the affective state of a user, bringing the machine closer to the human by including emotional content in the communication [22].

Several strategies have been proposed for emotion recognition by means of non-invasive techniques that allow registering biosignals as electroencephalography (EEG) [22,54,57,65,80,89], galvanic skin response (GSR) [82,91], skin temperature variation (ST), electrodermal activity [53] and electrocardiography (ECG) [9,47,83,106], among others.

Among all the techniques mentioned, this work has been focused on emotion recognition by means of heart rate variability (HRV) analysis extracted from the ECG, because, as explained above, emotional stimuli cause an action on the hypothalamus-pituitary-adrenal axis, which has an effect on the ANS, in both branches, sympathetic and parasympathetic, and subsequently ANS has a field of action on the heart. The spectral analysis of HRV is considered a non-invasive technique for evaluating the relationship between these two main branches of ANS and has been proposed for the recognition of human emotions in previous studies [22, 83].

The influence of ANS in the high frequency (HF) band is mainly due to respiratory sinus arrhythmia (RSA). Therefore, HRV is influenced by respiration and not taking it into account can lead to a misunderstanding of the results, as some works have already pointed out [5, 7, 8, 42].

One of the methodologies developed in this thesis will attempt to overcome such limitations. Therefore, an estimation of the spectral bands particularized for each subject will be taken into account, which will avoid the subjectivity of selection of the width of the HF band that depends to a great extent on considerations such as the age and physiological conditions of each person. This methodology will be developed based on algorithms of linear analysis of the signal.

In addition, within the framework of this thesis it is intended to expand the study of linear analysis with techniques based on the analysis of non-linear dynamics, in order to study the complexity of the related cardiac signals. The study of the non-linear dynamics of these signals can provide very meaningful information on the characterization of the ANS [53, 88, 105]. The most important limitation presented by these techniques is that they need a sufficient signal length to be applied [53]. Therefore, it will be necessary to adapt the algorithms developed to be robust methods of analyzing short-term signals.

1.2 Work hypothesis

The starting hypotheses of this research work are listed below:

First work hypothesis: ***emotions cause alterations on the autonomic nervous system.***

The effects of ANS on the heart are mediated through hypothalamic communications with spinal cardiovascular centers. This explains why cardiovascular responses are usually connected with some emotional responses, because an emotional stimulus regulates the activation and inhibition of communication between the hypothalamus, the pituitary and other peripheral glands. Therefore, the hormonal release of these glands has a direct effect on the heart. For example, the cardiovascular reaction to a stressful event is to increase BP, caused by an increase in the activity of the sympathetic system, a decrease in parasympathetic activity and the secretion of hormones from the adrenal gland: adrenaline, noradrenaline and glucocorticoids [10, 19, 70].

Second work hypothesis: ***the alterations that cause the emotions on the ANS can be measured by means of analysis of physiological signals.***

An objective and non-invasive measurement of the ANS is done by studying the variability of the heart rhythm by processing the HRV signal which allows the balance between the sympathetic and the parasympathetic system of the measured subject to be obtained [93] and therefore the emotional response. Many studies have been published showing the existing changes in HRV during different emotional states [102, 105], however, there are some limitations in the methods currently used. Within this thesis, several robust methods are proposed, both in the linear and non-linear analysis for the characterization of the response of the ANS to emotional stimuli, which take into account the limitations of the HRV analysis, such as changes in heart rate, and a respiratory rate outside the classic range, among others.

Third work hypothesis: ***the inclusion of respiratory information improves HRV ability to discriminate emotions.***

The combination of information from different physiological signals, such as HRV and respiration (RSP), improves the characterization of the ANS for the discrimination of emotions as suggested in [47].

1.3 Physiological aspects

1.3.1 The autonomic nervous system

The autonomic nervous system is the component of the peripheral nervous system that controls cardiac muscle contraction, visceral activities, and glandular functions of the body. Specifically the ANS can regulate heart rate, BP, rate of respiration, body temperature, sweating, gastrointestinal motility and secretion, as well as other visceral activities that maintain homeostasis [15, 45, 61, 85]. The ANS functions continuously without conscious effort. The ANS, however, is controlled by centers located in the spinal cord, brain stem, and hypothalamus [41].

The ANS is composed of a sympathetic division and a parasympathetic division (Fig. 1.1). The sympathetic nervous system is named for acting in sympathy with emotions. In combination with anger or fear, the sympathetic nervous system prepares the body for fight or flight. It produces the heart rate increases, the pupils dilate, the skin sweats, the blood is directed from the skin and the intestinal tube to the skeletal muscles and the sphincters of the digestive tract and the urinary system are closed. The parasympathetic nervous system usually counteracts the effect of the sympathetic nervous system. It adapts the eyes to the near vision, slows down the heart, favors the secretion of saliva and intestinal secretions and accelerates intestinal peristalsis [95].

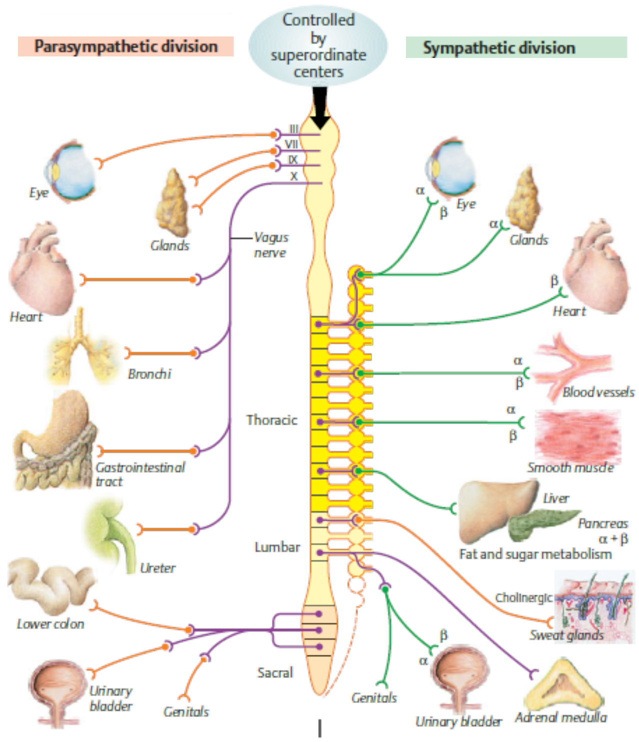

Figure 1.1: Schematic view of the autonomic nervous system composed of a sympathetic division and a parasympathetic division (From [29]).

Messages from sympathetic and parasympathetic nervous systems are conveyed as electrical impulses that travel along axons and cross synaptic clefts using chemical neurotransmitters. Both sympathetic and parasympathetic pathways are composed of a preganglionic neuron and a postganglionic neuron. The neurotransmitter between the preganglionic and postganglionic neurons is norepinephrine for the sympathetic nervous system, while the parasympathetic nervous system releases acetylcholine [41].

In the sympathetic system (thoracolumbar division), these nerves originate from the thoracolumbar region of the spinal cord (T1-L2) and radiate out towards the target organs. In contrast, the nerves of the parasympathetic system originate within the midbrain, pons and medulla oblongata of the brain stem and part of these fibers originate in the sacral region (S2-S4 sacral spinal nerves) of the spinal cord. While sympathetic nerves utilize a short preganglionic neuron followed by a relatively long postganglionic neuron, parasympathetic nerves (e.g., the vagus nerve, which carries about 75 percent of all parasympathetic fibers) have a much longer pregan-

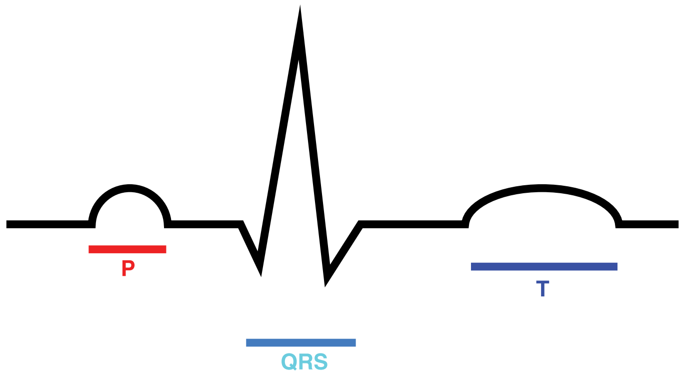

Figure 1.2: Schematic view of a normal electrocardiogram: P = P wave, QRS = QRS complex and T = T wave.

glionic neuron, followed by a short postganglionic neuron [41].

1.3.2 The autonomic nervous system control of the heart

The heart is divided into four chambers: upper left and right atria; and lower left and right ventricles. It serves as the pump that moves blood through blood vessels thereby providing the needed oxygen and nutrients to the body. To achieve this goal, the heart must beat with a rhythm determined by a group of pacemaking cells in the SA node located in the right atrium. These cardiac cells generate action potentials that causes contraction of the heart, traveling through the atrioventricular node and along the conduction system of the heart [41].

The electrical activity in the heart is coordinated by the intrinsic conduction system which can be seen on an ECG [41].

Under normal conditions, the P wave of a ECG recording reflects atrial depolarization followed by atrial contraction. The QRS wave reflects ventricular depolarization followed by ventricular contraction and the T wave reflects ventricular repolarization and ventricular relaxation (Fig. 1.2) [41].

In the absence of extrinsic neural or hormonal influences, the SA node pacing rate would be about 100 beats per minute. The heart rate and cardiac output, however, must vary in response to the needs of the bodys cells for oxygen and nutrients under varying conditions. In order to respond rapidly to changing requirements of the bodys tissues, the heart rate and contractility are regulated by the autonomic nervous system, hormones, and other factors [41].

The regulation of the heart by the ANS is accomplished by control centers in the medulla that receive descending input from higher neural areas in the brain and afferent input from mechanically and chemically sensitive receptors located throughout the body [68]. The principal mechanisms in the brain that regulate the cardiovascular system are: 1) feedforward regulation, often referred to as central command, and 2) feedback or reflex regulation. These cardiovascular regulatory mechanisms are closely coordinated with respiratory and other regulatory mechanisms to maintain homeostasis [26].

The SA node responds clearly to emotional states. Sympathetic hyperactivity, in response to emotions of rapprochement of a sexual or combative nature, can cause the heart to lose a beat (extrasystole) or the pulse run (tachycardia). Parasympathetic hyperactivity in response to aversive emotions is usually of olfactory or visual origin, can cause bradycardia, or even cardiac arrest [95].

During rest, sleep, or emotional tranquility, the parasympathetic nervous system predominates and controls the heart rate at a resting rate of 60-75 beats per minute (bpm). At any given time, the effect of the ANS on the heart is the net balance between the opposing actions of the sympathetic and parasympathetic systems [41].

1.3.3 Heart rate variability

Heart rate variability describes variations in consecutive cardiac cycles. Other terms have been used in the literature, for example cycle length variability, heart period variability, RR variability where R is the main positive deflection of the QRS complex of the ECG wave, and RR interval tachogram [93]. In Fig. 1.3, 10 seconds of an ECG are shown with its corresponding RR time series. HRV exhibit temporal fluctuations, as shown in Fig. 1.3, which are synchronized with respiration, increa-

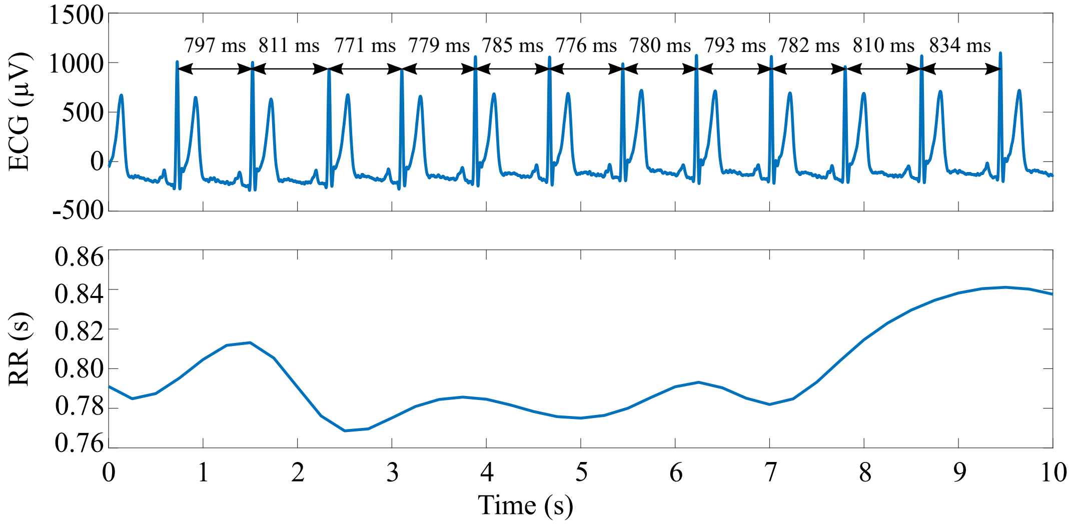

Figure 1.3: Ten seconds of an (a) electrocardiogram (ECG) - Lead I with the time duration of all RR intervals, and (b) its corresponding RR time series interpolated to 4 Hz.

sing during inspiration and decreasing during expiration. This phenomenon called RSA reflects the changes in cardiac autonomic regulation [11].

The HRV analysis provides a tool for the evaluation of cardiac autonomic changes in patients. In fact, reduced HRV is associated with a variety of cardiovascular risk factors and disease states including diabetes, smoking, obesity, work stress, hypertension and heart failure [11].

Many techniques have been proposed to quantify the HRV in order to provide indices of cardiac autonomic regulation in both health and disease. Most of them were included in the Task Force of 1996 [87, 93]. There are two primary approaches for the analysis of HRV: linear and non-linear methods [11]. The linear methods are divided in the time domain and frequency domain methods, and they are reported in Table 1.1, and Table 1.2, respectively. And the most used non-linear methods applied to HRV series are reported in Table 1.3.

The time domain measures, reported in Table 1.1, are easier to calculate but less useful than the frequency domain approaches in identifying specific components of this variability [11]. Regarding the frequency domain measures, three main peaks are often identified for shorter duration recordings (2-5 min): a very low frequency component (VLF) in the range between 0 Hz and 0.04 Hz, a low frequency component

(LF) between 0.04 Hz and 0.15 Hz, and a high frequency component (HF) between 0.15 Hz and 0.4 Hz [93]. A fourth peak, ultra low frequency (ULF) ($f \in$[0.03-0.04] Hz) appears during longer recording periods (24 h).

The sympathetic modulation of cardiac activity is encompassed in LF band and the parasympathetic activity affects both LF and HF band power [93]. The ratio of LF to HF (LF/HF) has been used as an index of the sympathetic/parasympathetic balance. However, this concept has been challenged as there is considerable controversy concerning the relationship between these frequency components and a particular division of the autonomic nervous system [11].

As was previously mentioned, non-linear dynamic analysis approaches have also been used to evaluate HRV: dominant Lyapunov exponent, detrended fluctuation analysis, approximate entropy, quadratic coupling, auto-mutual information function or cross mutual information function [1, 48, 49, 101–105].

1.3.4 Physiology of emotions

Paul Ekman described in 1992 a theory about the six basic emotions as anger, disgust, fear, happiness, sadness and surprise [33]. These 6 basic emotions were discretely categorized because several theories believes they are distinguishable by biological processes and an individuals facial expression [25].

Emotions activate biochemical mechanisms at the level of the hypothalamus, pituitary, and other peripheral glands. These tend to restore or suppress the immune and endocrine responses, making the development of diverse pathological processes possible [40].

Transient behavior of the cardiovascular function is often linked with some emotional responses. In particular, heart rate is profoundly influenced by neural inputs from sympathetic and parasympathetic divisions of the ANS, which allows the modification of cardiac function to meet the changing homeostatic needs of the body [70]. For example, cardiovascular reaction to a perceived stress situation creates an increase in BP as a consequence of a general increase in cardiovascular sym-

Table 1.1: Time-domain measures of HRV, from [93].

Variable (Units)	Description
SDNN (ms)	SD of all NN.
SDANN (ms)	SD of the averages of NN in all 5 min segments of the entire recording.
RMSSD (ms)	The square root of the mean of the sum of the squares of differences between adjacent NN.
SDNN index (ms)	Mean of the SD of all NN for all 5 min segments of the entire recording.
SDSD (ms)	SD of differences between adjacent NN.
NN50 count	Number of pairs of adjacent NN differing by more than 50 ms in the entire recording.
pNN50 (%)	NN50 count divided by the total number of all NN.
HRV triangular index	Total number of all NN divided by the height of the histogram of all NN measured on a discrete scale with bins of 7.8125 ms (1/128 s).
TINN (ms)	Baseline width of the minimum square difference triangular interpolation of the highest peak of the histogram of all NN.
Differential index (ms)	Difference between the widths of the histogram of differences between adjacent NN measured at selected heights.
Logarithmic index	Coefficient ø of the negative exponential curve $ke^{-øt}$ which is the best approximation of the histogram of absolute differences between adjacent NN.

NN = NN intervals corresponding to heart period during sinus rhythm.

SD = Standard deviation.

Table 1.2: Frequency-domain measures of HRV, from [93].

Variable (Units)	Description
power (ms^2)	The variance of NN over 5 minutes.
VLF (ms^2)	Power in very low frequency range ($f \leqslant 0.04$ Hz).
LF (ms^2)	Power in low frequency range ($f \in$[0.04-0.15] Hz).
LF norm (n.u.)	Low frequency power in normalized units (LF/(LF+HF)x100).
HF (ms^2)	Power in high frequency range ($f \in$[0.15-0.40] Hz).
HF norm (n.u.)	High frequency power in normalized units (HF/(LF+HF)x100).
LF/HF	Ratio LF(ms^2)/HF(ms^2).

Table 1.3: Bibliographic summary of non-linear techniques applied to HRV series.

Technique	Description
DLEs	Dominant Lyapunov Exponents
ApEn	Approximate Entropy
SEn	Sample Entropy
FMEn	Fuzzy Measure Entropy
CSEn	Cross Sample Entropy
CFMEn	Cross Fuzzy Measure Entropy
PE	Permutation Entropy
PME	Permutation Min-Entropy
PD2	Pointwise Correlation Dimension
DFA	Detrended Fluctuation Analysis
LLP	Lagged Poincaré Plot
AMIF	Auto-Mutual Information Function
CMIF	Cross-Mutual Information Function

pathetic nerve activity and a decrease in parasympathetic activity [3, 10, 70]. When adrenergic sympathetic fibers activate, they release noradrenaline on cardiac cells, increasing the heart rate. When cholinergic parasympathic nerve fibers activate, they release acetylcholine on cardiac muscle cells and the heart rate decelerates [95]. Sympathetic and parasympathetic activation work to increase and decrease cardiac pumping, respectively [29]. Usually, an increment in parasympathetic nerve activity is accompanied by a reduction in sympathetic nerve activity, and vice versa.

1.3.5 Heart rate variability and emotions

Several strategies have been proposed for recognition of emotional states assessed by means of HRV spectral analysis [14, 23, 28, 39, 67, 83, 84]. As well, non-linear techniques such as the Dominant Lyapunov Exponents, the Detrended Fluctuation Analysis, the Approximate Entropy, the Sample Entropy, the Fuzzy Measure Entropy, the Cross Sample Entropy, the Cross Fuzzy Measure Entropy, the Permutation Entropy, Permutation Min-Entropy, the Pointwise Correlation Dimension, the Lagged Poincaré Plot or the Quadratic Coupling have been applied to HRV signals to detect emotional stimuli [12, 30, 43, 101–105, 109, 111]. Some of these techniques have also been used to study non-linear relationships between HRV and RSP signals [55, 103–105, 111].

Hernando, A., published that the HRV analysis methods are a suitable technique for the evaluation of stress [47], as long as respiratory information is taken into account. Rantanen, A., et al. [84] shows the evidence that the elicitation of the negative valence increases sympathovagal activity in women and Quintana, D. S., et al. [83] suggests that the increase in HRV may provide a new marker for recognizing emotions in humans.

On the other hand, Nyguyen, V.T., et al. [72], found that cardiac activity is represented in the center of the posterior insula and demonstrated the perception of internal physiological processing states during the natural emotional experience providing an ecologically valid framework to elucidate the neuronal bases of emotional deficits in the neuropsychiatric disorders.

Several studies have revealed that patients with anxiety and phobias exhibit a low HRV. Therefore, a low HRV has been linked to psychological problems [14, 16, 31, 37, 38, 66, 69]. In addition, subjects with post-traumatic stress disorder consistently show a lower HRV [23, 24, 92]. Similarly to these studies, others researchers also suggest a connection between a low HRV and depression [20,21,52]. It is important to note that the relationship of a low HRV between anxiety, phobias, stress and depression exists independently of age, gender, cardiorespiratory capacity, heart rate, BP and respiratory rate [31].

Most of these studies do not take into account the joint analysis of heart rate variability and respiration particularized for each subject, which might be important to discriminate emotions since emotional characterization strongly depends on individual considerations such as age and physiological conditions. In this PhD thesis, human emotion recognition is proposed based on linear and non-linear methodologies which address current limitations by characterizing the relationship between HRV and respiration for each specific subject to avoid subjectivity in emotion identification.

1.4 Objectives and outline of the thesis

The objective of this thesis is to develop a methodology that allows the characterization of emotional responses based on the study of HRV. This methodology will take into account some of the current limitations of HRV analysis to characterize emotional responses, considering both linear and non-linear HRV analysis parameters and including information of respiration. For spectral indices, an estimation of the spectral bands particularized for each subject will be proposed. Regarding non-linear parameters, this work is focused on the definition of robust and complexity measurements in short time series also taking into account respiratory information.

This general objective can be subdivided into:

In chapter 3: it is proposed the joint analysis of HRV and RSP based on the spectral correlation of the high frequency band to improve human emotion characterization.

This methodology is based on the automatic detection of spectral limits, particularized for each subject, to take into account that the bandwidth of the HF band is different for each subject and condition depending on the breathing pattern. Therefore, HF band will be defined based on the maximum spectral correlation between HRV and RSP. The maximum spectral correlation itself is proposed as an index to identify emotions. The hypothesis is that this index, characterizing the relationship between RSP and HRV, can add relevant information to HRV analysis to describe human emotions.

First, a simulation study is designed to evaluate the ability of the proposed HF band to quantify RSA. The performance of the proposed HF band will be compared to other commonly used HF band definitions. Then, the ability of the proposed indices to characterize human emotions will be tested on a database of video-induced emotions.

The work presented in this chapter has been published in:

- Valderas, M.T., Bolea, J., Laguna, P., Vallverdú, M. and Bailón, R., Human emotion recognition using heart rate variability analysis with spectral bands based on respiration, *37th International Conference on IEEE EMBS International Conference on Engineering in Medicine and Biology Society*, 2015, 6674-6677, DOI: 10.1109/EMBC.2015.7319792.

- Valderas, M.T., Bolea, J., Orini, M., Laguna, P., Orrite, C., Vallverdú, M. and Bailón, R., Human emotion characterization by heart rate variability analysis guided by respiration, *IEEE Journal of Biomedical and Health Informatics*, 2019, DOI: 10.1109/JBHI.2019.2895589.

In chapter 4: it is proposed to use non-linear techniques for HRV analysis because it has been demonstrated that it is a complementary tool of HRV analysis based on linear statistics for ANS analysis [49].

In the present work, both non-linear Auto-Mutual Information Function (AMIF) and Cross-Mutual Information Function (CMIF) techniques are proposed for human emotion recognition. On the one hand, the AMIF technique is applied to HRV signals to study complex communication within the ANS, and on the other hand the CMIF technique is considered to quantify the complex coupling between HRV and respiratory signals.

Both algorithms will be adapted to short term time series and applied to the redefined HF band described in chapter 3, as well as to classic LF and HF bands. Both AMIF and CMIF algorithms will be calculated on these spectral bands with regard to different time scales as specific complexity measures. The ability of the parameters derived from the AMIF and the CMIF to discriminate emotions will be evaluated on a database of video-induced emotion elicitation.

The work presented in this chapter has been published in:

- Valderas, M.T., Bolea, J., Laguna, P., Bailón, R. and Vallverdú, M., Mutual information between heart rate variability and respiration for emotion characterization, *Physiological Measurement*, Volume 40, Number 8, 2019, DOI: 10.1088/1361-6579/ab310a.

In chapter 5: it is proposed to use a linear classifier to identify the linear and non-linear characteristics that discriminate between pairs of emotions and between emotional valences to determine which parameters allow differentiating between the groups and how many of them are necessary to achieve the best classification.

Chapter 2

Materials

Contents

2.1 Registered signals

A database of 25 volunteers was recorded at the University of Zaragoza during an induced emotion experiment. It contains the simultaneous recording of ECG and RSP, BP, ST and GSR signals acquired with a MP100 BIOPAC device. The signals used were: the limb ECG leads (I, II and III) which were sampled at 1 kHz and the respiratory signal, *r(t)*, at 125 Hz (Fig. 2.1).

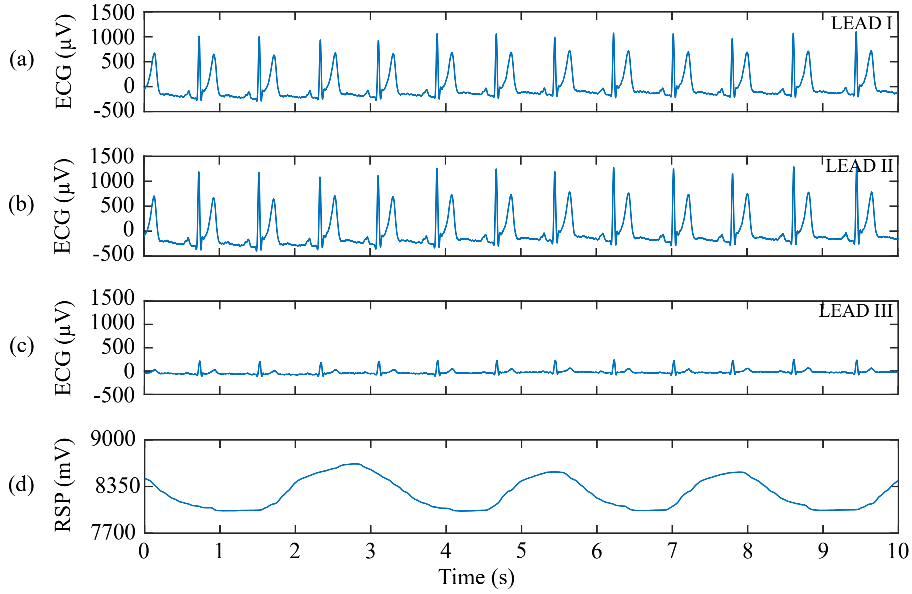

Figure 2.1: Ten seconds of the simultaneous recorded signals: (a) ECG Lead I, (b) ECG Lead II, (c) ECG Lead III, and (d) RSP.

The distribution of the subjects was: four men and five women for the age range 18 to 35 years, four men and four women for the age range 36 to 50 years and four men and four women over 50 years. All subjects were University students or employees with an estimated BMI of 22.9 kg/m^2. Previous to the inclusion in the study, the adequacy of each subject was evaluated with a General Health Questionnaire.

2.2 Registered emotions

The experiment consisted on eliciting each subject by four emotions (joy, fear, anger and sadness) using videos (two videos per emotion). Despite the classification described by Paul Ekman consisted in six basic emotions, disgust and surprise were discarded because the psychologists involved in the study decided these two emotions were specific reactions rather than prolonged moods.

All the experiment extended over 2 consecutive days and two sessions were recorded each day. The experiment was split into two days, with the aim to have more than one sample per day for each emotion; therefore the recording is more representative of the emotion and not particularly biased for the specific mood of the day that was recorded. During sessions 1 and 4, the subject was stimulated with videos of joy (J) and fear (F), and during sessions 2 and 3 with videos of anger (A) and sadness (S). Therefore, each of the 25 subjects was elicited with 2 videos of the same emotion, resulting in a total of 50 recordings per emotion. All videos were presented in randomized order.

To ensure that the physiological parameters returned to the baseline condition, each video was preceded and followed by a relaxing video considered as baseline, which were excerpts from nature images with classical music. All sessions were recorded at the same time of the day and the order of the participant was maintained during all sessions to mitigate the circadian variations of HRV parameters. A schema of the organization of the video-induced emotion sessions is represented in Fig. 2.2.

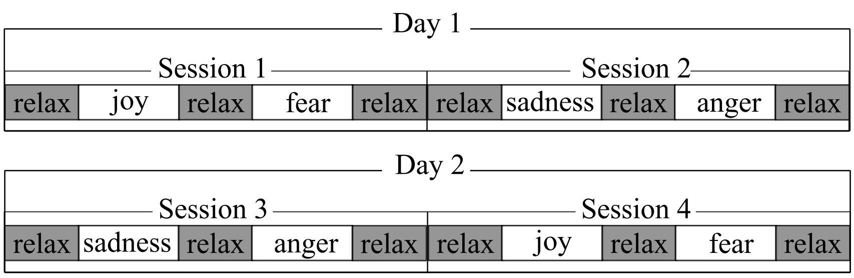

Figure 2.2: Scheme of the organization of the video-induced emotion sessions. Session 1 and 2 were recorded the first day, and session 3 and 4 were recorded the second day. In session 1 and 4, the subject was stimulated with videos of joy and fear, and with videos of sadness and anger in session 2 and 3. All videos were presented in randomized order.

The contents of the videos were: the joy videos were excerpts from laughing monologues; the fear videos were excerpts from scary movies, like Alien and Misery;

Table 2.1: Specific time segments studied for each video: total video length, time range and video length studied. The unit time are expressed in hh:mm:ss.

	Video	Total video length	Time range studied	Video length studied
Session 1	Relax	00:06:46	[00:01:00-00:06:00]	00:05:00
	Joy	00:10:36	[00:02:00-00:07:00]	00:05:00
	Fear	00:02:47	[00:00:00-00:02:45]	00:02:45
Session 2	Relax	00:06:51	[00:01:00-00:06:00]	00:05:00
	Sadness	00:07:25	[00:01:00-00:06:00]	00:05:00
	Anger	00:09:18	[00:01:00-00:06:00]	00:05:00
Session 3	Relax	00:06:35	[00:01:00-00:06:00]	00:05:00
	Sadness	00:07:07	[00:01:00-00:06:00]	00:05:00
	Anger	00:06:29	[00:01:00-00:06:00]	00:05:00
Session 4	Relax	00:07:36	[00:01:00-00:06:00]	00:05:00
	Joy	00:06:13	[00:01:00-00:06:00]	00:05:00
	Fear	00:09:42	[00:04:00-00:09:00]	00:05:00

the sadness videos were an excerpt from the film The Passion of the Christ and a documentary film about history wars; the anger videos were an excerpt of the documentary film of the Columbine High School massacre in 1999 and a documentary about domestic violence; and the relax videos were excerpts from nature images with classical music.

Although each video had a different length, five minutes long were studied for all videos, except one of the videos corresponding to emotion fear, which lasted three minutes. In Table 2.1 the total video length for each emotion, the time range evaluated and the resulting video length studied are specified. The selected time range was defined by means of analyzing all recordings one by one and avoiding those segments which contain noise or part of the signal was distorted. Regarding to the analysis of the relax, only the first relax of each session was analyzed as a basal condition during all the session.

Institutional Ethical Review Boards approved all experimental procedures involving human beings, and subjects gave their written consent. The experiments were conducted following the protocol approved by the Aragón Research Agency under contract: #PM055, 2005.

Table 2.2: PANAS-X scale with the 60-item scale of different feelings and emotions.

PANAS-X SCALE		
I1: Cheerful	I21: Shaky	I41: Lively
I2: Disgusted	I22: Happy	I42: Ashamed
I3: Attentive	I23: Timid	I43: At ease
I4: Bashful	I24: Alone	I44: Scared
I5: Sluggish	I25: Alert	I45: Drowsy
I6: Daring	I26: Upset	I46: Angry at self
I7: Surprised	I27: Angry	I47: Enthusiastic
I8: Strong	I28: Bold	I48: Downhearted
I9: Scornful	I29: Blue	I49: Sheepish
I10: Relaxed	I30: Shy	I50: Distressed
I11: Irritable	I31: Active	I51: Blameworthy
I12: Delighted	I32: Guilty	I52: Determined
I13: Inspired	I33: Joyful	I53: Frightened
I14: Fearless	I34: Nervous	I54: Astonished
I15: Disgusted with self	I35: Lonely	I55: Interested
I16: Sad	I36: Sleepy	I56: Loathing
I17: Calm	I37: Excited	I57: Confident
I18: Afraid	I38: Hostile	I58: Energetic
I19: Tired	I39: Proud	I59: Concentrating
I20: Amazed	I40: Jittery	I60: Dissatisfied with self

2.3 Emotion database validation

The emotion database has been validated by 16 subjects, different from the ones participating in the database, using the Positive and Negative Affect Schedule - Expanded Form (PANAS-X) [108]. To assess specific emotional states, a 60-item scale of different feelings and emotions was used as shown in Table 2.2. Each subject watched each video, and right after each display the person marked from 1 to 5 each item (I) with the appropriate answer indicating to what extent he or she felt, being 1 = very slightly, 2 = a little, 3 = moderately, 4 = quite a bit and 5 extremely.

Based on the sum of subject responses of specific items of the PANAS-X scale, the following affect scales can be computed: fear scale (S_{fear}) (Eq. 2.1), sadness scale ($S_{sadness}$) (Eq. 2.2), guilt scale (S_{guilt}) (Eq. 2.3), hostility scale ($S_{hostility}$) (Eq. 2.4), shyness scale ($S_{shyness}$) (Eq. 2.5), fatigue scale ($S_{fatigue}$) (Eq. 2.6), surprise scale ($S_{surprise}$) (Eq. 2.7), joviality scale ($S_{joviality}$) (Eq. 2.8), self-assurance scale ($S_{self-assurance}$) (Eq. 2.9), attentiveness scale ($S_{attentiveness}$) (Eq. 2.10) and serenity scale ($S_{serenity}$) (Eq. 2.11).

$$S_{fear} = I18 + I44 + I53 + I34 + I40 + I21 \tag{2.1}$$

$$S_{sadness} = I16 + I29 + I48 + I24 + I35 \tag{2.2}$$

$$S_{guilt} = I32 + I42 + I51 + I46 + I15 + I60 \tag{2.3}$$

$$S_{hostility} = I37 + I38 + I11 + I9 + I2 + I56 \tag{2.4}$$

$$S_{shyness} = I30 + I4 + I49 + I23 \tag{2.5}$$

$$S_{fatigue} = I36 + I19 + I5 + I45 \tag{2.6}$$

$$S_{surprise} = I20 + I7 + I54 \tag{2.7}$$

$$S_{joviality} = I22 + I33 + I12 + I1 + I37 + I47 + I41 + I58 \tag{2.8}$$

$$S_{self-assurance} = I39 + I3 + I57 + I28 + I6 + I14 \tag{2.9}$$

$$S_{attentiveness} = I25 + I3 + I59 + I52 \tag{2.10}$$

$$S_{serenity} = I17 + I10 + I43 \tag{2.11}$$

Then, a Basic Negative Emotion (BNE) scale is defined as the average of $S_{sadness}$, S_{guilt}, $S_{hostility}$ and S_{fear} (Eq. 2.12), and a Basic Positive Emotion (BPE) scale as the average of $S_{joviality}$, $S_{self-assurance}$ and $S_{attentiveness}$ (Eq. 2.13). In this work it is studied the BPE, BNE, $S_{joviality}$, S_{fear}, $S_{sadness}$ and $S_{hostility}$.

$$BNE = (S_{sadness} + S_{guilt} + S_{hostility} + S_{fear})/4 \tag{2.12}$$

$$BPE = (S_{joviality} + S_{self-assurance} + S_{attentiveness})/3 \tag{2.13}$$

Statistical analysis was done by T-test or Wilcoxon-test when necessary, depending on normality test results to evaluate differences for all followed paired conditions: relax vs. joy (R-J), relax vs. fear (R-F), relax vs. sadness (R-S), relax vs. anger (R-A), joy vs. fear (J-F), joy vs. sadness (J-S), joy vs. anger (J-A), fear vs. sadness (F-S), fear vs. anger (F-A) and sadness vs. anger (S-A).

The significant statistical level was p-value ≤ 0.05, that provides a reliable value for statistical discrimination [86].

In Table 2.3, the mean and standard deviation ($\mu \pm \sigma$) of the scales evaluated for each emotion are shown. It could be observed that the highest mean value of BPE scale corresponds to the emotion with positive valence (joy), while mean value of BNE was higher for emotions with negative valence (fear, sadness and anger). In addition, the affect scale with highest value in joy is $S_{joviality}$ and the highest value in fear emotion is S_{fear}. However, there is not a single affect scale for sadness and anger that defines each emotion, resulting in high values for the S_{fear}, $S_{sadness}$ and $S_{hostility}$.

Table 2.4 displays the p-values obtained in the comparison of PANAS-X scales between different emotions. All affect scales showed statistically significant differen-

Table 2.3: Mean and standard deviation ($\mu \pm \sigma$) of the PANAS-X scales: Basic Positive Emotion (BPE), Basic Negative Emotion (BNE), $S_{joviality}$, S_{fear}, $S_{sadness}$ and $S_{hostility}$.

	Emotions			
Scales	Joy	Fear	Sadness	Anger
BPE	13.1±4.8	8.1±1.7	7.4±1.5	7.8±2.2
BNE	6.5±0.8	12.2±3.9	14.3±4.4	12.8±3.8
$S_{joviality}$	22.3±8.6	9.0±2.4	8.4±0.8	8.8±1.6
S_{fear}	6.4±1.1	19.0±6.6	14.8±5.3	13.8±5.9
$S_{sadness}$	5.2±0.6	8.7±4.6	14.8±5.5	11.7±4.5
$S_{hostility}$	8.1±1.7	14.3±5.3	15.7±5.4	15.8±4.8

Table 2.4: p-values of the PANAS-X scales: Basic Positive Emotion (BPE), Basic Negative Emotion (BNE), $S_{joviality}$, S_{fear}, $S_{sadness}$ and $S_{hostility}$ for the pair of emotional conditions induced by videos: joy vs. fear (J-F), joy vs. sadness (J-S), joy vs. anger (J-A), fear vs. sadness (F-S), fear vs. anger (F-A) and sadness vs. anger (S-A).

	Emotions analyzed					
Scales	J−F	J−S	J−A	F−S	F−A	S−A
BPE	$p\leq 0.001$	$p\leq 0.001$	$p\leq 0.001$	0.011	0.043	n.s.
BNE	$p\leq 0.001$	$p\leq 0.001$	$p\leq 0.001$	0.005	n.s.	0.007
$S_{joviality}$	$p\leq 0.001$	$p\leq 0.001$	$p\leq 0.001$	n.s.	n.s.	n.s.
S_{fear}	$p\leq 0.001$	$p\leq 0.001$	$p\leq 0.001$	$p\leq 0.001$	$p\leq 0.001$	n.s.
$S_{sadness}$	$p\leq 0.001$	$p\leq 0.001$	$p\leq 0.001$	$p\leq 0.001$	0.002	$p\leq 0.001$
$S_{hostility}$	$p\leq 0.001$	$p\leq 0.001$	$p\leq 0.001$	n.s.	n.s.	n.s.

ces between positive valence and negative valence emotions (J-F, J-S, J-A). Affect scales showing largest statistically significant differences between negative valence emotions were: S_{fear} (F-S, F-A) and $S_{sadness}$ (F-S, S-A).

According to the analysis of the affect scales derived from the PANAS-X scale, shown in Table 2.3, it could be stated that: joy emotion presents the highest values for the BPE and $S_{joviality}$; all negative emotions presented lower BPE and higher BNE, as expected; fear emotion obtains the highest mean value for the affect scale S_{fear}; however, sadness and anger emotions have a high mean value for S_{fear}, $S_{sadness}$ and $S_{hostility}$.

As shown in Table 2.4, all PANAS-X affect scales were significantly different between joy and all negative valence emotions (fear, sadness, anger). Statistical differences between negative valence emotions were only found in a subset of PANAS-X affect scales, which might challenge their discrimination using physiological signals (Table 2.4).

Additionally, all subjects in this experiment reported an agreement between the theoretical positive valence of joy elicitation and the emotion felt, and fear, sadness and anger were identified as negative emotions. The duration of all videos is considered enough to induce an autonomic response, since those times are longer than the reported delay response to individuals who were exposed to emotions, at least when induced by musical stimulus [73].

Chapter 3

Linear Analysis Methodology

Contents

3.1 Introduction

Developing a tool which identifies human emotions may have a potential value in several fields. First, in the clinical practice, it may have value to reduce the diagnostic time of a psycho-neural illness, and, subsequently, it could directly represent a beneficial economic impact for the health system. Secondly, it can improve on the human-machine interaction since it could provide knowledge regarding the affective state of a user, bringing the machine closer to the human by including emotional content in the communication [22].

This work has been focused on emotion recognition by means of HRV analysis. In previous studies, recognition of emotional states assessed by means of HRV spectral analysis has been reported [14, 23, 28, 39, 67, 83, 84].

As mention before in chapter 1, HRV is influenced by respiration. Heart rate is increased during inspiration and reduced during expiration, phenomenon described as RSA. RSA has been used as an index of cardiac vagal or parasympathetic function, usually measured by the HF component of the HRV [110], while the LF component is affected by both sympathetic and parasympathetic activity. The necessity of redefining the HF band to be centered on the respiratory frequency (F_R) when F_R is above 0.40 Hz, has already been highlighted, as well as the misinterpretation of spectral HRV indices when respiratory frequency lies within the LF band [5].

Several studies have already used respiratory information to define the HF band. Most of them define the HF band centered at respiratory frequency and use a fixed bandwidth. Only a few of them use variable HF bandwidth dependent on respiration. In [8], respiratory frequency as well as its rate of variation were used to estimate HF power based on a parametric decomposition of the instantaneous autocorrelation function. In [96], an HF bandwidth dependent on respiration stability was used to analyze HRV in critically ill patients. Recently, spectral coherence between respiration and HRV has been used to define the HF band [27, 56].

Moreover, the relationship between respiration and HRV might be further exploited to add relevant information regarding ANS regulation. Interactions between respiration and HRV have been continuously assessed using time-varying spectral coherence, partial coherence and phase differences during orthostatic test and under selective autonomic blockade [74, 76]. Characterization of these interactions might be crucial in applications where both respiration and HRV are altered, such as during stress [47].

In this work, it is proposed the joint analysis of HRV and respiration to improve human emotion characterization. HF band is defined based on the maximum spectral correlation between HRV and respiration. Both the center and bandwidth of HF band depend on respiration. The maximum spectral correlation itself is proposed as an index to identify emotions. The hypothesis is that this index, characterizing the relationship between respiration and HRV, can add relevant information to HRV analysis to describe human emotions.

First, a simulation study is designed to evaluate the ability of the proposed HF band to quantify RSA. The performance of the proposed HF band is compared to other commonly used HF band definitions. Then, the ability of the proposed indices to characterize human emotions will be tested on a database of video-induced emotions.

3.2 Methods and materials

3.2.1 Signal preprocessing

Beat occurrence times were detected from the recorded ECG using a wavelet-based detector [63]. Instantaneous heart rate $(d_{HR}(t))$ was estimated from the beat occurrence times based on the integral pulse frequency modulation (IPFM) model, which takes into account the presence of ectopic beats [64]. A time-varying mean heart rate $(d_{HRM}(t))$ was computed by low pass filtering (cut-off frequency 0.03 Hz) $d_{HR}(t)$, and then the HRV was obtained as $d_{HRV}(t) = d_{HR}(t) - d_{HRM}(t)$. The modulating signal, *m(t)*, which is assumed to carry the ANS information according to the IPFM model [6], was estimated as *m(t)* = $(d_{HR}(t) - d_{HRM}(t))/\overline{d_{HRM}}$ [6], being

$\overline{d_{HRM}}$ the mean of $d_{HRM}(t)$. The *m(t)* was resampled at 4 Hz.

The respiratory signal, *r(t)*, was filtered by a band pass filter from 0.04 Hz to 0.80 Hz, which is assumed to cover the physiological frequency range for *m(t)* and *r(t)*, and undersampled at 4 Hz.

Spectral HRV indices were estimated from the power spectrum density (PSD) of *m(t)* ($S_m(f)$), computed by means of the Welch Periodogram. Then, the power content in the HF band (P_{HF}) and in the LF band (P_{LF}), the normalized power in the LF band (i.e. P_{LFn} = P_{LF}/(P_{LF}+P_{HF})) and the ratio $R = P_{LF}/P_{HF}$ were computed. The limits of the bands are defined in Section *3.2.2 Frequency band definition*. The respiratory frequency F_R was estimated from the location of the largest peak in the PSD obtained from *r(t)* ($S_r(f)$).

$$\rho^{ab}_{(Sm,Sr)} = \frac{\int_a^b \left(S_m(f) - \overline{S_m}(f)\right)\left(S_r(f) - \overline{S_r}(f)\right) df}{\sqrt{\int_a^b \left(S_m(f) - \overline{S_m}(f)\right)^2 df \int_a^b \left(S_r(f) - \overline{S_r}(f)\right)^2 df}} \tag{3.1}$$

3.2.2 Frequency band definition

Shifted and resized HF band based on Spectrum Correlation (SCHF)

The HF band is redefined based on the correlation between $S_m(f)$ and $S_r(f)$ as given in Eq. (3.1), where a and b are the lower and upper limits of the analyzed frequency range. The maximum value of $\rho^{ab}_{(Sm,Sr)}$ is searched, following the steps detailed below:

- Step 1: the spectral correlation of $S_m(f)$ and $S_r(f)$, $\rho^{ab}_{(Sm,Sr)}$, is computed within a bandwidth of 0.02 Hz centered at F_R.
- Step 2: the integration frequency range [a, b] is symmetrically expanded 0.02 Hz and $\rho^{ab}_{(Sm,Sr)}$ is recomputed. This step is repeated until the physiological range from 0.1 Hz to $\overline{d_{HRM}}/2$ is covered, with the following restrictions: (1) the lower limit a must be above 0.10 Hz, (2) the upper limit b must be below half the mean heart rate ($\overline{d_{HRM}}/2$) and (3) $S_r(b)$ must be above 5% of the

maximum value of $S_r(f)$ to avoid including in the correlation estimation frequencies with no respiratory power. In these cases, the restricted limit (lower or upper) is kept fixed and the other limit is increased in 0.01 Hz. The resulting integration frequency ranges are no longer symmetric with respect to F_R.

- Step 3: the maximum value of $\rho^{ab}_{(Sm,Sr)}$, denoted by $\rho_{max} = \rho^{a_{max}b_{max}}_{(Sm,Sr)}$, determines the lower and upper limits [a_{max}, b_{max}] of the redefined HF band (HF$_{SC}$).

Only those recordings showing $\rho_{max} \geq 0.5$ were considered for further analysis, being this value selected empirically as a trade-off between subject number inclusion and correlation strength. Fig. 3.1 shows a diagram of the SCHF method.

Standard LF band was considered in the range of [0.04, 0.15] Hz, except when the HF band encroached the LF band. In these cases, the upper limit of the LF band was reduced to the lower limit of the HF band, i.e., LF band was $\in$ [0.04, a_{max}] Hz.

Classic HF band

The classic HF band described in Task Force [93] was analyzed, i.e. [0.15, 0.40] Hz.

Shifted HF band centered at F_R with fixed bandwidth

As defined in previous studies [5, 99], the HF band was centered at F_R and had a fixed bandwidth of 0.11 Hz (HF_{F_R}).

In approaches to HF_{SC} and HF_{F_R}, which take into account respiratory information, those recordings with $F_R < 0.1$ Hz are excluded from the analysis due to the overlapping between the LF and HF bands.

3.2.3 Simulation study

A simulation study was carried out to validate the proposed HF_{SC} definition.

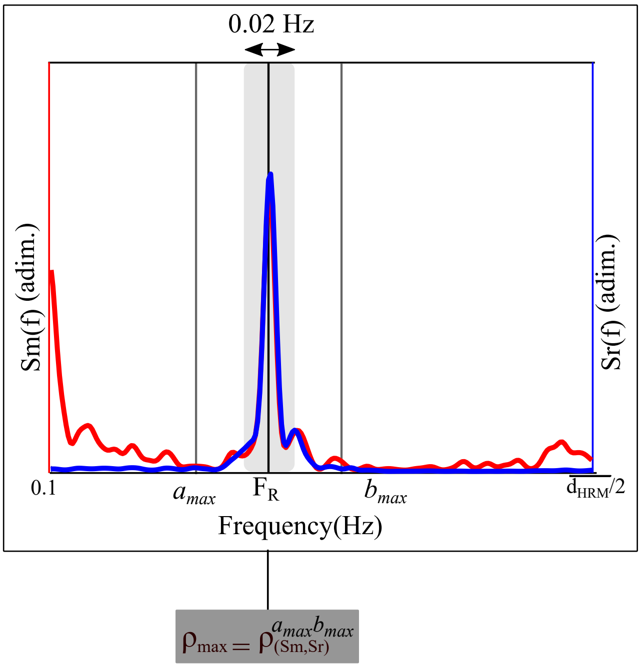

Figure 3.1: Diagram of the SCHF methodology: PSD of *m(t)* ($S_m(f)$) and PSD of *r(t)* ($S_r(f)$). The correlation between $S_m(f)$ and $S_r(f)$ was calculated by expanding symmetrically the $[a, b]$ range in steps of 0.02 Hz per iteration. The maximum value of the correlation between $S_m(f)$ and $S_r(f)$ (ρ_{max}) determines the lower and upper limits $[a_{max}, b_{max}]$ of the redefined HF band (HF_{SC}).

Synthetic modulating signals ($m_s(t)$) were generated as the sum of a HF and a LF component, following the steps detailed below:

- Step 1: the HF component was obtained by filtering a respiration signal *r(t)* from the emotion database from 0.25 Hz to $\overline{d_{HRM}}/2$. This HF component is denoted by $m_{HF_i}(t)$, i = 1, ..., I, where I is the number of cases with $F_R > 0.35$ Hz since those are the most challenging for the classic HF band. A total of I = 59 cases were identified.

- Step 2: the LF component was simulated based on a time-varying autoregressive moving average (ARMA) model [75]. The frequency for the ARMA model was obtained as the maximum of the original modulating signal spectrum $S_m(f)$, associated with the i-th subject, in the band from 0.04 Hz to 0.15 Hz and the amplitude was fixed to 0.1. A total of 50 realizations of the LF component were generated for each considered subject, yielding ${m_{LF_i}}^k(t)$ with k = 1, ..., 50.

- Step 3: the simulated modulating signals were constructed as ${m_{s_i}}^k(t) = {m_{LF_i}}^k(t) + \alpha m_{HF_i}(t)$, where the α parameter allows to simulate a set of sympathovagal ratios, R. The following R were considered: 0.5, 1, 2, 5, 10, 15, 20 and 30, as shown in Fig. 3.2. This range allows to cover the physiological R values computed during pure parasympathetic stimulation, median (interquartile range) of $1.53(0.83|2.11)$ and pure sympathetic stimulation $19.52(11.80|27.75)$ in a database of healthy subjects during pharmacological blockade and body position changes [13].

- Step 4: finally, each modulating signal ${m_{s_i}}^k(t)$ fed an IPFM model with time-varying threshold which generates the beat occurrence time series [6]. The time-varying threshold is defined as $1/d_{HRM_i}(t)$. From the simulated beat occurrence time series, a simulated instantaneous heart rate was obtained ${d_{HR_{s_i}}}^k(t)$. The same processing described in Section *3.2.1 Signal preprocessing* for real signals was applied to simulated ${d_{HR_{s_i}}}^k(t)$. A diagram of the whole process is shown in Fig. 3.3.

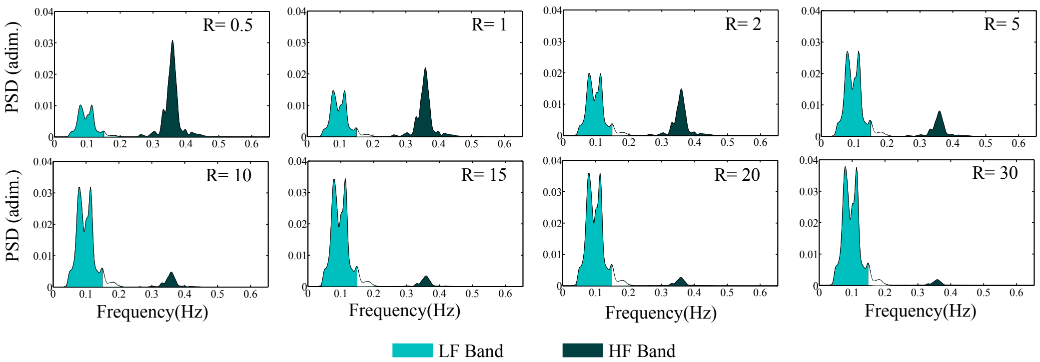

Figure 3.2: PSD of the modulating signal simulated ${d_{HR_{s_i}}}^k(t)$ for the physiological sympathovagal ratios: 0.5, 1, 2, 5, 10, 15, 20 and 30.

3.2.4 Performance measurement

The mean relative error (MRE) of HF power was calculated for each ratio Eq. (3.2).

$$MRE(\%) = mean\left(\frac{{P_{HF_i}}^k - P_{HFr_i}}{P_{HFr_i}}\right)100 \tag{3.2}$$

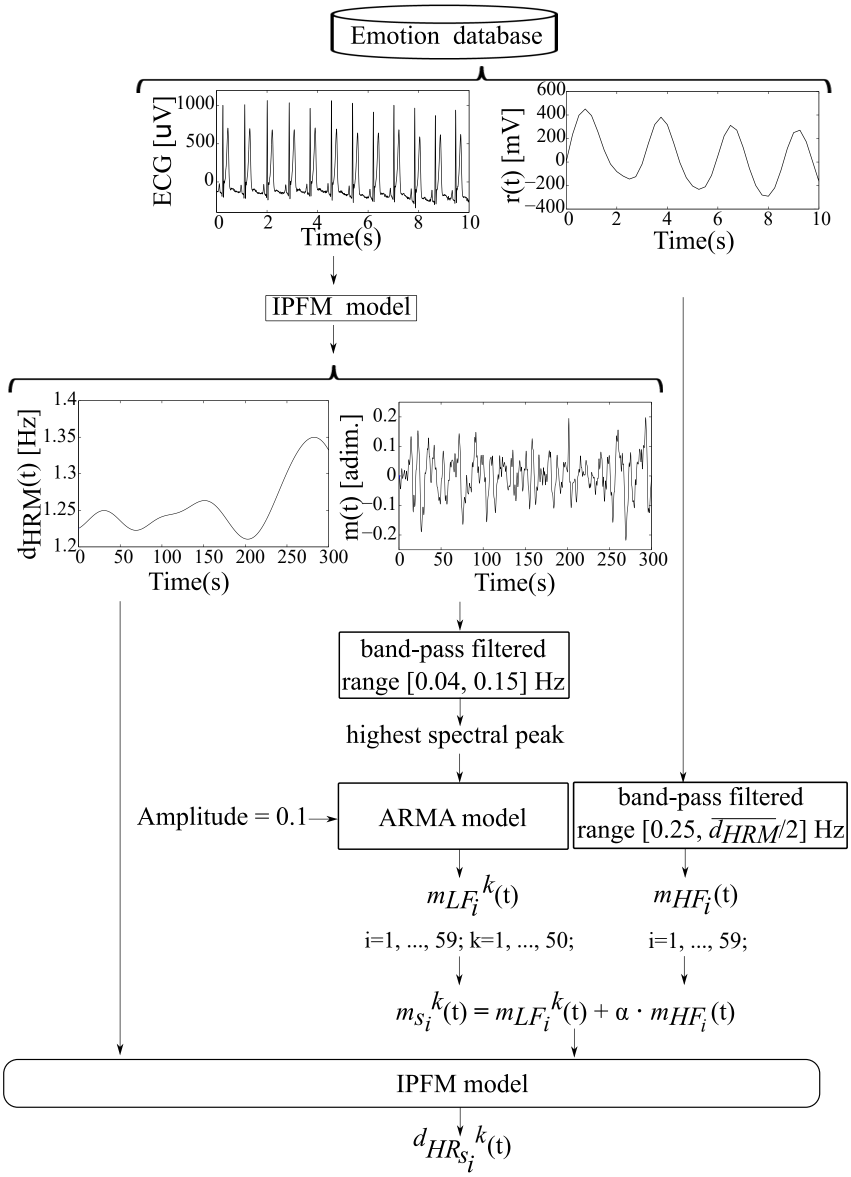

Figure 3.3: Schema of the simulation process for a single recording detailed in the following steps: (1) the HF component of the synthetic *m(t)* signals was obtained by filtering the *r(t)* of the emotion database from 0.25 Hz to the $\overline{d_{HRM}}/2$, resulting in $m_{HF_i}(t)$, (2) the LF component was simulated by an ARMA model with a fixed amplitude of 0.1 and a frequency calculated by the maximum of the original $S_m(f)$, associated with the *i-th* subject, resulting in $m_{LF_i}{}^k(t)$, (3) the simulated modulating signals $m_{s_i}{}^k(t)$ were constructed as the sum of the LF and HF components, where i is the number of the subject analyzed and k the number of the realization performed and (4) each modulating signal $m_{s_i}{}^k(t)$ fed an IPFM model with time-varying threshold $(1/d_{HRM_i}(t))$ which generates the beat occurrence times, and from them the HRV signal $d_{HR_{s_i}}{}^k(t)$ is derived.

Where $P_{HF_i}{}^k$ was the spectral content in the HF band, calculated as explained in Section *3.2.2 Frequency band definition*, from the simulated $d_{HR_{s_i}}{}^k(t)$ signal (Fig. 3.3) for each simulation and the P_{HFr_i} was the reference spectral content $\in [0.25, \overline{d_{HRM}}/2]$ Hz derived from ${d_{HR_{s_i}}}^k(t)$ signal.

The proposed SCHF methodology was compared with the other HF band definitions. Therefore, ${P_{HF_i}}^k$ and P_{HFr_i} for the MRE calculation were computed according to the bandwidth definitions detailed in Section *3.2.2 Frequency band definition*: (1) HF$_{SC}$, (2) HF and (3) HF$_{F_R}$.

3.2.5 Statistical analysis

Prior to the statistical analysis, normality distribution of all indices was evaluated by Lillie test.

Statistical analysis was done by T-test or Wilcoxon-test when necessary, depending on normality test results to evaluate differences for all followed paired conditions: relax vs. joy (R-J), relax vs. fear (R-F), relax vs. sadness (R-S), relax vs. anger (R-A), joy vs. fear (J-F), joy vs. sadness (J-S), joy vs. anger (J-A), fear vs. sadness (F-S), fear vs. anger (F-A) and sadness vs. anger (S-A).

The following HRV indices have been analyzed:

- Indices derived from the HF$_{SC}$ band: $P_{HF_{SC}}$, $P_{LFn_{SC}}$, R_{SC}, ΔHF=b_{max}-a_{max}, a_{max} and b_{max} and the novel index proposed in this work ρ_{max}. The respiratory frequency of the recordings which accomplishes all the restrictions imposed in Section *3.2.2 Frequency band definition*, denoted by $F_{R_{SC}}$ was also considered.
- Indices derived from the classic HF band: P_{HF}, P_{LFn} and R. The respiratory frequency, F_R, of all recordings was also studied.
- Indices derived from the HF$_{F_R}$ band: $P_{HF_{F_R}}$, $P_{LFn_{F_R}}$ and R_{F_R}. The respiratory frequency of the recordings which accomplishes the unique restriction of $F_R \geq 0.10$ Hz, denoted by $F_{R_{F_R}}$ was also considered.

The significant statistical level was p-value ≤ 0.05, that provides a reliable value for statistical discrimination [86]. To analyze the capability of the indices to discriminate emotions, the area under the receiver operating characteristic curve (AUC) was calculated and only those indices with AUC $\geq$ 0.70 were further considered. Finally, sensitivity, specificity and accuracy for each index in 2-class emotion classification were calculated using the leaving-one-out cross validation method [71].

3.3 Results

3.3.1 Evaluation of the methods for synthetic data

Fig. 3.4 presents the mean and standard deviation ($\mu \pm \sigma$) of the relative errors in P_{HF} estimation obtained from HF$_{SC}$, HF and HF$_{F_R}$ for several physiological sympathovagal ratios, R i.e. 0.5, 1, 2, 5, 10, 15, 20 and 30. The standard HF bandwidth presents relative error values strongly dependent on the ratio, while the HF$_{F_R}$ and the HF$_{SC}$ bandwidth presents lower relative error values regardless of the ratio values. Furthermore, the HF$_{SC}$ bandwidth presents lower relative errors than the HF$_{F_R}$ one.

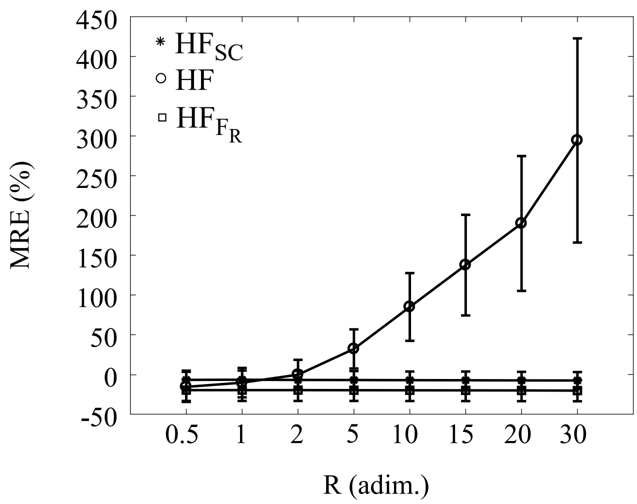

Figure 3.4: Mean and standard deviation ($\mu \pm \sigma$) of the mean relative errors (MRE) obtained by Eq. (3.2) for HF$_{SC}$, HF and HF$_{F_R}$ bands for eight physiological sympathovagal ratios studied: 0.5, 1, 2, 5, 10, 15, 20 and 30.

3.3.2 Evaluation of the methods for real data

All indices derived from the HF_{SC}, HF and HF_{F_R} bands have been evaluated and compared between each pair of emotions. In Table 3.1, the results obtained by the studied indices in terms of median and interquartile ranges as first (Q1) and third (Q3) quartile, median (Q1|Q3), for all emotional conditions (i.e. relax, joy, fear, sadness and anger) are shown. And Table 3.2 displays the p-values obtained from the statistical analysis and AUC values for the comparison of all pair of emotions.

Table 3.1: Median (Q1|Q3) values of the parameters studied for relax, joy, fear, sadness and anger.

	Relax	Joy	Fear	Sadness	Anger
P_{HF} (10^{-4}) (adim.)	3.60(1.52|8.01)	3.30(1.54|6.62)	3.62(1.67|5.91)	2.56(1.61|5.49)	2.76(1.34|4.60)
P_{LFn} (%)	73.93(56.44|83.34)	81.74(75.52|88.30)	70.21(56.89|80.85)	75.86(62.19|80.81)	78.61(69.13|83.75)
R (adim.)	2.84(1.30|5.00)	4.48(3.09|7.55)	2.37(1.32|4.22)	3.14(1.64|4.21)	3.67(2.24|5.16)
$\overline{d_{HRM}}$ (bpm)	0.61(0.57|0.69)	0.63(0.57|0.69)	0.64(0.58|0.69)	0.64(0.58|0.72)	0.64(0.60|0.69)
F_R (Hz)	0.29(0.24|0.35)	0.18(0.08|0.33)	0.31(0.27|0.35)	0.31(0.28|0.36)	0.30(0.25|0.35)
$P_{HF_{F_R}}$ (10^{-4}) (adim.)	1.93(0.73|4.95)	2.50(0.44|9.68)	1.91(0.86|4.08)	1.44(0.88|2.54)	1.58(0.78|2.71)
$P_{LFn_{F_R}}$ (%)	78.94(61.49|90.24)	83.42(68.42|93.55)	73.64(61.92|89.24)	82.57(63.97|90.51)	85.96(76.35|91.01)
R_{F_R} (adim.)	3.75(1.60|9.27)	5.03(2.19|14.50)	2.79(1.63|8.29)	4.75(1.80|9.61)	6.12(3.23|10.12)
$F_{R_{F_R}}$ (Hz)	0.30(0.27|0.35)	0.32(0.15|0.35)	0.32(0.28|0.35)	0.32(0.28|0.36)	0.31(0.27|0.35)
$P_{HF_{SC}}$ (10^{-4}) (adim.)	2.42(0.95|6.21)	2.25(0.46|4.21)	2.61(0.97|4.36)	1.65(0.11|2.95)	1.86(0.94|2.64)
$P_{LFn_{SC}}$ (%)	76.32(58.39|86.03)	82.45(77.40|90.69)	71.70(59.39|88.58)	80.60(61.57|88.10)	84.29(73.72|90.41)
R_{SC} (adim.)	3.22(1.40|6.16)	4.70(3.60|13.46)	2.53(1.46|7.76)	4.17(1.62|7.41)	5.37(2.81|9.43)
ΔHF (Hz)	0.16(0.12|0.20)	0.18(0.14|0.23)	0.14(0.12|0.18)	0.16(0.12|0.18)	0.14(0.12|0.18)
a_{max} (Hz)	0.21(0.18|0.27)	0.25(0.22|0.27)	0.24(0.20|0.26)	0.24(0.20|0.27)	0.24(0.21|0.27)
b_{max} (Hz)	0.40(0.35|0.42)	0.41(0.39|0.51)	0.40(0.36|0.44)	0.40(0.36|0.45)	0.40(0.36|0.43)
ρ_{max} (adim.)	0.95(0.88|0.98)	0.89(0.76|0.92)	0.93(0.89|0.97)	0.96(0.90|0.98)	0.93(0.89|0.98)
$F_{R_{SC}}$ (Hz)	0.30(0.27|0.35)	0.33(0.31|0.38)	0.32(0.29|0.35)	0.32(0.28|0.36)	0.32(0.29|0.36)

Only those parameters that revealed statistical differences to discriminate between pairs of emotions are shown in Fig. 3.5 by means of boxplots in terms of median and interquartile ranges as first (Q1) and third (Q3) quartile, median (Q1|Q3) of: (a) $P_{LFn_{SC}}$, (b) P_{LFn}, (c) $P_{LFn_{F_R}}$, (d) R_{SC}, (e) R, (f) R_{F_R} and (g) ρ_{max} for the emotions studied.

The spectral indices P_{LFn} and R revealed statistically significant differences between R-J, J-F and J-S. However, $P_{LFn_{F_R}}$, $P_{LFn_{SC}}$, R_{F_R} and R_{SC} only show statistically significant differences between R-J and J-F. Additionally, the novel ρ_{max} provided statistically significant differences between R-J, J-F, J-S, J-A and F-S. Since ρ_{max} obtained AUC $\geq$ 0.8, its discrimination capability was further analyzed, calculating sensitivity, specificity and accuracy using cross validation (Table 3.3).

Therefore, among all the emotions compared, neutral state vs. positive valence,

Table 3.2: *p*-values and AUC indices of the parameters studied for the emotional conditions: relax vs. joy (R-J), relax vs. fear (R-F), relax vs. sadness (R-S), relax vs. anger (R-A), joy vs. fear (J-F), joy vs. sadness (J-S), joy vs. anger (J-A), fear vs. sadness (F-S), fear vs. anger (F-A) and sadness vs. anger (S-A).

		R-J	R-F	R-S	R-A	J-F	J-S	J-A	F-S	F-A	S-A
Number of comparisons		35	43	30	34	34	21	26	25	31	22
P_{HF}	*p*-value	n.s.	n.s.	n.s.	n.s.	n.s.	n.s.	n.s.	n.s.	n.s.	n.s.
	AUC index	0.52	0.48	0.52	0.52	0.49	0.56	0.51	0.50	0.56	0.55
P_{LFn}	*p*-value	**≤0.001**	n.s.	n.s.	n.s.	**≤0.001**	**≤0.01**	≤0.05	n.s.	≤0.05	n.s.
	AUC index	**0.70**	0.50	0.48	0.53	**0.72**	**0.76**	0.59	0.57	0.62	0.54
R	*p*-value	**≤0.01**	n.s.	n.s.	n.s.	**≤0.001**	**≤0.01**	≤0.05	n.s.	≤0.05	n.s.
	AUC index	**0.70**	0.50	0.52	0.53	**0.72**	**0.76**	0.59	0.57	0.62	0.54
$\overline{d_{HRM}}$	*p*-value	≤0.05	≤0.01	n.s.	n.s.	n.s.	n.s.	n.s.	n.s.	n.s.	n.s.
	AUC index	0.55	0.56	0.54	0.51	0.50	0.46	0.51	0.53	0.52	0.51
F_R	*p*-value	≤0.05	≤0.05	n.s.	≤0.05	≤0.01	≤0.05	n.s.	n.s.	n.s.	n.s.
	AUC index	0.65	0.58	0.56	0.54	0.68	0.67	0.60	0.51	0.58	0.55
Number of comparisons		17	38	26	28	17	12	16	21	25	19
$P_{HF_{F_R}}$	*p*-value	≤0.05	n.s.	n.s.	n.s.	n.s.	n.s.	n.s.	n.s.	n.s.	n.s.
	AUC index	0.61	0.48	0.52	0.52	0.58	0.38	0.43	0.45	0.47	0.52
$P_{LFn_{F_R}}$	*p*-value	**≤0.01**	n.s.	n.s.	n.s.	**≤0.01**	≤0.05	≤0.05	n.s.	n.s.	n.s.
	AUC index	**0.72**	0.50	0.53	0.58	**0.75**	0.67	0.60	0.54	0.57	0.56
R_{F_R}	*p*-value	**≤0.01**	n.s.	n.s.	n.s.	**≤0.01**	≤0.05	≤0.05	n.s.	n.s.	n.s.
	AUC index	**0.72**	0.50	0.47	0.58	**0.75**	0.67	0.60	0.54	0.57	0.56
$F_{R_{F_R}}$	*p*-value	≤0.05	≤0.05	n.s.	≤0.05	n.s	n.s	n.s	n.s	n.s	n.s
	AUC index	0.63	0.58	0.54	0.55	0.51	0.62	0.60	0.52	0.54	0.49
Number of comparisons		12	33	22	26	12	9	11	17	21	17
$P_{HF_{SC}}$	*p*-value	≤0.05	n.s.	n.s.	n.s.	n.s.	n.s.	n.s.	n.s.	n.s.	n.s.
	AUC index	0.59	0.49	0.53	0.54	0.62	0.48	0.60	0.5	0.54	0.50
$P_{LFn_{SC}}$	*p*-value	**≤0.05**	n.s.	n.s.	n.s.	**≤0.01**	n.s.	n.s.	n.s.	n.s.	n.s.
	AUC index	**0.72**	0.49	0.53	0.59	**0.76**	0.63	0.49	0.56	0.61	0.56
R_{SC}	*p*-value	**≤0.05**	n.s.	n.s.	n.s.	**≤0.01**	n.s.	n.s.	n.s.	n.s.	n.s.
	AUC index	**0.72**	0.51	0.47	0.59	**0.76**	0.63	0.49	0.44	0.61	0.56
ΔHF	*p*-value	n.s.	n.s.	n.s.	n.s.	n.s.	n.s.	n.s.	n.s.	n.s.	n.s.
	AUC index	0.62	0.62	0.57	0.54	0.62	0.67	0.69	0.5	0.52	0.53
a_{max}	*p*-value	n.s.	n.s.	n.s.	n.s.	n.s.	n.s.	n.s.	n.s.	n.s.	n.s.
	AUC index	0.57	0.55	0.56	0.58	0.55	0.49	0.53	0.55	0.50	0.51
b_{max}	*p*-value	n.s.	n.s.	n.s.	n.s.	≤0.05	n.s.	n.s	n.s.	n.s.	n.s.
	AUC index	0.65	0.52	0.51	0.52	0.63	0.62	0.64	0.49	0.50	0.50
ρ_{max}	*p*-value	**≤0.01**	n.s.	n.s.	n.s.	**≤0.05**	**≤0.05**	**≤0.01**	**≤0.05**	n.s.	n.s.
	AUC index	**0.90**	0.54	0.63	0.55	**0.77**	**0.84**	**0.82**	**0.70**	0.47	0.55
$F_{R_{SC}}$	*p*-value	n.s.	n.s.	n.s.	≤0.05	n.s.	n.s.	n.s.	n.s.	n.s.	n.s.
	AUC index	0.65	0.54	0.53	0.56	0.55	0.59	0.62	0.51	0.54	0.49

n.s. Stands for non-significant.

Note that parameters with $p \leq 0.05$, AUC index ≥ 0.70, sensitivity, specificity, accuracy values $\geq 70\%$ are remarked are remarked in bold type.

Table 3.3: Sensitivity, specificity and accuracy calculated using cross validation for the parameter ρ_{max} with AUC ≥ 0.8: relax vs. joy (R-J), joy vs. sadness (J-S) and joy vs. anger (J-A).

	R-J	J-S	J-A
Sensitivity (%)	66.7	88.9	99.9
Specificity (%)	91.7	66.7	63.6
Accuracy (%)	79.2	77.8	77.3

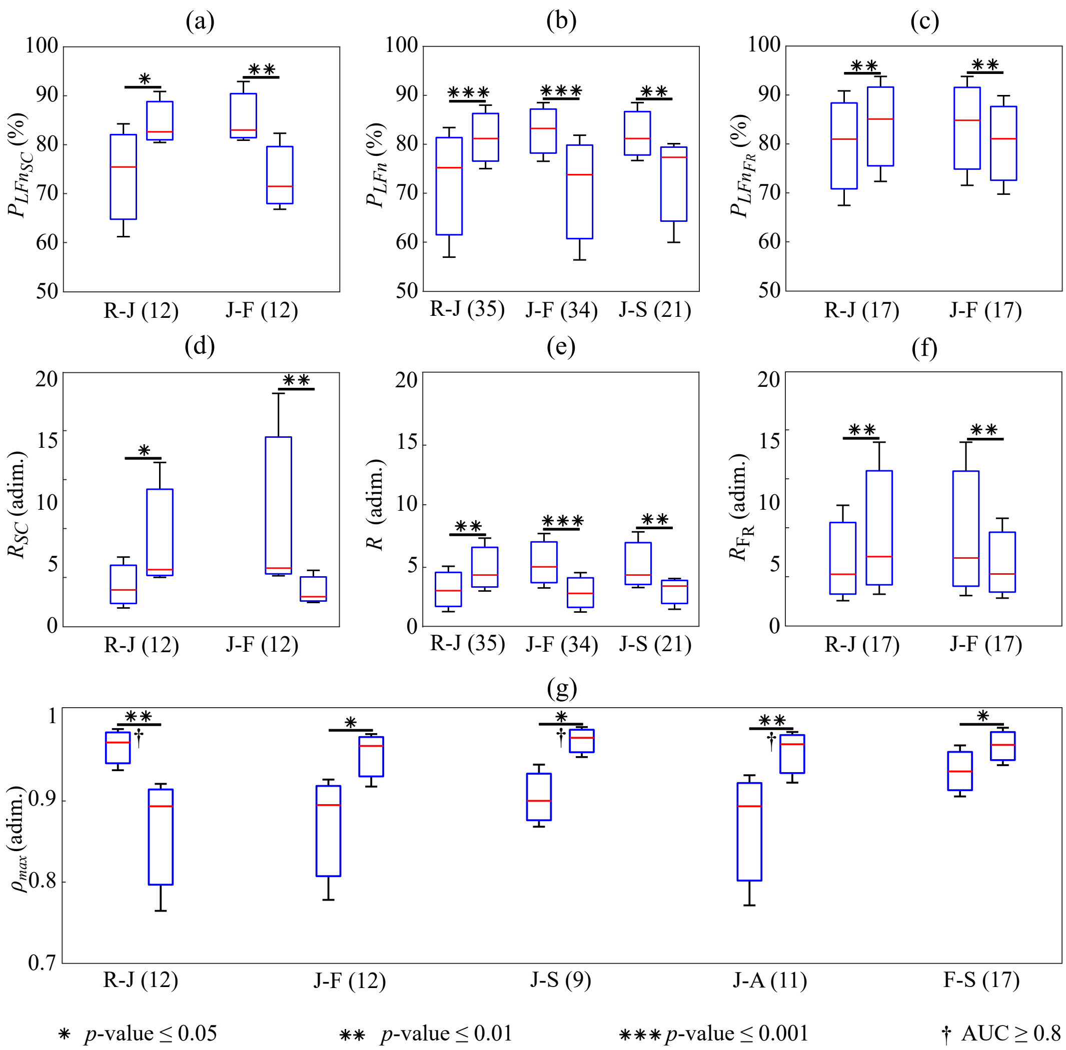

Figure 3.5: Boxplots of the median (Q1|Q3) values of only those parameters which present statistical differences between the emotional conditions induced by videos: (a) $P_{LFn_{SC}}$, (b) P_{LFn}, (c) $P_{LFn_{F_R}}$, (d) R_{SC}, (e) R, (f) R_{F_R} and (g) ρ_{max}. The nomenclature used for each pair of emotions is: relax vs. joy (R-J), joy vs. fear (J-F), joy vs. sadness (J-S), joy vs. anger (J-A) and fear vs. sadness (F-S). The statistical differences between the pair of emotions are indicated by $*$ for p-value ≤ 0.05, $**$ for p-value ≤ 0.01, $***$ for p-value ≤ 0.001 and † for AUC ≥ 0.80. It can be noted that those indices which are not marked by a † have an AUC ≥ 0.70. Together to the label of the pair of studied emotions in parentheses, it is the number of comparisons.

positive valence vs. all negative valences and F-S were significantly different. No statistically significant differences were found in the comparison between neutral state vs. negative valences and anger vs. negative valences.

Fig. 3.6 displays two examples where the SCHF method is especially useful:

(a) The F_R is below 0.15 Hz and therefore the HF_{SC} band encroaches the classic LF band. In this particular case the HF_{SC} band limits are: a_{max} = 0.10 Hz and b_{max} = 0.29 Hz. The LF_{SC} band is redefined from 0.04 Hz to 0.10 Hz.

(b) F_R is 0.40 Hz and the HF_{SC} upper band limit should be shifted to the right to consider all the RSA information. In this particular case, the HF_{SC} band limits are: a_{max} = 0.34 Hz and b_{max} = 0.46 Hz.

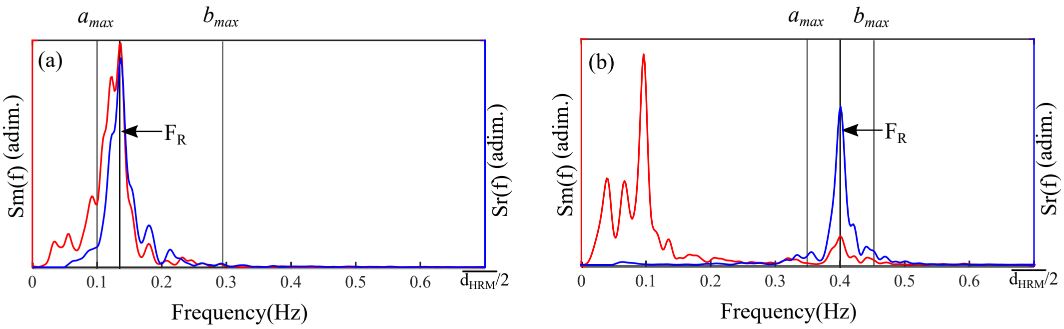

Figure 3.6: Correlation between $S_m(f)$ and $S_r(f)$ in two particular cases: (a) F_R is below 0.15 Hz and (b) F_R is 0.40 Hz.

3.4 Discussion

According to the simulation results, the SCHF method presented the lowest relative error values for HF content estimation independently of the considered low-to-high frequency ratio, R, values (Fig. 3.4). In this way, the choice of adaptive HF frequency limits may avoid physiological misinterpretations of HF power content, because frequency limits depend strongly on age and physiological conditions [42].

The statistical analysis presented in Table 3.2 and in Fig. 3.5 revealed statistically significant differences between: (1) neutral state vs. positive valence by means of P_{LFn}, R, $P_{LFn_{F_R}}$, R_{F_R}, $P_{LFn_{SC}}$, R_{SC} and ρ_{max}, (2) joy vs. fear by means of P_{LFn}, R, $P_{LFn_{F_R}}$, R_{F_R}, $P_{LFn_{SC}}$, R_{SC} and ρ_{max}, (3) joy vs. sadness by means of P_{LFn}, R and ρ_{max}, (4) joy vs. anger by means of ρ_{max} and (5) fear vs. sadness by means of ρ_{max}.

The SCHF methodology proposed in this study differentiated R-J, J-F, J-S, J-A and F-S by means of ρ_{max}. No statistically significant differences were found for neutral state vs. negative valences and anger vs. negative valences.

Classic frequency indices P_{LFn} and R were able to discriminate between R-J, J-F and J-S. It can be noted that emotions J-A and F-S were only distinguished by parameter ρ_{max} derived from the new method SCHF, which offered additional statistically significant information based on the relationship between HRV and respiration.

Regarding respiratory information, neither F_R, nor $F_{R_{F_R}}$, nor $F_{R_{SC}}$ showed statistically significant differences between all pairs of emotions studied. Hernando et al. [47] did not found significant differences in respiratory frequency between relax and stress. The F_R index, computed from all recordings, showed a median value around 0.30 Hz and with a first quartile above 0.15 Hz for relax, fear, sadness and anger. Therefore, in all these cases, the redefined HF band HF_{SC} does not encroach the classic LF band. However, in the case of joy, F_R presented the lowest median value of 0.18 Hz with a first quartile of 0.08 Hz. For this reason and during joy elicitation, the HF_{SC} could encroach the classic LF band. Therefore, this highlights the need to redefine the HF band, especially in joy condition.

For this reason, all cases presenting a F_R inside the classic LF band, a redefinition of the HF classic band could improve the measurement of the HF band, as shown in Fig. 3.6 (a). A similar situation occurs in Fig. 3.6 (b) when F_R is near to or above the classic upper limit of the HF band (0.40 Hz), where the classic range [0.15, 0.40] Hz could miss the RSA information. With a redefinition of the HF band in these cases, a more refined description of the physiological information could be extracted from the signals. However, only recordings which accomplished the restrictions of the SCHF method could be analyzed. This implies to discard an amount of signals from the analysis, and subsequently the number of analyzed subjects in each case is reduced. It can be noted that the percentage of subjects excluded is different for each of the comparisons, with a minimum of 22.7% for the comparison S-A and a maximum of 65.7% for the comparison R-J.

Classic ΔHF [0.15, 0.40] Hz has a bandwidth of 0.25 Hz. Analyzing the results obtained by the SCHF method, the ΔHF presented a median bandwidth value of 0.16 Hz for relax, 0.18 Hz for joy, 0.14 Hz for fear and anger and 0.16 Hz for sadness. The lower and upper limit of the HF_{SC}, i.e., a_{max} and b_{max}, showed similar values within the different emotions, although both are subject dependent. The SCHF reveals a slight improvement in the reliability of sympathovagal balance estimation capable of discriminating neutral (relax) vs. positive (joy) valence, positive vs. negative (fear, sadness and anger) valences and negative (fear) vs. negative (sadness) valence. In accordance with our results, Goren Y. et al. [42] concluded the importance of redefining the boundary of the HF band for a correct evaluation of physiological changes of the ANS.

$P_{HF_{SC}}$ was found higher for fear and relax than for joy, sadness and anger. These results are different from the ones in previous studies [73] where P_{HF} values were higher during listening to unpleasant than pleasant music. This difference may be due to the different stimuli utilized in [67] and [73] where music was used as opposed to videos as in the present study.

Mikuckas A. et al. [67] found that P_{LF} and LF/HF ratio increased during exciting and sedative music, but decreased during silence. Moreover, Rantanen A. et al. [84] evidenced that negative valence elicitation, induced by unpleasant pictures, produced a higher LF/HF ratio than neutral and pleasant pictures in a female cohort. Valenza G. et al. [104] investigated the synchronization between breathing patterns and heart rate during emotional visual elicitation by means of a set of neutral vs. increasing level of arousal images. In that study, it was found that the LF/HF ratio presented statistically significant differences between neutral and arousal sessions with higher LF/HF ratio values while arousal sessions, in which sympathetic activity should be dominant. In this study, an increase in the $P_{LFn_{SC}}$ and R_{SC} indices during joy (Fig. 3.5 (a-f)) was observed. Thus, joy could be associated with a sympathetic predominance. Additionally, $P_{LFn_{SC}}$ and R_{SC} presented statistically significant differences discriminating neutral sessions vs. positive valence and J-F.

Besides the aforementioned elicitation types and emotions, population characteristics such as age could influence the results [42]. Thus, interpretation of the results should be addressed within this framework.

Chapter 4

Non-Linear Analysis Methodology

Contents

4.1 Introduction

Interest in emotion recognition has burgeoned in recent years aiming to provide a useful tool in the field of emotion regulation. In that sense, a subject's emotional response is mediated by individual influences depending on which emotions the subject has and how he/she experiences and expresses them [44]. Many clinical features of depression, stress, anxiety and mood disorders may be construed as maladaptive attempts to regulate unwanted emotions [17]. A system for emotion recognition could help people to manage their own emotions, providing a tool to record their feelings and consequently, focusing their attention on modulating their emotional responses.

A complex mixture of cognitive, affective, behavioral, and physiological factors contributes to individual differences in health and disease. All these factors produce wide variation in outcomes of HRV, blood pressure and autonomic balance which have important implications for both physical and mental health [94].

As before mentioned, HRV analysis based on linear methods (such spectral analysis) is a usual strategy for ANS analysis, although non-linear HRV analysis has also been demonstrated as a useful complementary tool [49]. Traditional time and frequency domain measures of HRV assess the amplitude of variations between subsequent intervals and the amplitude distributions in the power spectra, respectively. However, none of them provide information about the complex communication involved in the control of the cardiovascular system that generates the HRV [77]. Non-linear techniques such as the Dominant Lyapunov Exponents, the Detrended Fluctuation Analysis, the Approximate Entropy, the Sample Entropy, the Fuzzy Measure Entropy, the Cross Sample Entropy, the Cross Fuzzy Measure Entropy, the Permutation Entropy, Permutation Min-Entropy, the Pointwise Correlation Dimension, the Lagged Poincaré Plot or the Quadratic Coupling have been used to detect emotional stimuli and all of them have shown better results than linear techniques [12, 30, 43, 101–105, 109, 111]. Some of these techniques have also been used to study non-linear relationships between HRV and respiration signals [55, 103–105, 111]. Table 4.1 reports a summary of different non-linear techniques applied to RR series during diverse emotional states.

Table 4.1: Bibliographic summary of non-linear techniques applied to HRV series in different emotional states.

Ref.	Technique	Emotional state	Results
[101]	DLEs ApEn	Neutral and arousal elicitation	Mean ApEn decrease and DLEs became negative during arousal elicitation.
[12]	AMIF	Depression	Increased total area under the AMIF curve are associated with major depression.
[111]	SEn FMEn CSEn CFMEn	Depression	Increased CSEn and CFMEn are associated with depression severity.
[109]	PE PME	Neutral, happiness, fear, sadness, anger, and disgust	Increased PE and PME during happiness, sadness, anger, and disgust. PME is more sensitive than PE for discriminating non-neutral from neutral emotional states.
[30]	DLEs ApEn SEn PD2 DFA	Anxiety	Decreased DLEs, ApEn, SEn, PD2 and increased $\alpha 1$ during anxiety state.
[43]	LPP	Peacefulness, happiness, fear, sadness	Maximum changes in LLP measures during happiness, and minimum changes during fear.

The nomenclature used is:
Dominant Lyapunov Exponents (DLEs), Approximate Entropy (ApEn), Sample Entropy (SEn), Fuzzy Measure Entropy (FMEn), Cross Sample Entropy (CSEn), Cross Fuzzy Measure Entropy (CFMEn), Permutation Entropy (PE), Permutation Min-Entropy (PME), Pointwise Correlation Dimension (PD2), Detrended Fluctuation Analysis (DFA), Lagged Poincaré Plot (LLP).

This complementary information can be assessed by non-linear methods such as the AMIF and the CMIF, which have been demonstrated to be independent of signal amplitudes and able to describe the predictability and regularity of the signals [48, 49]. Both functions, the AMIF and the CMIF, have been proposed as predictors of cardiac mortality [49]. The AMIF has been studied as an indicator of the increased cardiac mortality in depressed patients [12] and in multiple organ dysfunction syndrome patients [48], and the CMIF has been applied to electroencephalographic signals for stress assessment [1].

In the present work, both the non-linear techniques, the AMIF and the CMIF are proposed for human emotion recognition. The AMIF technique is applied to HRV signals to study complex communication within the ANS, while the CMIF technique is considered to quantify the complex coupling between HRV and respiratory signals. Both algorithms are, in this work, adapted to short-term time series modifying the number of histogram bins involved in the methodology. Traditional RR band filtering is considered (i.e. LF and HF band), and also a redefined HF band, HF_{SC}, centered at the F_R and whose width is determined based on the SCHF method, are investigated [100]. The aim of including the HF_{SC} band is the analysis of RSA influences on HRV, mainly when F_R is above 0.40 Hz or F_R lies within the LF band [5, 100]. The ability of the parameters derived from the AMIF and the CMIF to discriminate elicited states is evaluated on a database of video-induced emotion elicitation, described in [100].

In [100], the discrimination between different emotional states was addressed using frequency domain HRV indices (linear features). However, it was not possible to discriminate between relax and all negative valences, as well as between fear and anger, and sadness and anger. Here, we aim to study the discrimination capability of the non-linear AMIF and CMIF techniques of emotions complementing the linear-feature information. We propose the use of these non-linear techniques for human emotion recognition hypothesizing that ANS response to different emotions will impinge differential regularity patterns in HRV and will change the complex interaction between respiration and heart rate variability.

4.2 Methods and materials

4.2.1 Signal preprocessing

The RR interval was defined as the time between two consecutive R wave peaks, detected from the ECG lead with the best signal-to-noise ratio using a wavelet-based detector [63]. The presence of ectopic beats and misdetections was detected and corrected [64]. Evenly sampled RR time series, $RR(t)$, were obtained by linear interpolation at 4 Hz.

Then, the $RR(t)$ was filtered in: (1) the LF band of [0.04, 0.15] Hz ($RR_{LF}(t)$), (2) the HF band of [0.15, 0.40] Hz ($RR_{HF}(t)$) and (3) the HF_{SC} band [100] based on the SCHF method, ($RR_{SC}(t)$). In the SCHF method, the HF band was redefined to be centered at the F_R and its limits were calculated by means of the cross-correlation function between the power spectrum of HRV and respiration, being subject-dependent. The maximum value of correlation determined the lower (a_{max}) and upper limit (b_{max}) of the HF_{SC} band.

The respiratory signal ($r(t)$) was filtered by a band pass filter from 0.04 Hz to 0.8 Hz, and downsampled at 4 Hz.

Then, a transformation of all time series was carried out by ranking data in order to have the best statistics in the entropy estimation and robustness against noise [81].

4.2.2 Auto-Mutual Information Function

The AMIF is a non-linear equivalent of the auto-correlation function, based on the Shannon entropy. The Shannon entropy of a time series $x(t)$ is calculated by the discrete probability distribution $p(x_i(t))$ of $x(t)$ leading $H_{x(t)}$ as shown in Eq. 4.1 [49].

$$H_{x(t)} = -\sum_{i=1}^{I} p(x_i(t)) log_2 p(x_i(t)) \tag{4.1}$$

where I is the number of bins needed for estimating the amplitude histogram of $x(t)$, an approximation to the probability distribution function of the signal.

Then, the AMIF of $x(t)$ is given by $H_{x(t)}$, by $H_{x(t+\tau)}$, obtained by shifting $x(t)$ a time lag τ as $x(t+\tau)$, and their bivariate probability distribution leading to $H_{x(t)x(t+\tau)}$ as shown in Eq. 4.2 [49].

$$AMIF_{xx}(\tau) = H_{x(t)} + H_{x(t+\tau)} - H_{x(t)x(t+\tau)} \tag{4.2}$$

Therefore, this function describes the amount of common information between the original time series $x(t)$ and the time shifted time series $x(t+\tau)$. In the case of statistically independent time series, the $AMIF_{xx}$ is zero, otherwise positive. The AMIF is normalized to its maximum amplitude (in $\tau = 0$) representing the entire information of a time series. The decay of this function over a time lag τ represents the loss of information with respect to this prediction time, and in the case of non-linear HRV analysis, it is assumed to quantify the complexity of autonomic communication [48]. In the case of a random and unpredictable time series, the AMIF decays to 0 for all prediction times τ apart from $\tau = 0$. On the contrary, in the case of a predictable time series the AMIF remains at 1 for all τ [77].

4.2.3 AMIF-based measures

In order to describe HRV complexity during emotion elicitation, the evolution of the information function over the time scale τ should be taken into consideration. The AMIF (Fig. 4.1) applied to the $RR(t)$ time series was characterized by the following parameters: BD is the beat decay that corresponds with the AMIF decay from $\tau = 0$ s to $\tau_B = 0.6$ s, which represents a standard mean beat period [77]. Also, $A_{T_{RR}}$ is the total area under the curve that has been proposed to characterize the morphology, predictability and regularity of the signal [12].

The AMIF applied to the filtered time series $RR_{LF}(t)$, $RR_{HF}(t)$ and $RR_{SC}(t)$ was characterized by the following parameters: PD_δ is the peak decay that shows the information decay at the maximum peak defined in the interval $[\tau_a, \tau_b]$; PD_{m_δ} is the mean peak decay within a time range $[\tau_a, \tau_b]$ that indicates the mean information decrease between two time lags τ_a and τ_b; and A_{T_δ} is the total area under the curve in the same time range $[\tau_a, \tau_b]$, where $\delta = \{LF, HF, SC\}$.

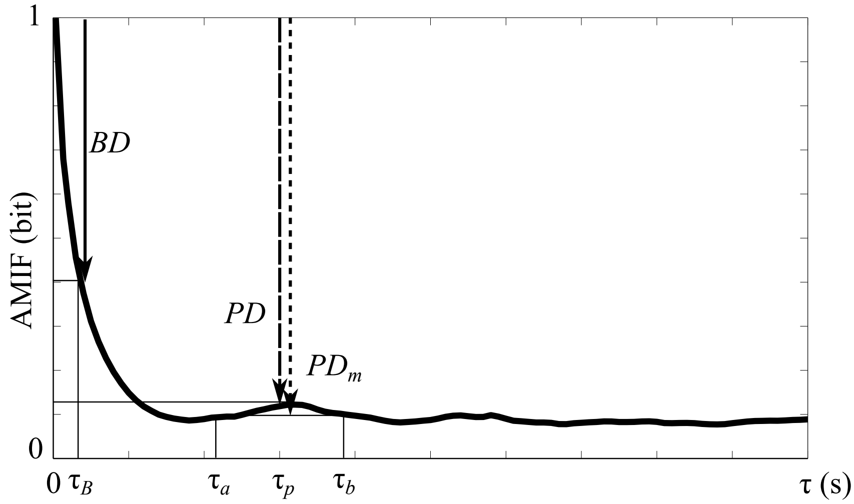

Figure 4.1: The normalized Auto-Mutual Information Function (AMIF) as function of the time scale τ. The AMIF value at $\tau = 0$ represents the entire information of a time series. Beat decay (*BD*) indicates the AMIF decay over a standard heart beat period (τ_B). Mean peak decay (PD_m) indicates the mean information decrease between τ_a and τ_b. Peak decay (*PD*) indicates the information decay at the maximum peak (τ_p) defined in the interval [τ_a, τ_b].

Since the information flow of oscillators has its peak starting at half the period τ = (1/(2*f*), 1/*f*, 3/(2*f*), ...), the lower and upper time scale boundaries [τ_a, τ_b] within the AMIF were chosen at τ = 1/(2*f*), where *f* is the frequency band boundaries used in the band pass filters [48] as: (1) the traditional LF range of [0.04, 0.15] Hz corresponds to a LF prediction time range of $\tau_{LF} = [\tau_a = 1/(2*0.15), \tau_b = 1/(2*0.04)]$ = [3.33, 12.5] s; (2) the traditional HF range corresponds to a HF prediction time range of [0.15, 0.40] Hz as $\tau_{HF} = [\tau_a = 1/(2*0.40), \tau_b = 1/(2*0.15)]$ = [1.25, 3.33] s and (3) the SCHF band [a_{max}, b_{max}] corresponds to a SCHF prediction time range of $\tau_{SC} = [\tau_a = 1/(2b_{max}), \tau_b = 1/(2a_{max})]$ s. In Table 4.2, the values for lower- and upper-time scale boundaries corresponding to the SCHF prediction time range of τ_{SC} in terms of median and interquartile ranges, as first and third quartile, (Median (Q1|Q3)) are specified.

4.2.4 Cross-Mutual Information Function

The CMIF is a non-linear equivalent of the cross-correlation function, based on the Shannon entropy similarly to the AMIF, but quantifying the coupling between two

Table 4.2: Median (Q1|Q3) values for lower- (τ_a) and upper-time (τ_b) scale boundaries corresponding to the SCHF prediction time range for relax, joy, fear, sadness and anger.

Elicitation	τ_a	τ_b
Relax	1.25 (1.19|1.43)	2.38 (1.85|2.78)
Joy	1.22 (0.98|1.28)	2.00 (1.85|2.27)
Fear	1.25 (1.14|1.39)	2.08 (1.92|2.50)
Sadness	1.25 (1.11|1.39)	2.08 (1.85|2.50)
Anger	1.25 (1.16|1.39)	2.08 (1.85|2.38)

signals $x(t)$ and $y(t)$. This function describes the amount of common information between a time series $x(t)$ and a time shifted time series $y(t+\tau)$. Then, the CMIF of $x(t)$ and $y(t+\tau)$ is given by $H_{x(t)}$, by $H_{y(t+\tau)}$, and their bivariate probability distribution leading to $H_{x(t)y(t+\tau)}$ as shown in Eq. 4.3 [49].

$$CMIF_{xy}(\tau) = H_{x(t)} + H_{y(t+\tau)} - H_{x(t)y(t+\tau)} \tag{4.3}$$

In contrast to the AMIF, the CMIF is not normalized for its analysis and it does not present a symmetric distribution around zero. Therefore, left and right sides of the CMIF around zero were analyzed. The non-linear analysis of the coupled signals using the CMIF was as described for the AMIF, i.e., the CMIF at $\tau = 0$ represents the common maximum information of both time series and the decay of this function over a prediction time describes the loss of information over this τ [49].

4.2.5 CMIF-based measures

In order to quantify and extract the amount of mutual information between the synchronized registered time series of HRV and respiration during emotion elicitation, the coupling between $RR(t)$ and $r(t)$, and between $RR_{SC}(t)$ and $r(t)$ was investigated. Only the $RR(t)$ and the $RR_{SC}(t)$ series have been taken into consideration because respiratory information is not consistently contained in the LF or HF bands for all subjects.

The following parameters were calculated from the CMIF of the synchronized cardiac and respiratory signals: $CMIF_0$ defined as the CMIF value at $\tau = 0$ that represents the amount of common information between both time series without time lag; $CMIF_{max}$ defined as the maximum CMIF value that shows the maximum coupling between the signals; and τ_{max} defined as the time lag between $CMIF_{max}$ and $CMIF_0$, that indicates the time lag between the amount of common information of the time series and the maximum coupling between the signals. For this analysis, the CMIF parameters were defined as follow: $CMIF_{0_\gamma}$, $CMIF_{max_\gamma}$ and τ_{max_γ} in the coupling between each $\gamma = \{RR, SC\}$ and $r(t)$. In Fig. 4.2, it is presented a CMIF function.

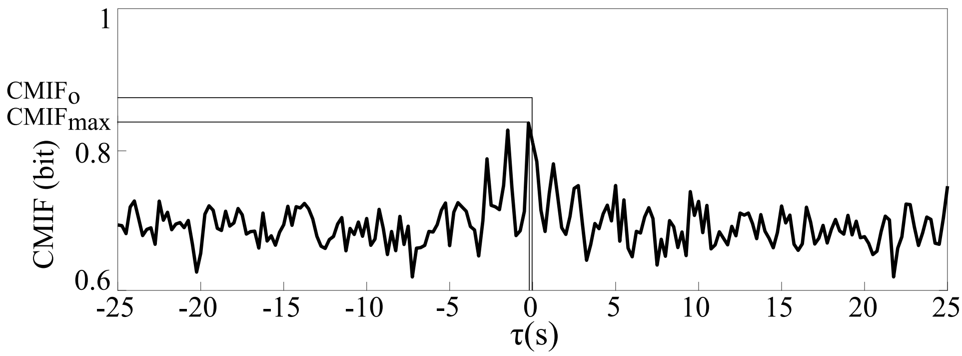

Figure 4.2: The Cross-Mutual Information Function (CMIF) of the coupling between $RR(t)$ and $r(t)$ as function of the time scale τ .The CMIF value at $\tau = 0$ ($CMIF_0$) represents the amount of common information of the time series without time lag and the maximum coupling between the signals is represented by $CMIF_{max}$.

4.2.6 Selection of the number of bins

The discrete probability distribution $p(x_i(t))$ corresponds to a partitioning of the amplitude range of each signal in a histogram, and $I = 2^N$ represents the maximum possible information that can be obtained (I is the number of bins of the histogram and N is the number of bits).

In order to adapt the algorithms of the AMIF and the CMIF to short-term time series, 2^N for $N = \{3, 4, 5, 6, 7, 8, 9\}$ bits were considered in the calculation methodology. The number of parameters able to statistically discriminate between relax and emotions and between pairs of emotions were assessed to determine the adequate number of histogram bins I.

4.2.7 Statistical analysis

Normality distribution of all parameters was evaluated by Lillie test. Then, the T-test or the Wilcoxon test when necessary, depending on normality test results, was applied to evaluate differences for the followed paired conditions: relax and each emotion and also each emotion was compared with each other.

The significance statistical level was p-value ≤ 0.05, since this threshold provides a reliable value for statistical discrimination [86]. Additionally, AUC index was studied to analyze the capability of the parameters to discriminate the studied elicitations and AUC ≥ 0.70 was used to determine statistically significant differences for each studied parameter. Furthermore, leaving-one-out cross validation method was used [71] to assess sensitivity, specificity and accuracy values for each parameter in 2-class emotion classification. These statistical parameters were required to be $\geq 70\%$ to determine statistically significant differences for each studied parameter. These thresholds have been selected as optimal cut-points values due to sensitivity and specificity being the closest to the value of the area under the ROC curve [97].

The number of bins I was selected as the value which yielded the highest number of parameters with statistically significant differences (p-value ≤ 0.001) between relax and each emotion and between pairs of emotions.

4.3 Results

4.3.1 Selection of the number of bins

The following analyzes have been performed to evaluate the adequate I for the AMIF and the CMIF calculation for emotion recognition using short-time HRV signals.

In Fig. 4.3, it is shown the percentage of the number of parameters that present statistically significant differences for each proposed I, when comparing relax with each emotions or between each pairs of emotions. The value $I = 2^5$ was selected, since it presents the highest number of parameters with statistically significant differences, p-value $\leq$ 0.001 and sensitivity, specificity and accuracy $\geq$ 70% and AUC index $\geq$ 0.70 for both non-linear techniques.

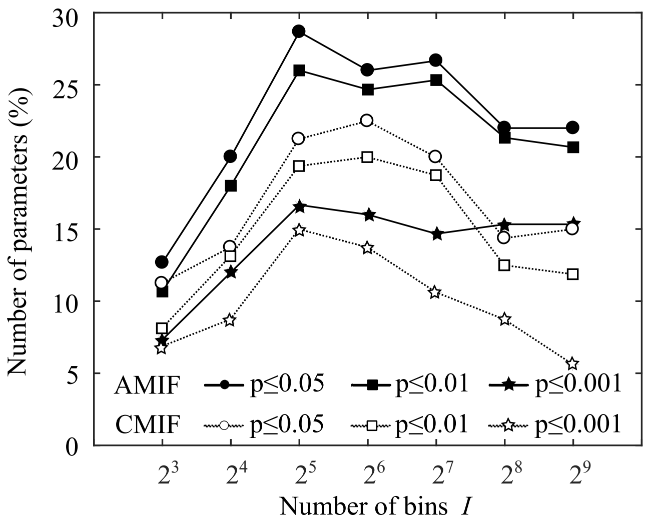

Figure 4.3: Percentage of number of parameters derived from the AMIF and the CMIF function of each proposed bin number I presenting statistically significant differences: (p-value $\leq$ 0.05, p-value $\leq$ 0.01 and p-value $\leq$ 0.001 when comparing relax and each emotion and between pairs of emotions. All these counted parameters also presented a sensitivity, specificity and accuracy $\geq$ 70% and AUC index $\geq$ 0.70).

4.3.2 AMIF-based measures

Those AMIF-based parameters that revealed statistically significant differences between relax and the different emotions or between pairs of emotions are presented in Fig. 4.4. In this figure, boxplots are shown in terms of median and interquartile ranges as first and third quartile: A_{T_γ} (Fig. 4.4a) for $\gamma = \{RR, LF, HF, SC\}$; BD (Fig. 4.4b) analyzed on $RR(t)$; and PD_{m_δ} (Fig. 4.4c) for $\delta = \{LF, HF, SC\}$.

In Table 4.3, p-value, AUC and accuracy values are remarked in bold type for those AMIF-based parameters that revealed statistically significant differences between the emotional states studied. The presented emotion conditions were those which revealed statistically significant differences.

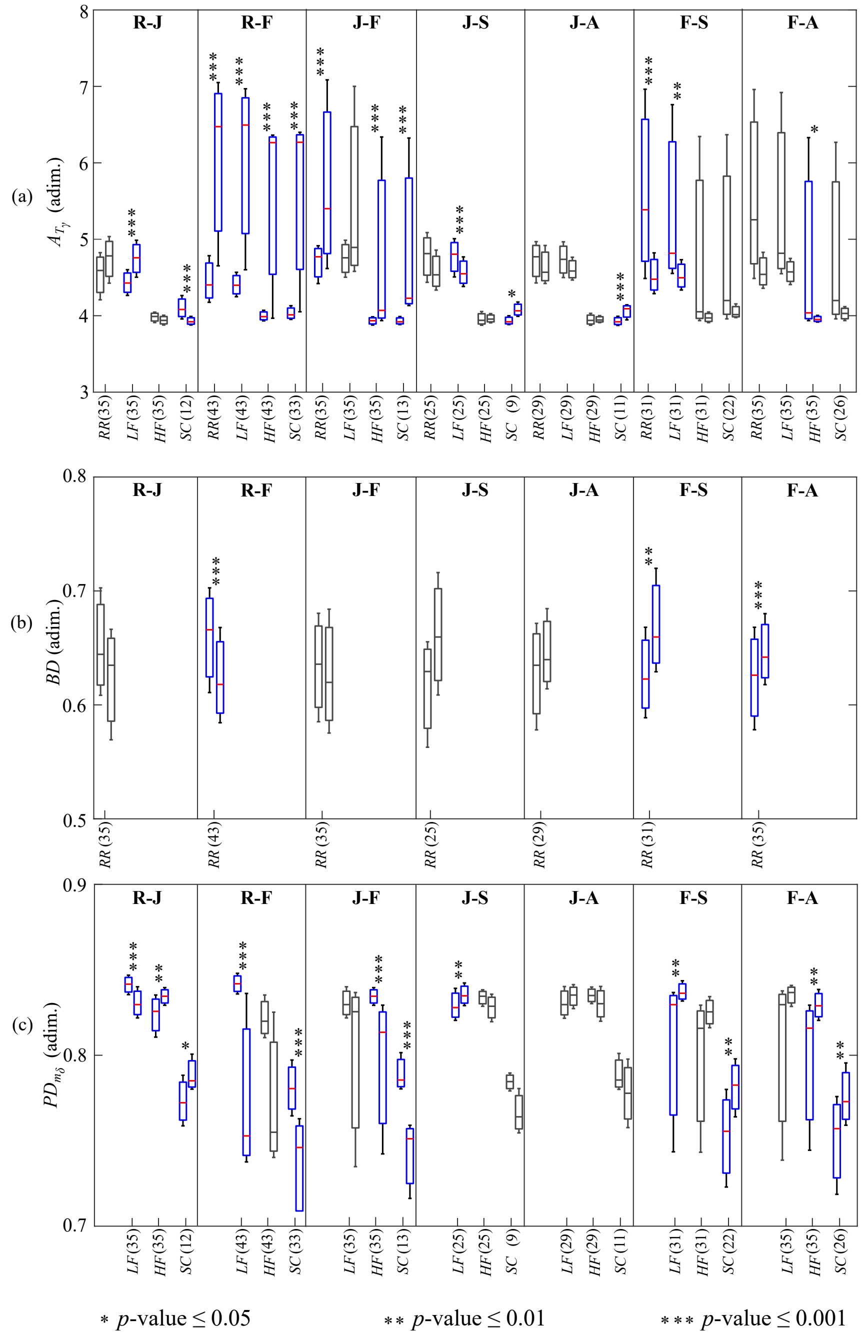

Figure 4.4: Boxplots of the parameters derived from the AMIF: (a) A_{T_γ} for $\gamma = \{RR, LF, HF, SC\}$; (b) BD analyzed on $RR(t)$; and (c) PD_{m_δ} for $\delta = \{LF, HF, SC\}$. Only compared elicitations with statistically significant differences are presented: relax and joy (R-J), relax and fear (R-F), joy and fear (J-F), joy and sadness (J-S), joy and anger (J-A), fear and sadness (F-S) and fear and anger (F-A). Statistical significance is denoted by: * for p-value ≤ 0.05, ** for p-value ≤ 0.01 and *** for p-value ≤ 0.001, all showed sensitivity, specificity and accuracy values $\geq 70\%$ and AUC index ≥ 0.70. The number of the analyzed subjects is indicated in parentheses.

Table 4.3: Values of p-value, AUC and accuracy for the parameters derived from the AMIF which statistically discriminate between some pair of elicitations: relax and joy (R-J), relax and fear (R-F), joy and fear (J-F), joy and sadness (J-S), joy and anger (J-A), fear and sadness (F-S) and fear and anger (F-A). The number of the analyzed subjects for each parameter and pair of elicitations is indicated in parentheses.

Parameters	R-J	R-F	J-F	J-S	J-A	F-S	F-A
$A_{T_{RR}}$	(35)	(43)	(35)	(25)	(29)	(31)	(35)
p-value	n.s.	**≤0.001**	**≤0.001**	n.s.	n.s.	**≤0.001**	≤0.001†
AUC	0.62	**0.81**	**0.72**	0.63	0.55	**0.73**	0.72
Accuracy (%)	61	**77**	**71**	64	60	**73**	73
$A_{T_{LF}}$	(35)	(43)	(35)	(25)	(29)	(31)	(35)
p-value	**≤0.001**	**≤0.001**	≤0.05	**≤0.001**	≤0.05	**≤0.01**	≤0.05
AUC	**0.76**	**0.82**	0.64	**0.71**	0.62	**0.73**	0.67
Accuracy (%)	**73**	**78**	66	**70**	62	**70**	64
$A_{T_{HF}}$	(35)	(43)	(35)	(25)	(29)	(31)	(35)
p-value	n.s.	**≤0.001**	**≤0.001**	n.s.	n.s.	≤0.001	**≤0.05**
AUC	0.63	**0.71**	**0.77**	0.58	0.53	0.67	**0.70**
Accuracy (%)	64	**70**	**71**	62	57	65	**70**
$A_{T_{SC}}$	(12)	(33)	(13)	(9)	(11)	(22)	(26)
p-value	**≤0.001**	**≤0.001**	**≤0.001**	**≤0.05**	**≤0.001**	≤0.01	≤0.05
AUC	**0.83**	**0.75**	**0.95**	**0.88**	**0.85**	0.66	0.68
Accuracy (%)	**75**	**74**	**92**	**78**	**77**	66	71
BD	(35)	(43)	(35)	(25)	(29)	(31)	(35)
p-value	≤0.01	**≤0.001**	≤0.01	≤0.01	n.s.	**≤0.01**	**≤0.001**
AUC	0.65	**0.78**	0.68	0.67	0.62	**0.72**	**0.71**
Accuracy (%)	67	**77**	67	66	60	**73**	**73**
$PD_{m_{LF}}$	(35)	(43)	(35)	(25)	(29)	(31)	(35)
p-value	**≤0.001**	**≤0.001**	≤0.01	**≤0.01**	n.s.	**≤0.01**	≤0.05
AUC	**0.76**	**0.81**	0.63	**0.71**	0.61	**0.70**	0.67
Accuracy (%)	**73**	**77**	69	**70**	60	**70**	63
$PD_{m_{HF}}$	(35)	(43)	(35)	(25)	(29)	(31)	(35)
p-value	**≤0.01**	≤0.001†	**≤0.001**	n.s.	n.s.	≤0.01	**≤0.01**
AUC	**0.70**	0.71	**0.81**	0.64	0.59	0.68	**0.72**
Accuracy (%)	**71**	72	**80**	66	64	68	**70**
$PD_{m_{SC}}$	(12)	(33)	(13)	(9)	(11)	(22)	(26)
p-value	**≤0.05**	**≤0.001**	**≤0.001**	n.s.	n.s.	**≤0.01**	**≤0.01**
AUC	**0.72**	**0.81**	**0.99**	0.79	0.64	**0.74**	**0.70**
Accuracy (%)	**75**	**77**	**96**	78	68	**70**	**70**

n.s. Stands for non-significant.

† Sensitivity or specificity ≤ 70%.

Note that parameters with $p \leq 0.05$, AUC index ≥ 0.70, sensitivity, specificity, accuracy values $\geq 70\%$ are remarked in bold type.

4.3.3 CMIF-based measures

All parameters derived from the CMIF have been evaluated, however, only those that revealed statistically significant differences for their ability to discriminate between pair of emotions are shown in Fig. 4.5. In this figure, boxplots are shown in terms of median and interquartile ranges as first and third quartile: $CMIF_{0_\gamma}$ (Fig. 4.5a); $CMIF_{max_\gamma}$ (Fig. 4.5b) and τ_{max_γ} (Fig. 4.5c) for the coupling between each signal $\gamma = \{RR, SC\}$ and $r(t)$.

In Table 4.4, p-value, AUC and accuracy values are remarked in bold type for those CMIF-based parameters that revealed statistically significant differences between the emotional states studied. The presented elicited conditions were those which revealed statistically significant differences.

4.4 Discussion

The AMIF and the CMIF techniques have been proposed to study the non-linear relationships between HRV and respiration for human emotion recognition. Both non-linear techniques may provide complementary information to that captured by linear techniques for emotion recognition.

The adequate number of bins I was estimated to adapt the AMIF and the CMIF algorithms to short-time signals for emotion recognition, since the values of I applied to long-term HRV may not be suitable for short-term. The value of I determines the histogram partitioning. The greater the I value is, the histogram represents more faithfully the probability density function. Nevertheless, each partitioning of the histogram needs to contain a minimum number of samples in order to capture the regularity and complexity signal contain more appropriately. Therefore, a compromise between the greatest number of partitioning of the histogram for faithfully describing the signal, and the adequate number of samples contained in each partitioning, should be taken into consideration.

In [49], the AMIF and the CMIF histogram were constructed by using 2^5 bins, when studying short-term RR signals according to Task Force guidelines [87, 93], in a group of patients after acute myocardial infarction and a control group. However, 2^3 bins were proposed in [48] for the AMIF histogram computation for short and

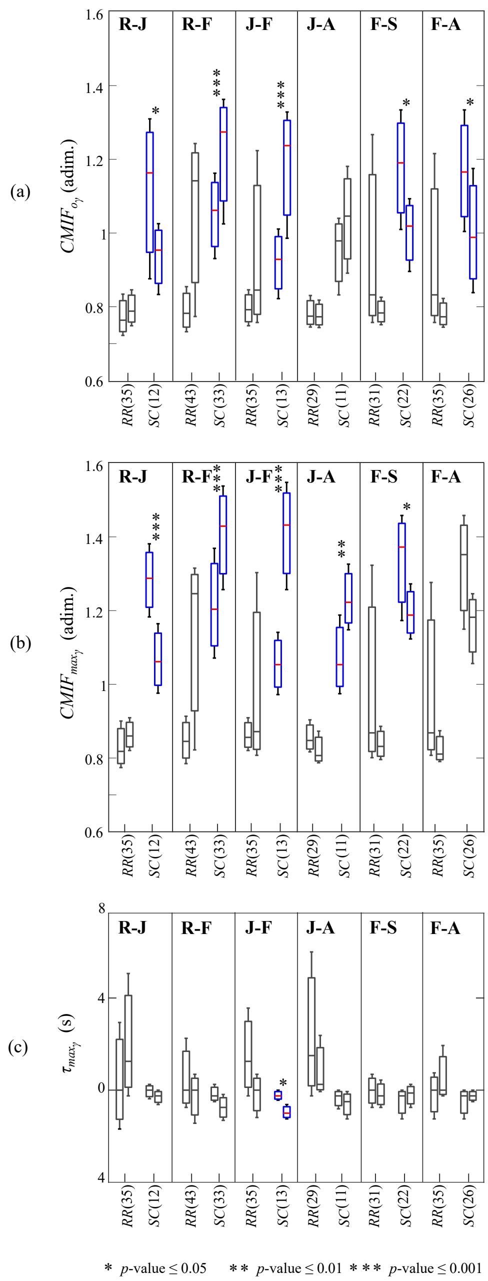

Figure 4.5: Boxplots of the parameters derived from the CMIF: (a) $CMIF_{0_\gamma}$, (b) $CMIF_{max_\gamma}$ and (c) τ_{max_γ}, for the coupling between each of the signals $\gamma = \{RR, SC\}$ and $r(t)$ and all emotion conditions studied with statistically significant differences: relax and joy (R-J), relax and fear (R-F), joy and fear (J-F), joy and anger (J-A), fear and sadness (F-S) and fear and anger (F-A). Statistical significance is denoted by: * for p-value ≤ 0.05, ** for p-value ≤ 0.01 and *** for p-value ≤ 0.001, all with sensitivity, specificity and accuracy $\geq 70\%$ and AUC index ≥ 0.70. In each x-axis the number of the analyzed subjects is indicated in parentheses.

long-term signals, to analyze the risk stratification of patients with multiple organ dysfunction syndrome, cardiac arrest patients and a control group. In this work, the

Table 4.4: Values of p-value, AUC and accuracy for the parameters derived from the CMIF which statistically discriminate between some pair of elicitations: relax and joy (R-J), relax and fear (R-F), joy and fear (J-F), joy and anger (J-A), fear and sadness (F-S) and fear and anger (F-A). The number of the analyzed subjects for each parameter and pair of elicitations is indicated in parentheses.

Parameters	R-J	R-F	J-F	J-A	F-S	F-A
$CMIF_{0_{RR}}$	(35)	(43)	(35)	(29)	(31)	(35)
p-value	n.s.	≤0.001†	≤0.01	n.s.	≤0.01	≤0.05
AUC	0.61	0.75	0.65	0.53	0.65	0.65
Accuracy (%)	61	78	70	53	66	64
$CMIF_{0_{SC}}$	(12)	(33)	(13)	(11)	(22)	(26)
p-value	**≤0.05**	**≤0.001**	**≤0.001**	n.s.	**≤0.05**	**≤0.05**
AUC	**0.70**	**0.73**	**0.85**	0.69	**0.72**	**0.70**
Accuracy (%)	**71**	**73**	**85**	64	**70**	**70**
$CMIF_{max_{RR}}$	(35)	(43)	(35)	(29)	(31)	(35)
p-value	n.s.	≤0.001†	≤0.05	n.s.	≤0.01	n.s.
AUC	0.62	0.72	0.60	0.64	0.63	0.66
Accuracy (%)	64	76	70	66	68	63
$CMIF_{max_{SC}}$	(12)	(33)	(13)	(11)	(22)	(26)
p-value	**≤0.001**	**≤0.001**	**≤0.001**	**≤0.01**	**≤0.01**	≤0.01
AUC	**0.88**	**0.74**	**0.95**	**0.79**	**0.77**	0.68
Accuracy (%)	**83**	**71**	**85**	**77**	**75**	69
$\tau_{max_{RR}}$	(35)	(43)	(35)	(29)	(31)	(35)
p-value	n.s.	n.s.	n.s.	n.s.	n.s.	n.s.
AUC	0.62	0.53	0.66	0.56	0.53	0.55
Accuracy (%)	66	55	67	57	56	57
$\tau_{max_{SC}}$	(12)	(33)	(13)	(11)	(22)	(26)
p-value	n.s.	≤0.01	**≤0.05**	n.s.	≤0.05	n.s.
AUC	0.62	0.68	**0.75**	0.66	0.62	0.51
Accuracy (%)	63	65	**77**	68	61	60

n.s. Stands for non-significant.

† Sensitivity or specificity $\leq$ 70%.

Note that parameters with $p \leq 0.05$, AUC index ≥ 0.70, sensitivity, specificity, accuracy values $\geq 70\%$ are remarked in bold type.

highest percentage of number of parameters that presents statistically significant differences (p-value ≤ 0.001) between each pair of elicited states was obtained for $I = 2^5$ bins, (see Fig. 4.3).

Table 4.5 displays the parameters which statistically discriminate between each pair of elicitations. The pair of elicited conditions which did not show statistically significant differences by means of any of the parameters considered in this work were: relax and sadness (R-S), relax and anger (R-A) and sadness and anger (S-A). It should be noted that no statistically significant differences between relax and emotions or between pairs of emotions were found by any parameter derived from analysis of the coupling between the signals $RR(t)$ and $r(t)$. As it was found by analyzing the AMIF technique, the pair of elicitation conditions which did not show statistically significant differences in the CMIF by means of any of the parameters considered was: relax and sadness (R-S), relax and anger (R-A), joy and sadness (J-S) and sadness and anger (S-A).

Table 4.5: Parameters derived from the AMIF and the CMIF which statistically discriminate between the studied elicitations.

Compared elicited states	R-J	R-F	J-F	J-S	J-A	F-S	F-A
Parameters derived from the AMIF							
$A_{T_{RR}}$	-	yes	yes	-	-	yes	-
$A_{T_{LF}}$	yes	yes	-	yes	-	yes	-
$A_{T_{HF}}$	-	yes	yes	-	-	-	yes
$A_{T_{SC}}$	yes	yes	yes	yes	yes	-	-
BD	-	yes	-	-	-	yes	yes
$PD_{m_{LF}}$	yes	yes	-	yes	-	yes	-
$PD_{m_{HF}}$	yes	-	yes	-	-	-	yes
$PD_{m_{SC}}$	yes	yes	yes	-	-	yes	yes
Parameters derived from the CMIF							
$CMIF_{0_{SC}}$	yes	yes	yes	-	-	yes	yes
$CMIF_{max_{SC}}$	yes	yes	yes	-	yes	yes	-
$\tau_{max_{SC}}$	-	-	yes	-	-	-	-

The nomenclature used for the elicited states is:
relax (R), joy (J), fear (F), sadness (S) and anger (A)

Regarding the ability of the AMIF parameters to discriminate emotions, the total areas (Fig. 4.4a), $A_{T_{SC}}$ was the only parameter capable of statistically distinguishing joy and anger among all the studied parameters derived from the AMIF. This result shows the importance of redefining the boundary of the HF band for a correct evaluation of physiological changes of the ANS [42,100]. Fear revealed a greater median value than any other emotion. It can be noted that an enlargement of the area under the AMIF curve indicates a better predictability of future heart beats, and therefore, a lower complexity [12].

Evaluating the beat decay BD (Fig. 4.4b), fear presented smaller median values than any other compared elicitation. Furthermore, this parameter was able to statistically distinguish between fear and relax, sadness and anger. However, the remaining pair of compared elicited states did not show such a clear pattern as fear. Additionally, PD_{m_δ} (Fig. 4.4c) presented a similar tendency as the BD for fear with a smaller median value than any other elicitation state. The BD and PD_{m_δ} presented results with complementary information, and statistically significant values, and also adequate sensitivity, specificity, accuracy and AUC index.

The CMIF has been proposed to reveal non-linear cardiorespiratory interdependencies [49], which might be altered during emotion elicitation. For example, a significant increase in the CMIF of electroencephalographic signals has been also observed in the presence of stress [1]. In our study, the parameter $CMIF_{0_{SC}}$ (Fig. 4.5a) and the parameter $CMIF_{max_{SC}}$ (Fig. 4.5b) provide similar information, although the slight differences in the calculation of both parameter revealed that $CMIF_{max_{SC}}$ is able to discriminate with an equal or better p-value, sensitivity, specificity, accuracy and AUC index than $CMIF_{0_{SC}}$ in all compared elicited states, except for fear and anger. Moreover, evaluating $CMIF_{0_{SC}}$ and $CMIF_{max_{SC}}$, it is possible to extract a similar pattern for fear presenting a greater median value than any other elicited state.

The time lag between $CMIF_0$ and $CMIF_{max}$ in the SCHF band was only able to distinguish between joy and fear, and it suggested less non-linear correlation between HRV and respiration during joy. A complexity reduction is observed during fear elicitation as reflected by a lower value of parameter $\tau_{max_{SC}}$.

Furthermore, joy or fear versus sadness can be discriminated by parameters obtained from $RR_{LF}(t)$ signals and joy or fear versus anger from $RR_{HF}(t)$ signals. Predominant autonomic rhythms can be assessed by the complex information loss over their respective prediction time horizon [49]. In this sense, those parameters studied in the LF band reflect the complexity of vagal and sympathetic mechanisms, and those parameters studied in the HF band reflect the complexity of vagal and respiratory rhythms [49].

Comparing the results obtained from the AMIF and the CMIF techniques, it is worth noting that filtering the HRV signals into a redefined HF band presents better discrimination power for parameters derived from the AMIF than from the CMIF ones. Furthermore, applying the CMIF into the RR time series filtered into the redefined HF band provided relevant complexity information to discriminate between HRV and respiratory mechanisms in the case of fear.

A complexity reduction is observed during fear elicitation as reflected by smaller BD, PD_{m_δ} and $\tau_{max_{SC}}$ values together with a greater total area, $CMIF_{0_{SC}}$ and $CMIF_{max_{SC}}$.

In [13], a physiological explanation of non-linear HRV parameters was reported. In this work, non-linear HRV indices during ANS pharmacological blockade and body position changes were studied in order to assess their relation with sympathetic and parasympathetic activities. Parasympathetic blockade caused a significant decrease in complexity values, while sympathetic blockade produced a significant increase in the non-linear parameters. We hypothesize that the decrease in complexity observed during fear elicitation reflects vagal activity, while more random RR series during joy might reflect sympathetic activity.

The results derived from this work have been compared with a previous work on the same emotion database, where a linear-based methodology was applied [100] (Table 4.6). In both cases the HF band was analyzed after redefining it considering the HRV-respiration interaction [100]. All the elicited states able to be discriminated with linear techniques, remain discriminated with the non-linear features (Table 4.6). In addition, during fear elicitation, heart rate presents a better predictability, implying lower complexity, as compared to other elicited states, resulting in extra discriminating power between fear and relax or anger (Table 4.6) non accessible from linear features. These results may indicate that the non-linear indexes are suitable for discrimination between different emotions.

Furthermore, other non-linear HRV parameters as the Correlation Dimension, the

Table 4.6: Discriminating possibility in comparing between elicited states with linear and non-linear techniques.

Compared elicited states	Linear techniques [100]	Non-linear techniques (This work)
R-J	yes	yes
R-F	no	yes
R-S	no	no
R-A	no	no
J-F	yes	yes
J-S	yes	yes
J-A	yes	yes
F-S	yes	yes
F-A	no	yes
S-A	no	no

The nomenclature used for the elicited states is:
relax (R), joy (J), fear (F), sadness (S) and anger (A)

Approximate Entropy and the Sample Entropy have been investigated in the same emotional database. However, these parameters did not present the ability to separate the emotional states in this analyzed database (Table 4.7, Table 4.8). Although in some comparisons exposed in Table 4.8 the p-value ≤ 0.05, AUC index ≥ 0.7, or sensitivity, specificity or accuracy $\geq 70\%$ criteria were not met.

Table 4.7: Median with the first and third interquartile ranges in terms of (m(1st|3th)) for the non-linear techniques Correlation Dimension (D2), Approximate Entropy (ApEn) and Sample Entropy (SampEn) for the elicitations: relax, joy, fear, sadness and anger.

Elicited states	D2	ApEn	SampEn
Relax	4.18 (3.72|4.63)	0.84 (0.78|0.91)	1.09 (0.96|1.29)
Joy	3.89 (3.32|4.60)	0.84 (0.71|0.93)	1.13 (0.81|1.23)
Fear	4.20 (3.69|4.87)	0.85 (0.79|0.95)	1.18 (0.93|1.33)
Sadness	4.42 (4.06|4.73)	0.87 (0.81|0.93)	1.14 (0.98|1.34)
Anger	4.21 (3.84|4.67)	0.89 (0.78|0.93)	1.15 (0.90|1.31)

In Table 4.1, there are summarized the non-linear techniques used to detect emotional stimuli based on HRV analysis. In [101], the emotional states were conceptualized in two dimensions by the terms of valence and arousal. The Dominant Lyapunov Exponent and the Approximate Entropy techniques showed differences between the neutral and the arousal elicitation. These results are in concordance with the ones obtained in this study by means of the AMIF and the CMIF techniques, since statistically significant differences between the neutral state of relax and the two high arousal elicitations of joy and fear were found. Furthermore, it was found in [101] that the Dominant Lyapunov Exponent became negative, and the mean Approximate Entropy decreased during arousal elicitation. In accordance with the Dominant Lyapunov Exponent and the Approximate Entropy, during fear elicitation the non-linear HRV parameters obtained in the present study revealed a reduced complexity level. In [12], an increment of the total area under the AMIF curve was observed revealing an indication of decreased complexity of cardiac regulation in depressed patients. However, in [111], a consistent increasing trend among most entropy measures for different depression levels was found. This suggested a reduced regularity and predictability of the depressed patients. The depression state is considered by means of the circumplex model of affect as having negative valence with low arousal, as can be sadness [101]. Considering the parameter $A_{T_{RR}}$ in the comparison between fear and sadness (emotional states with the same negative valence but different arousal), it could be observed that sadness presents a lower median value, being an indicator of decreased complexity as reported in [12], and being in agreement with the results obtained by [111]. In [109], a significantly increase of the entropy measures was found during the emotional states of happiness, sadness, anger, and disgust. These results are in concordance with the ones obtained in this study for fear, which revealed increased regularity and a reduced unpredictability. In [30], significant decreases in the Entropy, the Dominant Lyapunov Exponent, and the Pointwise Correlation Dimension, and an increase in the short-term fractal-like scaling exponent of the Detrended Fluctuation Analysis were found during anxiety situations, compared with the rest period. These results suggest that an increase of anxiety was related to the decrease in the complexity. The anxiety state can be considered by means of the circumplex model of affect [101] as having negative valence with high arousal, similar to fear. Both the state of anxiety studied in [30] and the emotional state of fear, studied in this work, presented the same tendency in level of complexity. In [43], maximum changes in the Lagged Poincaré Plot measures were found during the happiness stimuli, and minimum changes were obtained during the fear inducements. These results are in agreement with the ones obtained by means the CMIF technique applied in the present study, were differences between joy and fear could be found.

There are also some limitations to note regarding this study. First, the sample size database used is small. Nonetheless, the results obtained advocated in support of using the proposed approaches, although a bigger sample size database could probably yield better statistics. Second, likewise, long-time emotional monitoring could probably provide additional information that cannot be detected in short-time series analyzes. Although, short-term emotional analyzes are more suitable for outpatient patient monitoring and applications where the result is urgently needed. Third, there are emotions that could not be expressed by the subject all the time the videos last, but they have been treated as if the subject expresses that emotion all the time.

Despite these limitations, the parameters derived from the AMIF and the CMIF techniques which presented statistically significant differences for emotion discrimination seem to be good candidates to be implemented on a biomedical equipment, providing a tool for mental illness diagnoses. In addition, analyzing the role of mutual information-based HRV measures to explore a multi-variable approach combining with other non-linear parameters could open a door to extract new suitable parameters for emotion recognition.

Table 4.8: Values of p-value, AUC index, sensitivity, specificity and accuracy for the non-linear techniques Correlation Dimension (D2), Approximate Entropy (ApEn) and Sample Entropy (SampEn) for all elicitation compared.

Compared elicited states	Parameter	D2	ApEn	SampEn
Relax vs. Joy	*p*-value	n.s.	n.s.	n.s.
	AUC	0.57	0.50	0.55
	Sensitivity (%)	51	40	46
	Specificity (%)	69	77	69
	Accuracy (%)	60	59	57
Relax vs. Fear	*p*-value	n.s.	0.03	n.s.
	AUC	0.52	0.58	0.53
	Sensitivity (%)	56	44	47
	Specificity (%)	49	77	72
	Accuracy (%)	52	60	59
Relax vs. Sadness	*p*-value	n.s.	n.s.	n.s.
	AUC	0.54	0.53	0.53
	Sensitivity (%)	63	57	57
	Specificity (%)	57	53	57
	Accuracy (%)	60	55	57
Relax vs. Anger	*p*-value	n.s.	n.s.	n.s.
	AUC	0.54	0.57	0.56
	Sensitivity (%)	56	62	59
	Specificity (%)	59	59	62
	Accuracy (%)	57	60	60
Joy vs. Fear	*p*-value	n.s.	n.s.	n.s.
	AUC	0.56	0.54	0.56
	Sensitivity (%)	60	63	43
	Specificity (%)	52	46	74
	Accuracy (%)	56	54	59
Joy vs. Sadness	*p*-value	0.01	0.05	0.01
	AUC	0.70	0.57	0.60
	Sensitivity (%)	80	68	76
	Specificity (%)	64	52	48
	Accuracy (%)	72	60	62
Joy vs. Anger	*p*-value	n.s.	n.s.	0.04
	AUC	0.62	0.55	0.60
	Sensitivity (%)	72	55	41
	Specificity (%)	55	62	83
	Accuracy (%)	64	59	62
Fear vs. Sadness	*p*-value	n.s.	n.s.	n.s.
	AUC	0.58	0.49	0.52
	Sensitivity (%)	84	68	65
	Specificity (%)	45	45	45
	Accuracy (%)	65	56	55
Fear vs. Anger	*p*-value	n.s.	n.s.	n.s.
	AUC	0.52	0.53	0.48
	Sensitivity (%)	66	71	57
	Specificity (%)	49	40	49
	Accuracy (%)	57	56	53
Sadness vs. Anger	*p*-value	n.s.	n.s.	n.s.
	AUC	0.58	0.53	0.50
	Sensitivity (%)	60	60	44
	Specificity (%)	60	44	68
	Accuracy (%)	60	52	56

Chapter 5

Classification Analysis

Contents

5.1 Introduction

New generations of human emotion recognition tools are based in classification analysis. A wide range of methods has been used to study affective states. Classifiers like Fisher Discriminant [60], Linear Discriminant Function [107], k-Nearest Neighbour [107], Multilayer Perceptron [107], Neural Networks [50, 59], Support Vector Machines [50, 53, 60] and others are useful to detect emotional elicitation states. Some of these techniques have also been used to study relationships between HRV and respiration signals [50, 107]. Table 5.1 reports a summary of different classification techniques applied to HRV parameters during diverse emotional states.

Table 5.1: Summary of classification techniques applied to HRV parameters in different emotional states.

Ref.	Emotional state	Technique	Classification rate
[50]	relax, neutral, startle, apprehension and very apprehension	ANN	77.3%
		SVM	78.5%
		RF	80.8%
		NFS	84.3%
[107]	joy, anger, sadness and pleasure	MP	88.6%
		kNN	90.9%
		LDF	92.1%
[53]	sadness, anger, stress, surprise	SVM	61.8%
[59]	sadness, anger, fear, surprise, frustration, amusement	kNN	72.3%
		LDF	75.0%
		MBP	84.1%
[60]	amusement, contentment, disgust, fear, neutrality, sadness	FD + SVM	92.0%

The nomenclature used is:
Articial Neural Networks (ANN), Support Vector Machines (SVM), Random Forests (RF),
Neuro-Fuzzy System (NFS), Linear Discriminant Function (LDF), k-Nearest Neighbour (kNN),
Multilayer Perceptron (MP), Marquardt Backpropagation (MBP), Fisher Discriminant (FD)

In this chapter the classification ability of the HRV parameters presented in previous chapters is investigated using a linear discriminant analysis. The choice of linear discriminant analysis instead of other more complex approaches, such as ANN or SVM, is motivated to facilitate the interpretation of the classification model and to prevent overfitting due to the reduced number of subjects in the database. A linear classifier has been used to identify the best subset of HRV parameters to discriminate between pairs of emotions and between emotional valences.

5.2 Methods

The linear discriminant analysis is a statistical method used to construct a predictive model of group classification based on the characteristics observed for each case [58]. The method generates a discriminant function based on linear combinations of the prediction parameters, which allows to obtain the best classification between groups.

The use of a statistical test, such as the analysis of variance (ANO-VA, *ANalysis Of VAriance*), quantitatively determines how separate the values that each characteristic of the analysis takes in the different groups through the significance obtained in the rejection or acceptance of the null hypothesis [2, 46]. In order the results derived from the statistical study to be considered valid, it is necessary that the characteristics studied meet the normality requirement: they must present a normal or Gaussian distribution and they have equal variances in the groups.

5.2.1 Estimation of discriminant function

The discriminant function is generated from the values of the prediction parameters of a set of cases whose classification in the different groups is known. Then, this function can subsequently be applied to new cases where the classification is not known, from measurements of the parameters on which the prediction is based. For the classification into two groups, a unique discriminating function needs to be built. The coefficients of the discriminant function are estimated by means of the Fisher procedure. This procedure assigns weights to the parameters which maximizes the variability between the groups (variance between groups) and minimizes the variability within the groups (intragroup variance).

Once the coefficients of the discriminant function have been obtained, the discriminant scores, d (equation (5.1)), for each case are calculated. The scores are the basis for the classification in one of the groups.

$$d = c_0 + c_1\chi^1 + + c_p\chi^p = c^T\chi \tag{5.1}$$

where c_j, j = 0, ..., p, are the coefficients of the discriminant function and χ^j represent the values of the p parameters selected for each case. The values of the discriminant scores d defined by the c_j coefficients should be close between cases of the same group, and differ as much as possible between cases of different groups. Therefore, this criterion maximizes the variability between the groups (maximizes the variance between groups) while minimizes the variability within the groups (intragroup variance).

Once the discriminant function has been obtained and the discriminant scores calculated for each case, a classification rule is used to make the assignment to a specific group. The classification of each case with a score of d in group g is done by means of the Bayes classification rule [79].

5.2.2 Parameter selection

During the process of parameter selection, all the parameters considered in this study could be included in order to have a greater number of degrees of freedom in the discriminant function, and thus obtain a better classification. However, a commonly accepted and widely used rule is that the number of classification parameters should be less than the square root of the number of cases in the smallest group. In fact, the use of an excessive number of parameters with respect to the number of cases leads to a biased estimate of the discriminant function, which decreases their ability to classify new cases [4].

It is applied a forward-backward selection method that allows a reduction in the number of parameters involved in discrimination. In each step new parameters are added or excluded, so that in each step it is obtained the set of parameters with greater discriminant power according to a certain statistical criterion. Among the criteria for selecting parameters in this study the Wilks′s Lambda minimization and the F statistic have been used.

Wilks′s Lambda (Λ) distribution is a probability distribution used especially in the context of the likelihood-ratio and multivariate analysis of variance [62]. Λ represents the proportion of the total variability due to differences within groups or, alternatively, the proportion of variability not explained by differences between groups. It is calculated as the ratio of the intragroup covariance, C_I, which is the sum of intragroup squares, measuring the variability within each group, and the total covariance matrix, C_T, which is the sum of total squares, measuring the total variability, according to the equation (5.2) [78].

$$\Lambda = \frac{|C_I|}{|C_T|} \tag{5.2}$$

The value of Wilks′s Lambda is limited between 0 and 1. Values close to 0 indicate that the means of the groups are different (the variability within the groups is small compared to the total variability) while values close to 1 indicate that the means are close. Although Wilks′s Lambda criterion identifies the parameters with the greatest discriminating power, it is the F statistic that determines which parameters should be taken into account in the model [78]. The F statistic is calculated based on the Wilks′s Lambda according to the equation (5.3).

$$F = \frac{N-G-p}{G-1} \frac{1-\frac{\Lambda_{p+1}}{\Lambda_p}}{\frac{\Lambda_{p+1}}{\Lambda_p}} \tag{5.3}$$

N is the total number of cases, G is the number of groups, p is the number of independent parameters, Λ_p is the Wilks′s Lambda calculated before the inclusion of the variable being evaluated, and Λ_{p+1} is the Wilks′s Lambda calculated after the inclusion of the variable. The F statistic represents the increase produced in discrimination after the inclusion of the parameter $p+1$ with respect to the total already reached with the p parameters previously included. The stepwise inclusion method are:

- First step: if the input criterion is met (F statistic is statistically significant

(F>3.84)) the parameter with the lowest value of the Wilks′s Lambda is included.

- Second step: if the input criterion is met, the included parameter is matched with each of the remaining parameters and that pair with the highest value of the F statistic is chosen.

- Third and subsequent steps: the third and subsequent parameters are selected in a similar way, but checking after each step if the previously included parameters remain significant or if, on the contrary, they can be excluded if they meet the exit criteria (F<2.1). When none of the parameters included meet the input and the exit criterion the process of parameter selection ends.

5.2.3 Performance measures of a classifier

To improve the estimation of the correct classification rate, the cross validation technique leaving-one-out method has been applied [71]. In this method, each case is classified by the discriminant function derived from all cases except it. This method is the one used in this study because it corresponds to a more realistic situation, since the case that is classified does not intervene in the elaboration of the model [32].

In addition to the classification rate, there are other classifier performance measures interesting to analyze. If the cases are available in two groups, positive and negative, the results of the classifier can be divided into:

- True positive (TP): cases that are positive, and the classifier considers positive.

- False negatives (FN): cases that are positive, but that are classified as negative.

- True Negative (TN): cases that are negative, and the classifier considers negative.

- False positives (FP): cases that are negative, and the classifier considers positive.

The parameters that allow evaluating the performance of a classifier are defined below:

- Sensitivity (Se): it is defined as the percentage of cases classified as positive among all positive cases (5.4).

$$Se(\%) = \frac{TP}{TP+FN}100 \tag{5.4}$$

- Specificity (Sp): it is defined as the percentage of cases considered negative by the classifier, among all the negative cases (5.5).

$$Sp(\%) = \frac{TN}{TN+FP}100 \tag{5.5}$$

- Positive predictive value (P+): it is the percentage of cases classified as positive, which are really positive (5.6).

$$P+(\%) = \frac{TP}{TP+FP}100 \tag{5.6}$$

- Negative predictive value (P-): it is the percentage of cases classified as negative, which are really negative (5.7).

$$P-(\%) = \frac{TN}{TN+FN}100 \tag{5.7}$$

- Accuracy (Acc): it is the percentage of cases classified correctly. It is, in fact, the classification rate (5.8).

$$Acc(\%) = \frac{TP+TN}{TP+FP+TN+FN}100 \tag{5.8}$$

In a good classifier, all values should be close to 100%. There is no point in obtaining a very high sensitivity value if the specificity is very low, and vice versa. In general, increasing sensitivity decreases specificity and vice versa, so a compromise between the two must be reached.

5.2.4 Parameters considered in the analysis

Only the parameters which presented statistically significant differences in chapter 3 (linear features) and in chapter 4 (non-linear features) were selected as characteristics to be investigated. Nine different subsets of parameters have been analyzed:

- Subset 1 (S1). Classic HRV analysis based on the standard definition of HF band [0.15,0.4 Hz] defined in [93]. The parameters analyzed in this group are: P_{HF}, P_{LFn}, R and F_R.
- Subset 2 (S2). HRV parameters based on the shifted HF band centered at F_R with fixed bandwidth: the HF band was centered at F_R and had a fixed bandwidth of 0.11 Hz (HF_{F_R}). The parameters analyzed in this group are: $P_{HF_{F_R}}$, $P_{LFn_{F_R}}$, R_{F_R} and $F_{R_{F_R}}$.
- Subset 3 (S3). HRV parameters based on the shifted and resized HF band based on Spectrum Correlation (SCHF): the HF band is redefined based on the correlation between the power content of HRV and respiration. The parameters analyzed in this group are: $P_{LFn_{SC}}$, R_{SC} and ρ_{max}.
- Subset 4 (S4). HRV parameters derived from the Auto-Mutual Information Function analysis of HRV: the parameters analyzed in this group are: $A_{T_{RR}}$, $A_{T_{LF}}$,$A_{T_{HF}}$, $PD_{m_{LF}}$ and $PD_{m_{HF}}$.
- Subset 5 (S5). HRV parameters derived from the Auto-Mutual Information Function analysis of HRV and respiration: the parameters analyzed in this group are: $A_{T_{SC}}$ and $PD_{m_{SC}}$.
- Subset 6 (S6). HRV parameters derived from the Cross-Mutual Information Function analysis of HRV: the parameters analyzed in this group are: $CMIF_{0_{RR}}$, $CMIF_{max_{RR}}$ and $\tau_{max_{RR}}$.
- Subset 7 (S7). HRV parameters derived from the Cross-Mutual Information Function analysis of HRV and respiration: the parameters analyzed in this group are: $CMIF_{0_{SC}}$, $CMIF_{max_{SC}}$ and $\tau_{max_{SC}}$.
- Subset 8 (S8). The best characteristics: those parameters which classify be-

tween the groups S1, S2, S3, S4, S5, S6 and S7.

- Subset 9 (S9). The best characteristics which only consider the HRV information: those parameters which classify between the groups S1, S2, S3, S4, S5, S6 and S7, but only take into account the HRV information.

All these nine subsets have been performed into three analyzes attending to the elicitations considered as well as to the normalization of the HRV parameters. And within each analysis, two groups of elicitations (G1 = Group 1; G2 = Group 2) are analyzed as presented below, and are schematized in Table 5.2:

- Analysis 1: classification between relax and emotions which comprises: relax vs. all emotions, relax vs. positive valence (joy), relax vs. all negative valences (fear, sadness and anger), relax vs. fear, relax vs. sadness and relax vs. anger. In this analysis, HRV parameters were considered without any normalization.

- Analysis 2: classification between positive and negative valences and between negative valences which comprise positive valence (joy) vs. all negative valences (fear, sadness and anger), joy vs. fear, joy vs. sadness, joy vs. anger, fear vs. sadness, fear vs. anger and sadness vs. anger. In this analysis, HRV parameters were considered without any normalization.

- Analysis 3: classification between positive and negative valences and between negative valences. In this analysis, HRV parameters were normalized by their value during the relax session which preceded each emotion.

Table 5.2: Relationship between analyzes and groups of elicitations (G1 = Group 1; G2 = Group 2).

Analysis 1		Analysis 2		Analysis 3 (*)	
G1	G2	G1	G2	G1	G2
relax	all emotions	joy	all negative valences	joy	all negative valences
relax	joy	joy	fear	joy	fear
relax	all negative valences	joy	sadness	joy	sadness
relax	fear	joy	anger	joy	anger
relax	sadness	fear	sadness	fear	sadness
relax	anger	fear	anger	fear	anger
		sadness	anger	sadness	anger

(*) HRV parameters were normalized by their value in the preceding relax session.

5.3 Results

In Table 5.3, 5.4 and 5.5, there are shown the number of comparison between each group (G1 for the first group and G2 for the second group), sensitivity, specificity, positive and negative predictive value and accuracy from the parameter set S1 to S9 when comparing between relax and emotions, between emotions and between emotions normalized by the basal condition, respectively.

It can be noted that when sensitivity, specificity and accuracy are all greater than 70% the results are remarked in bold type.

5.3.1 Evaluation of the analysis 1

Regarding the results obtained by the analysis 1 (Table 5.3), it can be observed that only the comparison between relax and joy can be classified by the set of parameters S8 with a sensitivity, sensitivity and accuracy greater than 80%. In the S8 analysis, it was considered the best classified characteristics derived from all set of parameters (i.e. S1, S2, S3, S4, S5, S6 and S7 analysis), therefore the resulting classified parameters are derived from the lineal and the non-linear analysis. The characteristics that classified relax vs. joy were: F_R, $F_{R_{F_R}}$ and R_{SC} for the linear analysis and $A_{T_{SC}}$ and $PD_{m_{HF}}$ for the non-linear analysis. It can be noted that all these parameters take into account the respiratory signal except $PD_{m_{HF}}$. However, it also accounts for the respiratory frequency band information.

5.3.2 Evaluation of the analysis 2

The results regarding the analysis 2 (Table 5.4) are presented by means of the comparisons between positive and negative valences or between negative valences. It can be observed that joy vs. fear could be classified by the sets of parameters S5, S7 and S8, and joy vs. sadness and joy vs. anger by means of the set of parameters S7. It can be noted that the classified characteristics of the S5 and S7 analyzes are based in the SCHF methodology which take into account the respiratory signal information of each subject, and they are also derived from the non-linear methodology, the AMIF and the CMIF, respectively.

The characteristics which best classify joy and fear are: F_R derived from the linear analysis, $PD_{m_{SC}}$ derived from the AMIF non-linear technique and considering the HF_{SC} band, and $CMIF_{max_{SC}}$ derived from the CMIF non-linear technique and also considering the HF_{SC} band. The characteristic which best classify joy vs. sadness and joy vs. anger is $CMIF_{max_{SC}}$. Therefore, the common characteristic which classify among all these groups is $CMIF_{max_{SC}}$.

5.3.3 Evaluation of the analysis 3

It can be observed in Table 5.5 that positive vs. all negative valences, joy vs. fear, joy vs. sadness, joy vs. anger and fear vs. sadness can be all classified by the set of parameters S7, which is derived from the CMIF non-linear technique and also it considers the SCHF method, with a sensitivity, sensitivity and accuracy greater than 80%. It needs to be pointed out that both methodologies, the CMIF and the SCHF combined, consider the cardiorespiratory coupling between the HRV and respiratory signals. It can be observed that the characteristic able to classify between all these groups is the parameter $CMIF_{max_{SC}}$.

Each of the comparisons is analyzed in detail below. Related to the comparison between joy with all negative valences together (fear, sadness and anger) the best results are obtained from the sets of parameters S7, S8, and S9. The resulting classificatory characteristics are: $CMIF_{max_{SC}}$ for S7; R, $F_{R_{F_R}}$, R_{F_R}, ρ_{max} and $CMIF_{max_{SC}}$ for S8; and R and $PD_{m_{HF}}$ for S9. With regard to analyzing joy with each single negative valence, the results obtained are the following. About joy vs. fear, the best classificatory characteristics are derived from S3, S7, S8 and S9 analysis. The resulting classificatory characteristics are: ρ_{max} for S3; $CMIF_{max_{SC}}$ for S7; F_R and $CMIF_{max_{SC}}$ for S8; and R and $PD_{m_{HF}}$ for S9. In respect of joy vs. sadness, the sets of characteristics which are good candidates to classify between both groups are ρ_{max}

for S3; $CMIF_{max_{SC}}$ for S7; and ρ_{max}, $A_{T_{LF}}$ and $CMIF_{max_{SC}}$ for S8. As regard joy vs. anger, again the analysis S3, S7 and S8 presents the best set of characteristics which discriminates between both emotions as ρ_{max} for S3; $CMIF_{max_{SC}}$ for S7; and ρ_{max}, $PD_{m_{LF}}$ and $CMIF_{max_{SC}}$ for S8. Analyzing fear vs. sadness, it can be observed that only the S7 analysis can provide a classificatory characteristic: $CMIF_{max_{SC}}$.

Table 5.3: Classification results obtained by the analysis 1: number of comparison between group 1 (G1) and group 2 (G2), sensitivity, specificity, positive and negative predictive value, accuracy and characteristics classified from the analysis S1 to S9.

	S1		S2		S3		S4		S5		S6		S7		S8		S9	
	G1	G2	G1	G2	G1	G2	G1	G2	G1	G2	G1	G2	G1	G2	G1	G2	G1	G2
Relax vs. all emotions																		
Number of comparisons	88	153	79	136	71	112	88	153	71	112	88	153	71	112	71	112	88	153
Se(%)/Sp(%)	–	–	–	–	45.1	64.3	80.7	41.8	87.3	24.1	73.9	32.7	63.4	41.1	78.4	45.8	80.7	41.8
P+(%)/P-(%)	–	–	–	–	44.4	64.9	44.4	79.0	42.2	75.0	38.7	68.5	40.5	63.9	45.4	78.7	44.4	79.0
Acc(%)	–		–		56.8		56.0		48.6		47.7		49.7		57.7		56.0	
Characteristics	–		–		$P_{LFn_{SC}}$		$A_{T_{LF}}$		$A_{T_{SC}}$		$CMIF0_{RR}$		$CMIF_{max_{SC}}$		$A_{T_{LF}}$		$P_{LFn_{SC}}, A_{T_{LF}}$	
Relax vs. Joy																		
Number of comparisons	88	36	79	25	71	13	88	36	71	13	88	36	71	13	71	13	88	36
Se(%)/Sp(%)	77.3	55.6	74.7	56.0	83.1	23.1	63.6	77.8	63.4	84.6	73.9	47.2	67.6	76.9	**81.7**	**84.6**	65.9	69.4
P+(%)/P-(%)	81.0	50.0	84.3	41.2	85.5	20.0	87.5	46.7	95.7	29.7	77.4	42.5	94.1	30.3	96.7	45.8	84.1	45.5
Acc(%)	71.0		70.2		73.8		67.7		66.7		66.1		69.0		**82.1**		66.9	
Characteristics	R, F_R		$R_{F_R}, F_{R_{F_R}}$		R_{SC}		$A_{T_{RR}}, A_{T_{LF}}, PD_{m_{HF}}$		$A_{T_{SC}}$		$CMIF_{max_{RR}}$		$CMIF_{max_{SC}}$		$F_R, F_{R_{F_R}}, R_{SC}, A_{T_{SC}}, PD_{m_{HF}}$		$R, PD_{m_{HF}}$	
Relax vs. all negative valences																		
Number of comparisons	88	117	79	111	71	99	88	117	71	99	88	117	71	99	88	117	88	117
Se(%)/Sp(%)	–	–	–	–	–	–	80.7	35.9	93.0	26.3	77.3	33.3	59.2	50.5	79.5	38.5	80.7	35.9
P+(%)/P-(%)	–	–	–	–	–	–	48.6	71.2	47.5	83.9	46.6	66.1	46.2	63.3	49.3	71.4	48.6	71.2
Acc(%)	–		–		–		55.1		54.1		52.2		54.1		56.1		55.1	
Characteristics	–		–		–		$A_{T_{LF}}$		$A_{T_{SC}}$		$CMIF0_{RR}$		$CMIF0_{SC}, CMIF_{max_{SC}}$		$A_{T_{LF}}$		$A_{T_{LF}}$	
Relax vs. Fear																		
Number of comparisons	88	46	79	45	71	41	88	46	71	41	88	46	71	41	71	41	88	46
Se(%)/Sp(%)	–	–	–	–	–	–	96.6	54.3	100.0	53.7	88.6	58.7	71.8	63.4	100.0	53.7	96.6	54.3
P+(%)/P-(%)	–	–	–	–	–	–	80.2	89.3	78.9	100.0	84.4	73.0	77.3	56.5	78.9	100.0	80.2	89.3
Acc(%)	–		–		–		82.1		83.0		78.4		68.8		83.0		82.1	
Characteristics	–		–		–		$A_{T_{LF}}$		$A_{T_{SCF}}$		$CMIF0_{RR}$		$CMIF0_{SC}, CMIF_{max_{SC}}, \tau_{max_{SC}}$		$A_{T_{SC}}$		$A_{T_{LF}}$	
Relax vs. Sadness																		
Number of comparisons	88	34	79	32	71	28	88	34	71	28	88	34	71	28	–	–	–	–
Se(%)/Sp(%)	–	–	–	–	–	–	–	–	–	–	–	–	–	–	–	–	–	–
P+(%)/P-(%)	–	–	–	–	–	–	–	–	–	–	–	–	–	–	–	–	–	–
Acc(%)	–		–		–		–		–		–		–		–		–	
Characteristics	–		–		–		–		–		–		–		–		–	
Relax vs. Anger																		
Number of comparisons	88	37	79	34	71	30	88	37	71	30	88	37	71	30	71	30	71	30
Se(%)/Sp(%)	–	–	–	–	47.9	70.0	53.4	59.5	–	–	–	–	–	–	47.9	70.0	47.9	70.0
P+(%)/P-(%)	–	–	–	–	79.1	36.2	75.8	34.9	–	–	–	–	–	–	79.1	36.2	79.31	36.2
Percentage[2]	–		–		54.5		55.2		–		–		–		54.5		54.5	
Characteristics	–		–		$P_{LFn_{SC}}$		$PD_{m_{HF}}$		–		–		–		$P_{LFn_{SC}}, PD_{m_{HF}}$		$P_{LFn_{SC}}, PD_{m_{HF}}$	

It can be noted that when sensitivity, specificity and accuracy are all greater than 70% the results are remarked in bold type.

Table 5.4: Classification results obtained by the analysis 2: number of comparison between group 1 (G1) and group 2 (G2), sensitivity, specificity, positive and negative predictive value, accuracy and characteristics classified from the analysis S1 to S9.

	S1		S2		S3		S4		S5		S6		S7		S8		S9	
	G1	G2	G1	G2	G1	G2	G1	G2	G1	G2	G1	G2	G1	G2	G1	G2	G1	G2
Positive valence vs. Negative valences																		
Number of comparisons	36	117	25	111	13	99	36	117	13	99	36	117	13	99	13	99	36	117
Se(%)/Sp(%)	58.3	83.8	56.0	77.5	23.1	83.8	80.6	59.8	100.0	29.3	77.8	33.3	76.9	65.7	69.2	88.9	61.1	70.9
P+(%)/P-(%)	52.5	86.7	35.9	86.7	15.8	89.2	38.2	90.9	15.7	100.0	26.4	83.0	22.7	95.6	45.0	95.7	39.3	85.6
Acc(%)	77.8		73.5		76.8		64.7		37.5		43.8		67.0		86.6		68.6	
Characteristics	R, F_R		R_{F_R}, $F_{R_{F_R}}$		R_{SC}		$A_{T_{LF}}$, $PD_{m_{HF}}$		$A_{T_{SC}}$		$CMIF_{0_{RR}}$		$CMIF_{max_{SC}}$		F_R, R_{SC}, $CMIF_{max_{SC}}$		R, $PD_{m_{HF}}$	
Joy vs. Fear																		
Number of comparisons	36	46	25	45	13	41	36	46	13	41	36	46	13	41	13	41	36	46
Se(%)/Sp(%)	55.6	78.3	56.0	80.0	23.1	85.4	100.0	54.3	**92.3**	**75.6**	91.7	58.7	**84.6**	**75.6**	**86.6**	**85.4**	100.0	53.3
P+(%)/P-(%)	66.6	69.2	60.9	76.6	33.3	77.8	63.1	100.0	54.5	96.9	63.5	90.0	52.4	94.0	64.7	94.6	63.2	100.0
Acc(%)	68.3		71.4		70.4		74.4		**79.6**		73.2		**77.8**		**85.2**		74.4	
Characteristics	P_{LFn}, F_R		R_{F_R}, $F_{R_{F_R}}$		R_{SC}		$PD_{m_{HF}}$		$PD_{m_{SC}}$		$CMIF_{0_{RR}}$		$CMIF_{max_{SC}}$		F_R, $CMIF_{max_{SC}}$		$PD_{m_{HF}}$	
Joy vs. Sadness																		
Number of comparisons	36	35	25	32	13	28	36	34	13	28	36	34	13	28	13	28	36	34
Se(%)/Sp(%)	58.3	91.1	–	–	–	–	61.1	64.4	76.9	60.7	–	–	**76.9**	**75.0**	53.8	92.9	50.0	85.3
P+(%)/P-(%)	87.5	67.4	–	–	–	–	64.7	61.1	47.6	85.0	–	–	58.8	87.5	77.8	81.3	78.3	61.7
Acc(%)	74.3		–		–		62.9		65.9		–		**75.6**		80.5		67.1	
Characteristics	R, F_R		–		–		$A_{T_{LF}}$		$A_{T_{SC}}$		–		$CMIF_{max_{SC}}$		R, F_R, $A_{T_{SC}}$		R	
Joy vs. Anger																		
Number of comparisons	36	37	25	34	13	30	36	37	13	30	36	37	13	30	13	30	36	37
Se(%)/Sp(%)	52.8	75.7	–	–	–	–	58.3	62.2	76.9	56.7	–	–	**76.9**	**70.0**	61.5	76.7	58.3	62.2
P+(%)/P-(%)	67.9	62.2	–	–	–	–	60.0	60.5	43.5	85.0	–	–	52.6	87.5	53.3	82.1	60.0	60.5
Acc(%)	64.4		–		–		60.3		62.8		–		**72.1**		72.1		60.3	
Characteristics	F_R		–		–		$A_{T_{LF}}$		$A_{T_{SC}}$		–		$CMIF_{max_{SC}}$		F_R, $A_{T_{SC}}$		$A_{T_{LF}}$	
Fear vs. Sadness																		
Number of comparisons	46	34	45	32	41	28	46	34	41	28	46	34	41	28	41	28	46	34
Se(%)/Sp(%)	–	–	–	–	–	–	54.3	97.1	53.7	100.0	58.7	88.2	68.3	75.0	53.7	100.0	54.3	97.1
P+(%)/P-(%)	–	–	–	–	–	–	96.2	61.1	100.0	59.6	87.1	61.2	80.0	61.8	100.0	59.6	96.2	61.1
Acc(%)	–		–		–		72.5		72.5		71.3		71.0		72.5		72.5	
Characteristics	–		–		–		$A_{T_{LF}}$		$A_{T_{SC}}$		$CMIF_{0_{RR}}$		$CMIF_{max_{SC}}$		$A_{T_{SC}}$		$A_{T_{LF}}$	
Fear vs. Anger																		
Number of comparisons	46	37	45	34	41	30	46	37	41	30	46	37	41	30	41	30	46	37
Se(%)/Sp(%)	50.0	64.9	–	–	–	–	60.9	97.3	53.7	96.7	58.7	94.6	68.3	80.0	53.7	96.7	58.7	94.6
P+(%)/P-(%)	63.9	51.1	–	–	–	–	96.6	66.7	95.6	60.4	93.1	64.8	82.4	64.9	95.7	60.4	93.1	64.8
Acc(%)	56.6		–		–		77.1		71.8		74.7		73.2		71.8		74.7	
Characteristics	P_{LFn}		–		–		$A_{T_{RR}}$		$A_{T_{SC}}$		$CMIF_{0_{RR}}$		$CMIF_{max_{SC}}$		$A_{T_{SC}}$		P_{LFn}, $A_{T_{RR}}$	
Sadness vs. Anger																		
Number of comparisons	34	37	32	34	28	30	34	37	28	30	34	37	28	30	–	–	–	–
Se(%)/Sp(%)	–	–	–	–	–	–	–	–	–	–	–	–	–	–	–	–	–	–
P+(%)/P-(%)	–	–	–	–	–	–	–	–	–	–	–	–	–	–	–	–	–	–
Acc(%)	–		–		–		–		–		–		–		–		–	
Characteristics	–		–		–		–		–		–		–		–		–	

It can be noted that when sensitivity, specificity and accuracy are all greater than 70% the results are remarked in bold type.

Table 5.5: Classification results obtained by the analysis 3: number of comparison between group 1 (G1) and group 2 (G2), sensitivity, specificity, positive and negative predictive value, accuracy and characteristics classified from the analysis S1 to S9.

	S1		S2		S3		S4		S5		S6		S7		S8		S9	
	G1	G2	G1	G2	G1	G2	G1	G2	G1	G2	G1	G2	G1	G2	G1	G2	G1	G2
Positive valence vs. Negative valences																		
Number of comparisons	35	107	23	94	12	81	35	107	12	81	35	107	12	81	12	81	35	107
Se(%)/Sp(%)	57.1	91.6	52.2	85.1	66.7	91.4	60.0	71.0	66.7	60.5	–	–	**83.3**	**79.0**	**83.3**	**85.2**	**71.4**	**73.8**
P+(%)/P-(%)	69.0	86.7	46.2	87.9	53.5	94.9	40.4	84.4	20.0	92.5	–	–	37.0	97.0	45.5	97.2	47.2	88.8
Acc(%)	83.1		78.6		88.2		68.3		61.3		–		**79.6**		**84.9**		**73.2**	
Characteristics	R, F_R		R_{F_R}, $F_{R_{F_R}}$		R_{SC}, ρ_{max}		$A_{T_{RR}}$, $PD_{m_{LF}}$, $PD_{m_{HF}}$		$PD_{m_{SC}}$		–		$CMIF_{max_{SC}}$		R, R_{F_R}, $F_{R_{F_R}}$, ρ_{max}, $CMIF_{max_{SC}}$		R, $PD_{m_{HF}}$	
Joy vs. Fear																		
Number of comparisons	35	43	23	38	12	33	35	43	12	33	35	43	12	33	12	33	35	43
Se(%)/Sp(%)	57.1	88.4	52.2	84.2	**75.0**	**81.8**	94.3	51.2	100.0	54.5	91.4	53.5	**91.7**	**81.8**	**75.0**	**78.8**	**85.7**	**70.0**
P+(%)/P-(%)	80.0	71.7	66.7	74.4	60.0	90.0	61.1	91.7	44.4	100.0	61.5	88.5	64.7	96.4	56.3	89.7	69.8	85.7
Acc(%)	74.4		72.1		**80.0**		70.5		66.7		70.5		**84.4**		**77.8**		**76.9**	
Characteristics	R, F_R		R_{F_R}, $F_{R_{F_R}}$		ρ_{max}		$PD_{m_{HF}}$		$A_{T_{SC}}$		$CMIF_{0_{RR}}$		$CMIF_{max_{SC}}$		F_R, $CMIF_{max_{SC}}$		R, $PD_{m_{HF}}$	
Joy vs. Sadness																		
Number of comparisons	35	30	23	27	12	22	35	30	12	22	35	30	12	22	12	22	35	30
Se(%)/Sp(%)	60.0	96.7	–	–	**83.3**	**77.3**	65.7	73.3	66.7	77.3	–	–	**75.0**	**72.7**	**100.0**	**77.3**	68.6	83.3
P+(%)/P-(%)	95.5	67.4	–	–	66.7	89.5	74.2	64.7	61.5	81.0	–	–	60.0	84.2	70.6	100.0	82.8	69.4
Acc(%)	76.9		–		**79.4**		69.2		73.5		–		**73.5**		**85.3**		75.4	
Characteristics	R, F_R		–		ρ_{max}		$A_{T_{RR}}$, $A_{T_{LF}}$		$A_{T_{SCF}}$		–		$CMIF_{max_{SC}}$		ρ_{max}, $A_{T_{LF}}$, $CMIF_{max_{SC}}$		R, $A_{T_{RR}}$, $A_{T_{LF}}$	
Joy vs. Anger																		
Number of comparisons	35	34	23	29	12	26	35	34	12	26	35	34	12	26	12	26	35	34
Se(%)/Sp(%)	54.3	79.4	–	–	**83.3**	**80.8**	60.0	73.5	66.7	73.1	57.1	52.9	**75.0**	**84.6**	**83.3**	**84.6**	60.0	73.5
P+(%)/P-(%)	73.1	62.8	–	–	66.7	91.3	70.0	64.1	53.3	82.6	55.6	54.5	69.2	88.0	71.4	91.7	70.0	64.1
Acc(%)	66.7		–		**81.6**		66.7		71.1		55.1		**81.6**		**84.2**		66.7	
Characteristics	P_{LFn}, F_R		–		ρ_{max}		$PD_{m_{LF}}$		$A_{T_{SC}}$		$CMIF_{max_{RR}}$		$CMIF_{max_{SC}}$		ρ_{max}, $PD_{m_{LF}}$, $CMIF_{max_{SC}}$		$PD_{m_{LF}}$	
Fear vs. Sadness																		
Number of comparisons	43	30	38	27	33	22	43	30	33	22	43	30	33	22	33	22	43	30
Se(%)/Sp(%)	–	–	–	–	–	–	51.2	100.0	54.5	100.0	53.5	93.3	**70.0**	**77.3**	54.5	100.0	51.2	48.8
P+(%)/P-(%)	–	–	–	–	–	–	100.0	58.8	100.0	59.5	92.0	58.3	82.1	63.0	100.0	59.5	100.0	58.8
Acc(%)	–		–		–		71.2		72.7		69.9		**72.7**		72.7		71.2	
Characteristics	–		–		–		$A_{T_{LF}}$		$A_{T_{SC}}$		$CMIF_{max_{RR}}$		$CMIF_{max_{SC}}$		$A_{T_{SC}}$		$A_{T_{LF}}$	
Fear vs. Anger																		
Number of comparisons	43	34	38	29	33	26	43	34	33	26	43	34	33	26	33	26	43	34
Se(%)/Sp(%)	–	–	–	–	–	–	58.1	100.0	54.5	96.2	53.5	100.0	66.7	76.9	54.5	96.2	58.1	100.0
P+(%)/P-(%)	–	–	–	–	–	–	100.0	65.4	94.7	62.5	100.0	63.0	78.6	64.5	94.7	62.5	100.0	65.4
Acc(%)	–		–		–		76.6		72.9		74.0		71.2		72.9		76.6	
Characteristics	–		–		–		$A_{T_{RR}}$		$A_{T_{SC}}$		$CMIF_{0_{RR}}$		$CMIF_{max_{SC}}$		$A_{T_{SC}}$		$A_{T_{RR}}$	
Sadness vs. Anger																		
Number of comparisons	30	34	27	29	22	26	30	34	22	26	30	34	22	26	–	–	–	–
Se(%)/Sp(%)	–	–	–	–	–	–	–	–	–	–	–	–	–	–	–	–	–	–
P+(%)/P-(%)	–	–	–	–	–	–	–	–	–	–	–	–	–	–	–	–	–	–
Acc(%)	–		–		–		–		–		–		–		–		–	
Characteristics	–		–		–		–		–		–		–		–		–	

It can be noted that when sensitivity, specificity and accuracy are all greater than 70% the results are remarked in bold type.

5.4 Discussion

The results derived from the three analyzes have been evaluated as shown below.

Regarding the results obtained by the analysis 1 (Table 5.3), it can be observed that only the comparison between relax and joy permits good classifications of the subjects by means of the characteristics: F_R, $F_{R_{F_R}}$, R_{SC}, $A_{T_{SC}}$ and $PD_{m_{HF}}$. Comparing these results with the linear analysis exposed in chapter 3, the statistics of the parameter R_{SC} are in concordance with the ones presented in chapter 3 where it was obtained that a p-value ≤ 0.05 and sensitivity, specificity and accuracy $\geq 70\%$ and AUC index ≥ 0.70. On the other hand, the parameters F_R and $F_{R_{F_R}}$ did not show significant statistical differences between this pair of elicitations but could classify as part of the parameter set S8. In addition, as in this classification analysis, no linear parameters were able to discriminate between relax and negative valences. In the non-linear analysis, exposed in chapter 4, among all parameters that presented statistically significant differences between relax and joy, $A_{T_{SC}}$ and $PD_{m_{HF}}$ both resulted in a p-value ≤ 0.01 and sensitivity, specificity and accuracy $\geq 70\%$ and AUC index ≥ 0.70. Furthermore, by means of the non-linear analysis, it was possible to extract parameters which differentiated between relax and fear.

Although in [60], different classifier methods are used compared to the ones applied in this work, it could be observed a classification rate of 92% among the basal state of neutrality against amusement, contentment, disgust, fear or sadness.

Regarding the results obtained by the analysis 2 (Table 5.4), it can be observed that joy vs. fear, joy vs. sadness and joy vs. anger can be classified with a common characteristic: $CMIF_{max_{SC}}$. Comparing these results with the non-linear analysis, exposed in chapter 4, $CMIF_{max_{SC}}$ resulted in a p-value ≤ 0.001, sensitivity and specificity $\geq 70\%$, accuracy $\geq 85\%$ and AUC index ≥ 0.95 for joy vs. fear. In addition, the parameter $CMIF_{max_{SC}}$ resulted in a p-value ≤ 0.01, sensitivity and specificity $\geq 70\%$, accuracy $\geq 75\%$ and AUC index ≥ 0.77 for joy vs. sadness and joy vs. anger.

The results regarding the analysis 3 are presented in Table 5.5 which shows that subjects can be well classified when positives vs. all negative valences, joy vs. fear, joy vs. sadness, joy vs. anger and fear vs. sadness are normalized by a basal condition of relax.

It can be observed that the parameter $CMIF_{max_{SC}}$, which considers the non-linear coupling between the HRV and the respiratory information in a HF band redefined by the SCHF method, is the recurrent characteristic that appears in all classifications between positive and all negative valences together, between joy and each single negative valence and between fear and sadness. Another interesting parameter to be mentioned is ρ_{max}, since it was able to classify between joy vs. all negative valences, joy vs. fear, joy vs. sadness and joy vs. anger. It can be noted that ρ_{max} also takes into account the common information between HRV and respiration.

Unfortunately, it is difficult to make comparisons between these results and the studies found in the bibliography because all differ on the database recording criteria that directly affect on the classification accuracy as happens with the number of participants, the emotion elicitation, the duration of the affective elicitation, the signals recorded and the classifier method [22]. Nonetheless, in Table 5.1 it has been reported studies close to the study developed in this thesis, that have taken into account HRV signals with visual or music elicitation, although with an elicitation with smaller duration or with different size database used. In [107], the same classifier technique than in the present thesis was performed to discriminate among joy, anger, sadness and pleasure with an overall result of 92.1%. In the present thesis, the percentage of original grouped cases correctly classified obtained comparing joy and all negative valences together was 84.9%, for joy vs. fear it was 84.4%, for joy vs. sadness it was 85.3%, for joy vs. anger it was 84.2% and fear vs. sadness it was 72.7%. Although [50, 53, 59, 60] used different classifier methods that those used in the present thesis, it could be observed that the best results are obtained for those studies which considered positive and negative valences, as it was reported here.

In some studies, more sophisticated methodologies have been used which have managed to improve the classification results in front of the linear classifiers. However, in [107], a linear methodology LDF has been used to distinguish between human emotions and it has offered a better result than the more sophisticated methodologies. This fact supports the choice of using a linear classifier to analyze between groups of human emotions.

There are some limitations to note regarding the classificatory study. The use of a linear classifier which is based on LDF makes results not optimal, since the features do not follow the assumption of normality and they are not independent. In addition, the sample size database used is small, and there are many emotions to classify and a high variability in the signals. That is why it has been selected a LDF algorithm in order to avoid an overtraining which could lead to a positive bias of the result.

The results extracted from this chapter suggest that although the analysis based on the analysis 2 has been able to obtain characteristics that classify between joy vs. fear, joy vs. sadness and joy vs. anger, the results obtained by the analysis 3 may be more reliable since it considers the emotions normalized by their baseline state and therefore eliminates the variability that these signals present. Furthermore, to take into account the relationship between the HRV and the respiratory information combined with lineal and non-lineal methodologies increases the reliability for human emotion recognition.

Chapter 6

Conclusions

Contents

Interest in emotion recognition has increased in recent years as a useful tool for diagnosing psycho-neural illnesses. In this dissertation, linear and non-linear methods based on the analysis of HRV were proposed for human emotion recognition.

For the linear analysis methodology, it was proposed the joint analysis of HRV and respiration to improve human emotion characterization. With this purpose, the HF band was defined based on the maximum spectral correlation between HRV and respiration. The ρ_{max} itself was proposed as an index to identify emotions. The hypothesis was that this index could add relevant information to HRV analysis to describe human emotions.

Regarding to the non-linear analysis methodologies, the AMIF technique was applied to HRV signals to study complex interdependencies, and the CMIF technique was considered to quantify the complex coupling between HRV and respiratory signals. Both algorithms were adapted to short term RR time series. Traditional band pass filtering was applied to the RR series at LF and HF band, and also the redefined HF based on the maximum spectral correlation between HRV and respiration was investigated. Both the AMIF and the CMIF algorithms were calculated with regard to different time scales as specific complexity measures.

The ability of the parameters derived from the linear and non-linear techniques was evaluated on the database of video-induced emotion elicitation.

6.1 Conclusions for linear analysis methodology

In chapter 3, human emotion recognition was assessed by HRV analysis. To increase the reliability of HRV measurements, a novel methodology based on spectral correlation of HRV signal and respiration was proposed.

The new proposed method, the Spectrum Correlation for High Frequency band, revealed an improvement in the reliability for sympathovagal balance estimation capable of discriminating between relax vs. joy, joy vs. each of the negative valences and fear vs. sadness.

This method provided the novel index, ρ_{max}, which offers additional information for emotion recognition, based on the relationship between HRV and respiration.

6.2 Conclusions for non-linear analysis methodology

The results extracted from chapter 4 suggested that the non-linear AMIF and the CMIF techniques characterized the negative valence of fear, by reflecting a lower complexity than the other emotions. Parameters derived from the AMIF allowed extending the description of the complexity of vagal and sympathetic autonomic rhythms. Parameters derived from the CMIF at the respiration-based bandwidth provided relevant information related to non-linear mechanisms between vagal and respiratory activity, especially for fear.

Furthermore, filtering the HRV signals into a redefined HF band provided a better discrimination for parameters derived from the AMIF between relax and joy, relax and fear, joy and all remaining emotion conditions as well as fear and all remaining emotion conditions.

The non-linear AMIF and CMIF techniques provided complementary information to other linear and non-linear methods.

6.3 Conclusions for the classification analysis

The results extracted from chapter 5 suggested that relax vs. joy, positive vs. all negative valences, joy vs. fear, joy vs. sadness, joy vs. anger and fear vs. sadness can be all classified.

Although the analysis based on the analysis 2 has been able to obtain characteristics that classify between joy vs. fear, joy vs. sadness and joy vs. anger, the results obtained by the analysis 3 may be more reliable since it considers the emotions normalized by their baseline state and therefore eliminates the variability that these signals present.

The parameter $CMIF_{max_{SC}}$, which considers the non-linear coupling between the HRV and the respiratory signal information in a HF band redefined by the SCHF method, is the recurrent characteristic that appear in all classifications between positive and all negative valences together, and between joy and each single negative valence. Another interesting parameter to be mentioned is ρ_{max}, since it was able to classify between joy vs. all negative valences, joy vs. sadness and anger. It can be noted that ρ_{max} also take into account the common information between HRV and respiration.

6.4 Future extensions

The current clinical practice for diagnosing patients affected by psychological or psychiatric disorders is based solely on verbal interviews and on specific questionnaire scores, and there are no reliable and objective psychophysiological markers that are taken into account. For these reason, the characterization of emotional patterns can have an impact in the treatment of certain psychological pathologies.

In future works, it will be proposed to implement the algorithms and indices derived from this research within a hardware like a biomedical equipment, an app or a remote server which sends the signal to a health professional to be analyzed. This tool opens the door to help in identifying emotional behaviors in people suffering from mental pathologies. However, further studies are needed to test the validity and reliability of the proposed index outside laboratory settings.

Another future extension to be considered is the outpatient monitoring, which consist on tracking changes in the health status of patients outside the classical hospital environment. Outpatient monitoring might be crucial after surgery, heart failure, diabetes, mental illness, among others to monitor emergency patients before they arrive at the hospital. This enables to improve the care patients receive and also their diagnosis.

For these reason, the algorithms and indices derived from this research could be implemented on mobile devices which record and transmit medical data, being a low cost and easy solution to obtain continuous and long term dynamic physiological data. This tool could provide an intelligent monitoring of outpatient individuals with mental illnesses with the purpose of designing individualized therapies. The importance of monitoring by means of an ambulatory system, individuals with depression or anxiety, between other mental illness, comes from the fact that it could alert during or before emergency crisis and also, it could maintain their attention on modulating their emotional responses.

Chapter 7

Conclusiones

Contents

El interés en el reconocimiento de emociones ha aumentado en los últimos años por ser una herramienta útil para diagnosticar enfermedades psico-neurales. En esta disertación se han propuesto métodos basados en análisis lineales y no lineales para analizar la variabilidad del ritmo cardíaco con la finalidad de identificar emociones humanas.

Para el análisis lineal se propuso analizar conjuntamente la variabilidad del ritmo cardíaco y la respiración para así mejorar la caracterización de las emociones humanas. Con este propósito, la banda de alta frecuencia se definió mediante la correlación espectral máxima entre la variabilidad del ritmo cardíaco y la respiración. Además, ρ_{max} fue propuesta como un índice para identificar emociones, con la hipótesis de que este índice podría agregar información relevante al análisis de la variabilidad del ritmo cardíaco para describir las emociones humanas.

Con respecto al análisis no lineal, la Función de Auto Información Mutua se aplicó a las señales de variabilidad del ritmo cardíaco para estudiar las interdependencias complejas, y se consideró la Función de Información Mutua Cruzada para cuantificar el acoplamiento complejo entre la variabilidad del ritmo cardíaco y las señales respiratorias. Ambos algoritmos se adaptaron a series temporales RR de corta duración. Se aplicó un filtro pasabanda tradicional a la serie RR en las bandas de baja y alta frecuencia, y también se investigó la banda de alta frecuencia redefinida según la correlación espectral máxima entre la variabilidad del ritmo cardíaco y la respiración. Los algoritmos de la Función de Auto Información Mutua y de la Función de Información Mutua Cruzada se calcularon con respecto a diferentes escalas de tiempo como medidas de complejidad específicas.

Se evaluó la capacidad de los parámetros derivados de las técnicas lineales y no lineales en la base de datos de emociones inducidas mediante videos.

7.1 Conclusiones del análisis lineal

En el capítulo 3, se evaluó el reconocimiento de emociones humanas mediante el análisis de variabilidad del ritmo cardíaco. Para aumentar la fiabilidad de las mediciones de variabilidad del ritmo cardíaco se propuso una nueva metodología basada en la correlación espectral máxima entre la señal de variabilidad del ritmo cardíaco y la respiración.

Este nuevo método propuesto, la correlación espectral en la banda de alta frecuencia, mejoró la estimación del equilibrio simpáticovagal capaz de discriminar entre la relajación versus alegría, alegría versus cada una de las valencias negativas y miedo versus tristeza.

Además este método proporcionó un nuevo parámetro, ρ_{max}, que ofrece información adicional para el reconocimiento de emociones, basado en la relación entre la variabilidad del ritmo cardíaco y la respiración.

7.2 Conclusiones del análisis no lineal

Los resultados extraídos del capítulo 4 sugirieron que las técnicas no lineales Función de Auto Información Mutua y Función de Información Mutua Cruzada caracterizan la valencia negativa del miedo, al reflejar una menor complejidad que las otras emociones. Los parámetros derivados de la Función de Auto Información Mutua permitieron ampliar la descripción de la complejidad de los ritmos autónomos vagales y simpáticos. Los parámetros derivados de la Función de Información Mutua Cruzada en la banda de alta frecuencia basada en la respiración proporcionaron información relevante relacionada con mecanismos no lineales entre la actividad vagal y respiratoria, especialmente para el miedo.

Además, filtrar las señales de variabilidad del ritmo cardíaco en una banda de alta frecuencia redefinida proporcionó una mejor discriminación de los parámetros derivados de la Función de Auto Información Mutua entre relajación y alegría, relajación y miedo, alegría y todas las condiciones emocionales restantes, así como el miedo y todas las condiciones emocionales restantes.

Las técnicas no lineales Función de Auto Información Mutua y Función de Información Mutua Cruzada proporcionaron información complementaria a otros métodos lineales y no lineales.

7.3 Conclusiones del análisis de clasificación

Los resultados extraídos del capítulo 5 sugirieron que ha sido posible clasificar relajación versus alegría, alegría versus todas las valencias negativas juntas, alegría versus miedo, alegría versus tristeza, alegría versus ira y miedo versus tristeza.

A pesar de que mediante el estudio basado en el análisis 2 se han podido obtener características que clasifican entre alegría versus miedo, alegría versus tristeza, y alegría versus ira, los resultados obtenidos mediante el análisis 3 pueden ser más significativos ya que este análisis considera las emociones normalizadas por su estado basal y, por lo tanto, elimina la variabilidad que presentan estas señales.

El parámetro $CMIF_{max_{SC}}$, que considera el acoplamiento no lineal entre la variabilidad del ritmo cardíaco y la información respiratoria en una banda de alta frecuencia redefinida por el método SCHF, ha sido una característica recurrente que aparece en todas las clasificaciones entre alegría versus todas las valencias negativas juntas, entre alegría versus cada valencia negativa individual, y entre miedo versus tristeza. Otro parámetro interesante a mencionar es ρ_{max}, ya que ha sido capaz de clasificar entre alegría versus miedo, alegría versus tristeza y alegría versus ira. Cabe señalar que ρ_{max} también tiene en cuenta la información común entre la variabilidad del ritmo cardíaco y la respiración.

7.4 Extensiones futuras

La práctica clínica actual para diagnosticar pacientes afectados por trastornos psicológicos o psiquiátricos se basa únicamente en entrevistas verbales y en puntajes de cuestionarios específicos, y no hay marcadores psicofisiológicos adecuados y objetivos que se tengan en cuenta. Por esta razón, la caracterización de los patrones emocionales puede tener un impacto en el tratamiento de ciertas patologías psicológicas.

En trabajos futuros, se propondrá implementar los algoritmos y parámetros derivados de esta investigación dentro de un hardware como por ejemplo puede ser un equipo biomédico, una aplicación o un servidor remoto que envíe la señal a un profesional de la salud para su posterior análisis. Esta herramienta abre la puerta para ayudar a identificar comportamientos emocionales en personas que sufren patologías mentales. Sin embargo, se necesitan más estudios para probar la validez y confiabilidad de los parámetros propuestos fuera de los entornos de laboratorio.

Otra extensión futura a considerar es la monitorización ambulatoria, que consiste en rastrear los cambios en el estado de salud de los pacientes fuera del entorno hospitalario clásico. El monitoreo ambulatorio puede ser crucial después de una cirugía, insuficiencia cardíaca, diabetes, enfermedades mentales, entre otros, para monitorear a los pacientes ante una emergencia antes de llegar al hospital. Esto permite mejorar la atención que reciben los pacientes y también su diagnóstico.

Por esta razón, los algoritmos y parámetros derivados de esta investigación podrían implementarse en dispositivos móviles que registran y transmiten datos médicos, siendo una solución fácil y de bajo coste para obtener datos fisiológicos dinámicos continuos y a largo plazo. Esta herramienta podría proporcionar un monitoreo inteligente de pacientes ambulatorios con enfermedades mentales con el propósito de diseñar terapias individualizadas. La importancia del monitoreo por medio de un sistema ambulatorio a individuos con depresión o con ansiedad, entre otras enfermedades mentales, viene del hecho de que podría alertar durante o antes de una crisis de emergencia y también, podría mantener su atención en la modulación de sus respuestas emocionales.

Chapter 8

Appendix

Contents

8.1 Scientific contributions

The methodologies and results presented in this dissertation and elaborated during my PhD studies have been published in the following works.

International Journals:

- [100] Valderas, M.T., Bolea, J., Orini, M., Laguna, P., Orrite, C., Vallverdú, M. and Bailón, R., Human emotion characterization by heart rate variability analysis guided by respiration, *IEEE Journal of Biomedical and Health Informatics*, 2019, DOI: 10.1109/JBHI.2019.2895589.

- [98] Valderas, M.T., Bolea, J., Laguna, P., Bailón, R. and Vallverdú, M., Mutual information between heart rate variability and respiration for emotion characterization, *Physiological Measurement*, Volume 40, Number 8, 2019, DOI: 10.1088/1361-6579/ab310a.

International conferences:

- [99] Valderas, M.T., Bolea, J., Laguna, P., Vallverdú, M. and Bailón, R., Human emotion recognition using heart rate variability analysis with spectral bands based on respiration, *37th International Conference on IEEE EMBS International Conference on Engineering in Medicine and Biology Society*, 2015, 6674-6677, DOI: 10.1109/EMBC.2015.7319792.

8.2 Acronyms

In this section a glossary with the most used abbreviations and parameters, with nomenclature and definition, is presented.

8.2.1 List of abbreviations

- μ: mean.

- σ: standard deviation.
- A: anger.
- AMIF: Auto-Mutual Information Function.
- ANN: Articial Neural Networks.
- ANO-VA: analysis of variance.
- ANS: autonomic nervous system.
- ApEn: Approximate Entropy.
- ARMA model: time-varying autoregressive moving average model.
- AUC: receiver operating characteristic curve.
- BNE: Basic Negative Emotion.
- BP: blood pressure.
- bpm: beats per minute.
- BPE: Basic Positive Emotion.
- CFMEn: Cross Fuzzy Measure Entropy.
- CMIF: Cross-Mutual Information Function.
- CSEn: Cross Sample Entropy.
- DFA: Detrended Fluctuation Analysis.
- DLEs: Dominant Lyapunov Exponents (DLEs).
- ECG: electrocardiography.
- EEG: electroencephalography.
- F: fear.
- FD: Fisher Discriminant.
- FMEn: Fuzzy Measure Entropy.

- GSR: galvanic skin response.
- HF: high frequency.
- HF_{F_R}: shifted HF band centered at F_R with fixed bandwidth.
- HF_{SC}: redefined HF band based in the Spectrum Correlation HF method.
- HRV: heart rate variability.
- IPFM model: integral pulse frequency modulation model.
- J: joy.
- kNN: k-Nearest Neighbour.
- LDF: Linear Discriminant Function.
- LF: low frequency.
- LLP: Lagged Poincaré Plot.
- MBP: Marquardt Backpropagation.
- MP: Multilayer Perceptron.
- MRE: mean relative error.
- NFS: Neuro-Fuzzy System.
- PANAS-X: the Positive and Negative Affect Schedule - Expanded Form.
- PD2: Pointwise Correlation Dimension.
- PE: Permutation Entropy.
- PME: Permutation Min-Entropy.
- PSD: power spectrum density.
- Q1: interquartile ranges in the first quartile.
- Q3: interquartile ranges in the third quartile.
- R: relax.

- RF: Random Forests.
- RSA: respiratory sinus arrhythmia.
- S: sadness.
- SA node: sinoatrial node.
- SCHF method: Spectrum Correlation HF method.
- SEn: Sample Entropy.
- ST: skin temperature variation.
- SVM: Support Vector Machines.
- ULF: ultra low frequency.
- VLF: very low frequency.

8.2.2 List of parameters

- ρ_{max}: maximum spectral correlation between HRV and respiration.
- τ: prediction time or time lag of the AMIF or the CMIF.
- τ_a: lower-time scale boundary corresponding to the SCHF prediction time range.
- τ_b: upper-time scale boundary corresponding to the SCHF prediction time range.
- $\tau_{max_{RR}}$: time lag between $CMIF_{max}$ and $CMIF_0$ studied in the $RR(t)$ series.
- $\tau_{max_{SC}}$: time lag between $CMIF_{max}$ and $CMIF_0$ studied in the ($RR_{SC}(t)$), which is the $RR(t)$ series filtered in the HF_{SC} band.
- ΔHF: distance between the lower and the upper limit of the HF_{SC} band.
- Λ: Wilks$'$s Lambda.
- a_{max}: lower limit of the HF_{SC} band.

- $A_{T_{RR}}$: total area under the curve $RR(t)$ series.
- $A_{T_{LF}}$: total area under the curve $RR_{LF}(t)$ series.
- $A_{T_{HF}}$: total area under the curve $RR_{HF}(t)$ series.
- $A_{T_{SC}}$: total area under the curve $RR_{SC}(t)$ series.
- Acc: accuracy.
- b_{max}: upper limit of the HF_{SC} band.
- BD: beat decay.
- $CMIF_{0_{RR}}$: CMIF value at $\tau = 0$ of the $RR(t)$ series.
- $CMIF_{0_{SC}}$: CMIF value at $\tau = 0$ of the $RR_{SC}(t)$ series.
- $CMIF_{max_{RR}}$: maximum CMIF value of the $RR(t)$ series.
- $CMIF_{max_{SC}}$: maximum CMIF value of the $RR_{SC}(t)$ series.
- $d_{HR}(t)$: instantaneous heart rate.
- $d_{HRM}(t)$: time-varying mean heart rate.
- $\overline{d_{HRM}}$: mean of $d_{HRM}(t)$.
- F_R: respiratory frequency.
- $F_{R_{F_R}}$: respiratory frequency of the recordings which accomplishes the restriction of $F_R \geq 0.10$ Hz.
- $F_{R_{SC}}$: respiratory frequency of the recordings which accomplishes all the restrictions imposed in Section *3.2.2 Frequency band definition*.
- FN: false negatives.
- FP: false positives.
- $H_{x(t)}$: Shannon entropy.
- I: Number of bins.
- *m(t)*: modulating signal.

- P-: negative predictive value.
- P+: positive predictive value.
- P_{HF}: power content in the HF band.
- $P_{HF_{F_R}}$: power content in the HF_{F_R} band.
- $P_{HF_{SC}}$: power content in the HF_{SC} band.
- P_{LF}: power content in the LF band.
- P_{LFn}: normalized power in the LF band.
- $P_{LFn_{F_R}}$: normalized power in the LF band considering the HF_{F_R} band.
- $P_{LFn_{SC}}$: normalized power in the LF band considering the HF_{SC} band.
- PD: Peak decay.
- PD_m: mean peak decay.
- $PD_{m_{LF}}$: mean peak decay of the $RR_{LF}(t)$ series.
- $PD_{m_{HF}}$: mean peak decay of the $RR_{HF}(t)$ series.
- $PD_{m_{SC}}$: mean peak decay of the $RR_{SC}(t)$ series.
- $r(t)$: respiratory signal.
- R: ratio LF/HF.
- R_{F_R}: ratio LF/HF_{F_R}.
- R_{SC}: ratio LF/HF_{SC}.
- $RR(t)$: RR time series.
- $RR_{LF}(t)$: $RR(t)$ series filtered in the LF band.
- $RR_{HF}(t)$: $RR(t)$ series filtered in the HF band.
- $RR_{SC}(t)$: $RR(t)$ series filtered in the HF_{SC} band.
- Se: sensitivity.

- Sp: specificity.
- $S_{attentiveness}$: attentiveness scale.
- $S_{fatigue}$: fatigue scale.
- S_{fear}: fear scale.
- S_{guilt}: guilt scale.
- $S_{hostility}$: hostility scale.
- $S_{joviality}$: joviality scale.
- $S_{sadness}$: sadness scale.
- $S_{self-assurancescale}$: self-assurance scale.
- $S_{serenity}$: serenity scale.
- $S_{shyness}$: shyness scale.
- $S_m(f)$: power spectrum density of *m(t)*.
- $S_r(f)$: power spectrum density of *r(t)*.
- $S_{surprise}$: surprise scale.
- TN: true negatives.
- TP: true positive.

Bibliography

[1] Alonso, J. F., Romero, S., Ballester, M. R., Antonijoan, R. M., and Mañanas, M. A. Stress assessment based on eeg univariate features and functional connectivity measures. *Physiological Measurement 36* (2015), 1351–1365.

[2] Anderson, T. W. *An introduction to Multivariate Statistical Analysis*. J. Wiley & Sons, New Jersey, 1984.

[3] Arza, A., Garzón-Rey, J. M., Lázaro, J., Gil, E., López-Antón, R., de la Cámara, C., Laguna, P., Bailón, R., and Aguiló, J. Measuring acute stress response through physiological signals: Towards a quantitative assessment of stress. *Medical & Biological Engineering & Computing* (2018), 1–17.

[4] Bailón, R. *Análisis de la señal electrocardiográfica durante prueba de esfuerzo y su aplicación en el diagnóstico de cardiopatías*. PhD thesis, Universidad de Zaragoza, 2006.

[5] Bailón, R., Laguna, P., Mainardi, L., and Sörnmo, L. Analysis of heart rate variability using time-varying frequency bands based on respiratory frequency. In *IEEE EMBS International Conference on Engineering in Medicine and Biology Society* (2007), 29th International Conference on, pp. 6674–6677.

[6] Bailón, R., Laouini, G., Grao, C., Orini, M., and Laguna, P. The integral pulse frequency modulation model with time-varying threshold: Ap-

plication to heart rate variability analysis during exercise stress testing. *IEEE Transactions on Biomedical Engineering 58*, 3 (2011), 642–652.

[7] BAILÓN, R., MAINARDI, L., AND LAGUNA, P. Time-frequency analysis of heart rate variability during stress testing using a priori information of respiratory frequency. In *Computers in Cardiology* (2006), pp. 169–172.

[8] BAILÓN, R., MAINARDI, L., ORINI, M., SÖRNMO, L., AND LAGUNA, P. Analysis of heart rate variability during stress testing using respiratory information. *Biomedical Signal Processing and Control 5*, 4 (2010), 299–310.

[9] BAILÓN, R., SÖRNMO, L., AND LAGUNA, P. A robust method for ECG-based estimation of the respiratory frequency during stress testing. *IEEE Transactions on Biomedical Engineering 53*, 7 (2006), 1273–1285.

[10] BALADA, F., MÁRQUEZ, C., NADAL, R., REDOLAR, D., AND SILVESTRE, J. *Farmacología y endocrinología del comportamiento*. Editorial UOC, Spain, 2012.

[11] BILLMAN, G. E. Heart rate variability - a historical perspective. *Frontiers in Physiology* (2011), 1–13.

[12] BOETTGER, S., HOYER, D., FALKENHAHN, K., KAATZ, M., YERAGANI, V. K., AND BR, K.-J. Nonlinear broad band dynamics are less complex in major depression. *Bipolar Disorders 10* (2008), 276–284.

[13] BOLEA, J., PUEYO, E., LAGUNA, P., AND BAILÓN, R. Non-linear HRV indices under autonomic nervous system blockade. In *36nd Annual International Conference of the IEEE EMBS* (2014), pp. 3252–3255.

[14] BORNASA, X., LLABRÉS, J., NOGUERAC, M., LÓPEZ, A. M., BARCELÓ, F., TORTELLA-FELIU, M., AND FULLANA, M. A. Looking at the heart of low and high heart rate variability fearful flyers: self-reported anxiety when confronting feared stimuli. *Biological Psychology 70*, 3 (2005), 182–187.

[15] BORON, W., AND BOULPAEP, E. *Medical physiology: a cellular and molecular approach.* Elsevier Saunders, Philadelphia, 2011.

[16] BROSSCHOT, J. F., DIJK, E. V., AND THAYER, J. F. Daily worry is related to low heart rate variability during waking and the subsequent nocturnal sleep period. *International Journal of Psychophysiology 63*, 1 (2007), 39–47.

[17] CAMPBELL-SILLS, L., AND BARLOW, D. H. *Incorporating Emotion Regulation into Conceptualizations and Treatments of Anxiety and Mood Disorders, Handbook of emotion regulation.* In: J. J. Gross (Ed.), Guilford Press, New York, 2007.

[18] CANNON, W. P. *Bodily Changes in Pain, Hunger, Fear and Rage.* D. Appleton, New York and London, 1927.

[19] CARLSON, N. R. *Physiology of behavior.* Pearson, USA, 2012.

[20] CARNEY, R. M., BLUMENTHAL, J. A., FREEDLAND, K. E., STEIN, P. K., HOWELLS, W. B., BERKMAN, L. F., WATKINS, L. L., CZAJKOWSKI, S. M., HAYANO, J., DOMITROVICH, P. P., AND JAFFE, A. S. Low heart rate variability and the effect of depression on postmyocardial infarction mortality. *JAMA Internal Medicine 165*, 3 (2005), 1486–1491.

[21] CARNEY, R. M., BLUMENTHAL, J. A., STEIN, P. K., WATKINS, L., CATELLIER, D., BERKMAN, L. F., CZAJKOWSKI, S. M., OCONNOR, C., STONE, P. H., AND FREEDLAND, K. E. Depression, heart rate variability, and acute myocardial infarction. *Circulation 104*, 17 (2001), 2024–2028.

[22] CHANEL, G., KIERKELS, J. M., SOLEYMANI, M., AND PUN, T. Short-term emotion assessment in a recall paradigm. *International Journal Human-Computer Studies 67*, 8 (2009), 607–627.

[23] COHEN, H., BENJAMIN, J., GEVA, A. B., MATAR, M. A., KAPLAN, Z., AND KOTLER, M. Autonomic dysregulation in panic disorder and in post-traumatic stress disorder: application of power spectrum analysis of heart rate

variability at rest and in response to recollection of trauma or panic attacks. *Psychiatry Research 96*, 1 (2000), 1–13.

[24] COHEN, H., KOTLER, M., MATAR, M. A., KAPLAN, Z., LOEWENTHAL, U., MIODOWNIK, H., AND CASSUTO, Y. Analysis of heart rate variability in posttraumatic stress disorder patients in response to a trauma-related reminder. *Biological Psychiatry 44*, 10 (1998), 1054–1059.

[25] COLOMBETTI, G. From affect programs to dynamical discrete emotions. *Philosophical Psychology 22 (4)* (2009), 407–425.

[26] DAMPNEY, R. A. L. Central neural control of the cardiovascular system: current perspectives. *Advances in physiology education 40(3)* (2016), 283–296.

[27] DAOUD, M., RAVIER, P., AND BUTTELLI, O. Use of cardiorespiratory coherence to separate spectral bands of the heart rate variability. *Biomedical Signal Processing and Control 46* (2018), 260–267.

[28] DEMAREE, H. A., AND EVERHART, D. E. Healthy high-hostiles: reduced parasympathetic activity and decreased sympathovagal flexibility during negative emotional processing. *Personality and Individual Differences 36* (2004), 457469.

[29] DESPOPOULOS, A., AND SILBERNAGL, S. *Color Atlas of Physiology*. Basic Sciences (Thieme), USA, 2003.

[30] DIMITRIEV, D. A., SAPEROVA, E. V., AND DIMITRIEV, A. D. State anxiety and nonlinear dynamics of heart rate variability in students. *PLoS ONE 11(1):e0146131* (2016).

[31] DISHMAN, R. K., NAKAMURA, Y., GARCIA, M. E. THOMPSON, R. W., DUNN, A. L., AND BLAIR, S. N. Heart rate variability, trait anxiety, and perceived stress among physically fit men and women. *International Journal of Psychophysiology 37*, 2 (2000), 121–133.

[32] EFRON, B. Estimating the error rate of a prediction rule: improvement on cross-validation. *Journal of the American Statistical Association 78* (1983), 316–331.

[33] EKMAN, P. An argument for basic emotions. *Cognition and Emotion 6 (3/4)* (1969), 169–200.

[34] EKMAN, P. *Emotions revealed: recognizing faces and feelings to improve communication and emotional life*. Times Books, Henry Holt and Company, LLC., New York, 2003.

[35] FELTEN, D. L. Neural influence on immune responses: underlying suppositions and basic principles of neural immune signaling. *Progress in brain research 122* (2000), 381–389.

[36] FELTEN, D. L., COHEN, N., ADER, R., FELTEN, S. Y., CARLSON, S. L., AND ROSZMAN, T. L. *Central neural circuits involved in neural immune interactions*. Eds. Psychoneuroinmmulogy. Academic Press, New York, 1991.

[37] FRIEDMAN, B. H. An autonomic flexibilityneurovisceral integration model of anxiety and cardiac vagal tone. *Biological Psychology 74*, 2 (2007), 185–199.

[38] FRIEDMAN, B. H., AND THAYER, J. F. Autonomic balance revisited: Panic anxiety and heart rate variability. *Journal of Psychosomatic Research 44*, 1 (1998), 133–151.

[39] GEISLER, F. C., VENNEWALD, N., KUBIAK, T., AND WEBER, H. The impact of heart rate variability on subjective well-being is mediated by emotion regulation. *Personality and Individual Differences 49* (2010), 723728.

[40] GÓMEZ, B., AND ESCOBAR, A. La psiconeuroinmunología: bases de la relación entre los sistemas nervioso, endocrino e inmune. *Facultad de Medicina de la Universidad Nacional Autónoma de México 45*, 1 (2002).

[41] GORDAN, R., GWATHMEY, J. K., AND XIE, L.-H. Autonomic and endocrine control of cardiovascular function. *World Journal of Cardiology 7(4)*

(2015), 204214.

[42] GOREN, Y., DAVRATH, L. R., PINHAS, I., TOLEDO, E., AND AKSELROD, S. Individual time-dependent spectral boundaries for improved accuracy in time-frequency analysis of heart rate variability. *IEEE Transactions on Biomedical Engineering 53*, 1 (2006), 35–42.

[43] GOSHVARPOUR, A., ABBASI, A., AND GOSHVARPOUR, A. Indices from lagged poincare plots of heart rate variability: an efficient nonlinear tool for emotion discrimination. *Australasian Physical & Engineering Sciences in Medicine 40(2)* (2016), 277–287.

[44] GROSS, J. J. The emerging field of emotion regulation: An integrative review. *Review of General Psychology 2(3)* (1998), 271–299.

[45] GWATHMEY, J. K., BRIGGS, G. M., AND ALLEN, P. D. *Heart Failure: Basic Science and Clinical Aspects*. Marcel Dekker Inc, New York, 1994.

[46] HAND, D. J., AND TAYLOR, C. C. *Multivariate Analysis of Variance and Repeated Measures*. Chapman & Hall, Florida, 1987.

[47] HERNANDO, A., LÁZARO, J., GIL, E., ARZA, A., MARIO, J., LÓPEZ-ANTÓN, R., DE LA CÁMARA, C., LAGUNA, P., AGUILÓ, J., AND BAILÓN, R. Inclusion of respiratory frequency information in heart rate variability analysis for stress assessment. *IEEE Journal of Biomedical and Health Informatics 20*, 4 (2016), 1016–1025.

[48] HOYER, D., FRIEDRICH, H., FRANK, B., POMPE, B., BARANOWSKI, R., ZEBROWSKI, J. J., AND SCHMIDT, H. Autonomic information flow improves prognostic impact of task force hrv monitoring. *Computer Methods and Programs in Biomedicine 81* (2006), 246–255.

[49] HOYER, D., LEDER, U., HOYER, H., POMPE, B., SOMMER, M., AND ZWIENER, U. Mutual information and phase dependencies: measures of reduced nonlinear cardiorespiratory interactions after myocardial infarction. *Medical Engineering and Physics 24* (2002), 33–43.

[50] KATSIS, C. D., KATERTSIDIS, N. S., AND FOTIADIS, D. I. An integrated system based on physiological signals for the assessment of affective states in patients with anxiety disorders. *Biomedical Signal Processing and Control 6*, 3 (2011), 261–268.

[51] KEMENY, M. E., AND GRUENEWALD, T. L. Affect, cognition, the immune system and health. *Progress in brain research 122* (2000), 291–308.

[52] KEMP, A. H., QUINTANA, D. S., GRAY, M. A., FELMINGHAM, K. L., BROWN, K., AND GATT, J. M. Impact of depression and antidepressant treatment on heart rate variability: A review and meta-analysis. *Biological Psychiatry 67*, 11 (2010), 1067–1074.

[53] KIM, K. H., BANG, S. W., AND KIM, S. R. Emotion recognition system using short-term monitoring of physiological signals. *Medical and Biological Engineering and Computing 42*, 3 (2004), 419–427.

[54] KOELSTRA, S., MÜHL, C., SOLEYMANI, M., LEE, J.-S., YAZDANI, A., EBRAHIMI, T., PUN, T., NIJHOLT, A., AND PATRAS, I. Deap: A database for emotion analysis using physiological signals. *IEEE Transactions on Affective Computing 3*, 1 (2012), 18–31.

[55] KONTAXIS, S., LÁZARO, J., GIL, E., LAGUNA, P., AND BAILÓN, R. Assessment of quadratic nonlinear cardiorespiratory couplings during tilt table test by means of real wavelet biphase. *IEEE Transactions Biomedical Engineering 66(1)* (2019), 187–198.

[56] KONTAXIS, S., ORINI, M., GIL, E., POSADAS-DE MIGUEL, M., BERNAL, M. L., AGUILÓ, J., DE LA CAMARA, C., LAGUNA, P., AND BAILÓN, R. Heart rate variability analysis guided by respiration in major depression disorder. In *Proceedings of the XLV International Conference on Computing in Cardiology* (2018), Maastricht, Netherlands, pp. 1–4.

[57] KUMAR, N., KHAUND, K., AND HAZARIKA, S. M. Bispectral analysis of EEG for emotion recognition. *Procedia Computer Science 84* (2016), 31–35.

[58] LACHENBRUCH, P. A. *Discriminant analysis*. Hafner Press, New York, 1975.

[59] LISETTI, C., AND NASOZ, F. Using noninvasive wearable computers to recognize human emotions from physiological signals. *Journal on Applied Signal Processing 11* (2004), 16721687.

[60] MAAOUI, C., AND PRUSKI, A. *Emotion recognition through physiological signals for human-machine communication, Cutting Edge Robotics*. Vedran Kordic, IntechOpen, France, 2010.

[61] MANN, D. L., ZIPES, D. P., LIBBY, P., AND BONOW, R. O. *Braunwalds Heart Disease: Textbook of Cardiovascular Medicine*. Elsevier - Health Sciences Division, Philadelphia, 2014.

[62] MARDIA, K., KENT, J. T., AND BIBBY, J. *Multivariate Analysis*. Academic Press, Massachusetts, 1979.

[63] MARTÍNEZ, J. P., ALMEIDA, R., OLMOS, S., ROCHA, A. P., AND LAGUNA, P. Wavelet-based ECG delineator: evaluation on standard databases. *IEEE Transactions on Biomedical Engineering 51* (2004), 570–581.

[64] MATEO, J., AND LAGUNA, P. Analysis of heart rate variability in the presence of ectopic beats using the heart timing signal. *IEEE Transactions on Biomedical Engineering 50*, 3 (2003), 334–343.

[65] MATTAVELLI, G., ROSANOVA, M., CASALI, A. G., PAPAGNO, C., AND ROMERO LAURO, L. J. Timing of emotion representation in right and left occipital region: Evidence from combined TMS-EEG. *Brain and Cognition 106* (2016), 13–22.

[66] MCCRATY, R., ATKINSON, M., TOMASINO, D., AND STUPPY, W. P. Analysis of twenty-four hour heart rate variability in patients with panic disorder. *Biological Psychology 56*, 2 (2001), 131–150.

[67] MIKUCKAS, A., MIKUCKIENE, I., VENCKAUSKAS, A., KAZANAVICIUS, E., LUKAS, R., AND PLAUSKA, I. Emotion recognition in human computer

interaction systems. *Elektronika ir Elektrotechnika 20*, 10 (2014), 1392–1215.

[68] MITCHELL, J. H., AND VICTOR, R. G. Neural control of the cardiovascular system: insights from muscle sympathetic nerve recordings in humans. *Medicine and science in sports and exercise 28(10)* (1996), 60–9.

[69] MIU, A. C., HEILMAN, R. M., AND MICLEA, M. Reduced heart rate variability and vagal tone in anxiety: Trait versus state, and the effects of autogenic training. *Autonomic Neuroscience 145*, 1-2 (2009), 99–103.

[70] MOHRMAN, D. E., AND HELLER, L. J. *Cardiovascular Physiology*. McGraw-Hill Interamericana, Mexico, 2006.

[71] NEY, H., MARTIN, S., AND WESSEL, F. *Statistical Language Modeling Using Leaving-One-Out.* In: Young S., Bloothooft G. (eds) Corpus-Based Methods in Language and Speech Processing. Text, Speech and Language Technology, vol 2., Springer, Dordrecht, 1997.

[72] NGUYEN, V. T., BREAKSPEAR, M., HU, X., AND GUO, C. C. The integration of the internal and external milieu in the insula during dynamic emotional experiences. *Neuroimage 124* (2016), 455–463.

[73] ORINI, M., BAILÓN, R., ENK, R., KOELSCH, S., MAINARDI, L., AND LAGUNA, P. A method for continuously assessing the autonomic response to music-induced emotions through HRV analysis. *Medical and Biological Engineering and Computing* (2010), 423–433.

[74] ORINI, M., BAILÓN, R., LAGUNA, P., MAINARDI, L. T., AND BARBIERI, R. A multivariate time-frequency method to characterize the influence of respiration over heart period and arterial pressure. *EURASIP Journal on Advances in Signal Processing 2012*, 214 (2012).

[75] ORINI, M., BAILÓN, R., MAINARDI, L. T., AND LAGUNA, P. Synthesis of HRV signals characterized by predetermined time-frequency structure by

means of time-varying arma models. *Biomedical Signal Processing and Control 7* (2012), 141–150.

[76] ORINI, M., BAILÓN, R., MAINARDI, L. T., LAGUNA, P., AND FLANDRIN, P. Characterization of dynamic interactions between cardiovascular signals by time-frequency coherence. *IEEE Transactions on Biomedical Engineering 59*, 3 (2012), 663–673.

[77] PALACIOS, M., FRIEDRICH, H., GÖTZE, C., VALLVERDÚ, M., BAYES DE LUNA, A., CAMINAL, P., AND HOYER, H. Changes of autonomic information flow due to idiopathic dilated cardiomyopathy. *Physiological Measurement 28* (2007), 677–688.

[78] PARDO, A., AND RUIZ, M. A. *SPSS 11. Guía para el análisis de datos*. Mc Graw Hill, Madrid, 2002.

[79] PARZEN, E. *Teoría moderna de probabilidades y sus aplicaciones*. Limusa Grupo Noriega Editores, España, 1973.

[80] PETRANTONAKIS, P. C., AND HADJILEONTIADIS, L. J. Emotion recognition from EEG using higher order crossings. *IEEE Transactions on Information Technology in Biomedicine 14*, 2 (2010), 186–197.

[81] POMPE, B. Ranking and entropy estimation in nonlinear time series analysis. *Nonlinear Analysis of Physiological Data* (1998), 67–90.

[82] POSTMA-NILSENOV, M., HOLT, E., HEYN, L., GROENEVELD, K., AND FINSET, A. A case study of vocal features associated with galvanic skin response to stressors in a clinical interaction. *Patient Education and Counseling 99*, 8 (2016), 1349–1354.

[83] QUINTANA, D. S., GUASTELLA, A. J., OUTHRED, T., HICKIE, I. B., AND KEMP, A. H. Heart rate variability is associated with emotion recognition: direct evidence for a relationship between the autonomic nervous system and social cognition. *International Journal of Psychophysiology 86*, 2 (2012), 168–172.

[84] RANTANEN, A., LAUKKA, S. J., LEHTIHALMES, M., AND SEPPAÄNEN, T. Heart rate variability reflecting from oral reports on negative experience. *Procedia, Social and Behavioral Sciences 5* (2010), 483–487.

[85] RHOADESAND, R. A., AND BELL, D. R. *Medical Physiology: Principles for Clinical Medicine*. Lippincott Williams and Wilkins, Wolters Kluwer Health, Philadelphia, 2009.

[86] RICE, W. R. Analyzing tables of statistical test. *Biomedical Signal Processing and Control 43(1)* (1989), 223–225.

[87] SASSI, R., CERUTTI, S., LOMBARDI, F., MALIK, M., HUIKURI, H. V., PENG, C.-K., SCHMIDT, G., AND YAMAMOTO, Y. Advances in heart rate variability signal analysis: joint position statement by the e-cardiology esc working group and the european heart rhythm association co-endorsed by the asia pacific heart rhythm society. *Europace 17(9)* (2015), 1341–53.

[88] SELVARAJ, J., MURUGAPPAN, M., WAN, K., AND YAACOB, S. Classification of emotional states from electrocardiogram signals: a non-linear approach based on hurst. *Biomedical Engineering Online 12*, 44 (2013).

[89] SOLEYMANI, M., ASGHARI-ESFEDEN, S., FU, Y., AND PANTIC, M. Analysis of EEG signals and facial expressions for continuous emotion detection. *IEEE Transactions on Affective Computing 7*, 1 (2016), 17–28.

[90] STERNBERG, E. M. Interactions between the immune and neuroendocrine system. *Progress in brain research 122* (2000), 35–42.

[91] SUDHEESH, N. N., AND JOSEPH, K. P. Investigation into the effects of music and meditation on galvanic skin response. *ITBM-RBM 21*, 3 (2000), 158–163.

[92] TAN, G., DAO, T. K., FARMER, L., SUTHERLAND, R. J., AND GEVIRTZ, R. Heart rate variability (HRV) and posttraumatic stress disorder (ptsd): A pilot study. *Applied Psychophysiology and Biofeedback 36*, 1 (2010), 27–35.

[93] TASK FORCE OF THE EUROPEAN SOCIETY OF CARDIOLOGY AND THE NORTH AMERICAN SOCIETY OF PACING ELECTROPHYSIOLOGY. Heart rate variability. Standards of measurement, physiological interpretation, and clinical use. *European Heart Journal 17* (1996), 354–381.

[94] THAYER, J. F., AND HANSEN, A. L. Heart rate variability, prefrontal neural function, and cognitive performance: The neurovisceral integration perspective on self-regulation, adaptation and health. *Annals of Behavioral Medicine 37* (2009), 141–153.

[95] TURLOUGH FITZGERALD, M. J., GRUENER, G., AND MTUI, E. *Clinical neuroanatomy and neuroscience*. Elsevier Saunders, España, 2012.

[96] TURON, M., FERNANDEZ-GONZALO, S., JODAR, M., GOMA, G., MONTANYA, J., HERNANDO, D., BAILÓN, R., DE HARO, C., GOMEZ-SIMON, V., LOPEZ-AGUILAR, J., MAGRANS, R., MARTINEZ-PEREZ, M., OLIVA, C., AND BLANCH, L. Feasibility and safety of virtual-reality-based early neurocognitive stimulation in critically ill patients. *Annals of Intensive Care 7*, 81 (2017), 1–11.

[97] UNAL, I. Defining an optimal cut-point value in roc analysis: An alternative approach. *Computational and Mathematical Methods in Medicine 2017* (2017), 1–14.

[98] VALDERAS, M. T., BOLEA, J., LAGUNA, P., BAILÓN, R., AND VALLVERDÚ, M. Auto-mutual information function and cross-mutual information function assessment for human emotion recognition. *Physiological Measurement 40*, 8 (2018).

[99] VALDERAS, M. T., BOLEA, J., LAGUNA, P., VALLVERDÚ, M., AND BAILÓN, R. Human emotion recognition using heart rate variability analysis with spectral bands based on respiration. In *IEEE EMBS International Conference on Engineering in Medicine and Biology Society* (2015), 37th International Conference on, pp. 6674–6677.

[100] Valderas, M. T., Bolea, J., Orini, M., Laguna, P., Orrite, C., Vallverdú, M., and Bailón, R. Human emotion characterization by heart rate variability analysis guided by respiration. *IEEE Journal of Biomedical and Health Informatics* (2018).

[101] Valenza, G., Allegrini, P., Lanatá, A., and Scilingo, E. P. Dominant lyapunov exponent and approximate entropy in heart rate variability during emotional visual elicitation. *Frontiers in neuroengineering 5*, 3 (2012).

[102] Valenza, G., Citi, L., Lanatá, A., Scilingo, E. P., and Barbieri, R. Revealing real-time emotional responses: a personalized assessment based on heartbeat dynamics. *Scientific Reports 4*, 4998 (2014).

[103] Valenza, G., Lanatá, A., and Scilingo, E. P. Improving emotion recognition systems by embedding cardiorespiratory coupling. *Physiological Measurement 34*, 4 (2012), 449–64.

[104] Valenza, G., Lanatá, A., and Scilingo, E. P. Oscillations of heart rate and respiration synchronize during affective visual stimulation. *IEEE Transactions on Information Technology in Biomedicine 16*, 4 (2012), 683–690.

[105] Valenza, G., Lanatá, A., and Scilingo, E. P. The role of nonlinear dynamics in affective valence and arousal recognition. *IEEE Transactions on Affective Computing 3*, 2 (2012), 237–249.

[106] Valenza, G., Nardelli, M., Lanatá, A., Gentili, C., Bertschy, G., Paradiso, R., and Scilingo, E. P. Wearable monitoring for mood recognition in bipolar disorder based on history-dependent long-term heart rate variability analysis. *IEEE Journal of Biomedical and Health Informatics 18*, 5 (2014), 1625–1635.

[107] Wagner, J., Kim, J., and André, E. From physiological signals to emotions: implementing and comparing selected methods for feature extraction and classification. In *2005 IEEE International Conference on Multimedia and Expo* (2005).

[108] WATSON, D., AND CLARK, L. A. *The PANAS-X: Manual for the Positive and Negative Affect Schedule - Expanded Form*. Department of Psychological & Brain Sciences Publications, University of Iowa, 1999.

[109] XIA, Y., YANG, L., ZUNINO, L., SHI, H., ZHUANG, Y., AND LIU, C. Application of permutation entropy and permutation min-entropy in multiple emotional states analysis of rri time series. *Entropy 20(3):430* (2018).

[110] YASUMA, F., AND HAYANO, J. I. Respiratory sinus arrhythmia: Why does the heartbeat synchronize with respiratory rhythm? *Chest 125(2)* (2004), 683–690.

[111] ZHAO, L., YANG, L., SU, Z., AND LIU, C. Cardiorespiratory coupling analysis based on entropy and cross-entropy in distinguishing different depression stages. *Frontiers in Physiology 10:359* (2019).